UNIVERSITY *of the*
WESTERN CAPE

The Colour Stability of Various Glass Ionomer Cements

A thesis submitted in fulfilment of the requirements for the

Degree of Masters in Restorative Dentistry in the

Department of Restorative Dentistry at the

University of the Western Cape

MSc (Restorative Dentistry)

Dr Farzana Karjiker
Student number: 9757851
Supervisor: Dr Desigar Moodley
Co-Supervisor: Dr Saadika Khan

Keywords

CIELAB

Glass ionomer cement

Polyalkenoate

Resin-modified glass ionomer

Nanotechnology

Staining

Spectrophotometry

Scanning Electron Microscopy (SEM)

Abstract

Introduction: Together with bonding to both enamel and dentine, an ideal restorative material would display physical properties similar to that of natural tooth tissue and would not be prone to degradation as a result of the oral environment. This includes changes in colour. Glass ionomer technology has undergone many changes to its original chemistry since it was developed in the early 1970's. In 1988 resin-modified glass ionomers were introduced and in 2008, nano-ionomers were introduced. As a result of the progression in material sciences and the use of more sophisticated techniques and methods in restorative dentistry, it is possible to accomplish much improved aesthetics and functional durability of a restoration, both anteriorly and posteriorly. However, for as long as aesthetic restorations have been available, and in spite of advances in material structure and performance, one of the greatest challenges facing clinicians still remains that aesthetic restorations have to be replaced relatively frequently as staining and discolouration is a common problem. **Aim of the study:** The aim of this study was to determine the stainability of four resin-modified glass ionomers and one glass ionomer cement when exposed to a staining broth. **Objectives:** To record any change in colour before and after exposing the sample with the staining broth using a spectrophotometer, to compare the stainability, to examine the depth of staining using a light microscope and to observe the particle size of the powder and the surface texture using Scanning Electron Microscopy of the four resin-modified glass ionomer cements and one glass ionomer cement. **Materials and**

Methods: Four resin-modified glass ionomers (one nano-ionomer) and one glass ionomer (zinc-reinforced ionomer) were selected. All were shade A2, except for Vitremer™ which was not available in A2. 15 discs of each material were prepared. The discs were 15 mm in diameter and 2 mm in thickness. All the materials were handled and cured according to the manufacturers' instructions. After curing, only one side of each disc was polished using Sof-Lex™ discs (3M ESPE, USA). The unpolished side of each disc was designated as a matrix finish. The specimens were all immersed in distilled water at 37 °C for one week. They were then immersed in a staining broth for a period of one week and readings were taken after a period of 2 hours, 4 hours, 8 hours, 24 hours and one week. Colour was read on each side of each disc at the indicated intervals with a spectrophotometer. The colour difference was calculated using the CIELAB colour co-ordinates. Sample discs were then sectioned to determine the depth of staining. An additional sample disc of each material was made for observation with the SEM and was therefore not stained. Also, an unmixed sample of each material was prepared for examination with the SEM. **Results:** In general, for all materials there was an increase in staining when assessed with the colour difference between the baseline colour and the 7 day reading. Ketac™ N100, showed the highest total colour change of 43.84 for the unpolished surface followed by Riva™ which showed the total colour change of 28.55 for the unpolished surface. This was similar to Fuji II LC® which had a total colour change of 28.16 for the unpolished surface. For Vitremer™, the total colour change increased to 18.07 for the unpolished surface. For the unpolished surfaces, ChemFil™ Rock showed the least colour difference from baseline to 7 days (ΔE^*_{ab}

= 10.45), followed by Vitremer™ (ΔE^*_{ab} = 18.07). Both Fuji II LC® and Riva™ Light Cure showed similar colour change from baseline to 7 days for unpolished surfaces (ΔE^*_{ab} of 28.16 and 28.55 respectively). Ketac™ N100 showed the highest staining after 7 days in the staining broth with a colour difference of 43.84. For the polished surfaces, the colour change for Fuji II LC® was 25.72 which was similar to Riva™ Light Cure which was 22.44 and Ketac™ N100 which showed a colour change of 22.79 on the polished surface. ChemFil™ Rock showed the least colour change of 17.69 for the polished surface followed by Vitremer™ which showed a colour change of 23.63 for the polished surface. Thus, for both the unpolished and polished surfaces there was a similar staining pattern. **Conclusion:** In this study it was demonstrated that all products evaluated in this study showed some degree of staining when exposed to a staining broth when evaluated using the ΔE^*_{ab} CIELAB colour evaluation. Ketac™ N100 showed the highest colour change compared to the other materials, but the reason for this was not explored. Both Vitremer™ and ChemFil™ Rock showed similar patterns of staining.

Declaration

I hereby declare that, "*The Colour Stability of Various Glass Ionomer Cements*" is my personal work, that it has not been submitted previously in its entirety or in part for any degree or examination at any other university, and that all the sources I have used or quoted have been indicated and acknowledged by a complete list of references.

Farzana Karjiker

Signature:  Date: 03/05/2019

Acknowledgement

All things are only possible by the grace and mercy of Allah. I am thankful to Allah, for in His infinite mercy and grace, I was able to complete this thesis.

To my supervisor, Dr. Desigar Moodley, I am grateful for your guidance, assistance, supervision and interest in my work and in me. You have been more than a supervisor and a colleague to me – you stepped in and took on a fatherly role. My admiration of you runs deep as a colleague, supervisor and researcher.

Dr. Saadika Khan, my co-supervisor, you became a mentor to me and allowed me to tap into your wealth of knowledge and experience which made me value your input and opinions. You were a source of light, information and guidance when it was needed. For this, you have my eternal gratitude.

My sincerest gratitude to Mr. Ahmed Eldud for his assistance in the statistical analysis of the data and for his guidance in the subject. In addition, thanks to Prof. Herman W. Kruijsse for his statistical assistance in the early stages of the project.

I am grateful for the time, assistance, guidance and input I received from Mr Adrian Joseph from the Electron Microscope Unit at the University of the Western Cape when doing the Scanning Electron Microscope studies.

I am grateful to Dr. Amir Omer for his invaluable input and editorial assistance, as well as his endless technical assistance during the final stages of this project.

To my parents, I will never be able to express the depth of my gratitude and appreciation for all that you have done. You instilled a thirst for knowledge in me and your support

and encouragement never wavered. You ensure that I always strive to be the best version of myself and for this, I will be eternally grateful.

I am blessed with four wonderful younger siblings. You all have been so supportive through this entire process. Thank you for the constant support.

And last, but not least, a heartfelt thank you to my friends who are my sisters too. Thank you for all the encouragement during this period.

Dedication

For Mom and Dad…who instilled in me the importance of always asking questions and finding answers in order to increase my knowledge and constantly improve myself.

"My Lord, increase me in knowledge." (Quran Chapter 20 : Verse 114)

Contents

Keywords ..... **ii**

Abstract ..... **iii**

Declaration ..... **vi**

Acknowledgement ..... **vii**

Dedication ..... **ix**

Contents ..... **x**

List of Figures ..... **xivv**

List of Tables ..... **xixix**

List of Abbreviations ..... **xx**

Presentations and Awards ..... **xxii**

Chapter 1 Literature Review **1**

1.1 Introduction 1

1.2 Review of the Literature 2

1.2.1 History of Glass Ionomers 2

1.2.2 The Ion-Leachable Glass 3

1.2.3 The Polyalkenoic Acid 4

1.2.4 The Setting Reaction 5

1.2.5 Structure of the Cement 9

1.2.6 Water Content 9

1.2.7 Resin-Modified Glass Ionomer 11

1.3 Nanotechnology 14

1.4 Materials and Filler Particles 15

1.5 Colour 33

1.5.1 Munsell Colour Tree 33

1.5.2 International Commission of Illumination (CIE) L*a*b* Colour System 34

1.6 Spectrophotometry 36

1.7 Staining 38

1.8 Scanning Electron Microscopy (SEM) 41

1.8.1 Description of the SEM 41

1.8.2 How the SEM Works 43

1.8.3 SEM Sample Preparation 44

Chapter 2 Aims and Objectives 46

2.1 Aim 46

2.2 Objectives 46

2.3 Null Hypothesis 46

Chapter 3 Materials and Methods 47

3.1 Sample Disc Preparation 48

3.2 Colour (Spectrophotometer) Analysis 54

3.2.1 Surface Examination Following Staining 55

3.3 Visual Assessment of Depth Penetration Using A Light Microscope 56

3.4 Scanning Electron Microscope Analysis 58

3.4.1 Analysis of Glass Ionomer Powder / Paste 58

3.4.2 Analysis of Surface Structure 63

Chapter 4 Data Analysis 66

Chapter 5 Results 68

5.1 Colour (Spectrophotometer) Analysis 68

5.1.1 Fuji II LC® CAPSULE Colour Changes 68

5.1.2 RIVA™ Light Cure Colour Changes 72

5.1.3 Ketac™ N100 Colour Changes 76

5.1.4 Vitremer™ Colour Changes 80

5.1.5 ChemFil™ Rock Colour Changes 84

5.2. Examination of Staining (Light Microscopy) 88

5.2.1. Surface Staining 88

5.2.2. Depth of Staining 92

5.3. Scanning Electron Microscopy 95

5.3.1. Fuji II LC® CAPSULE 95

5.3.2. Riva™ Light Cure 97

5.3.3. Ketac™ N100 99

5.3.4. Vitremer™ 101

5.3.5. ChemFil™ Rock 103

Chapter 6 Discussion **105**

Chapter 7 Conclusion **1155**

Chapter 8 Limitations and Recommendations **1188**

Chapter 9 References **12020**

List of Figures

Figure 1.1: The initial stages of the glass ionomer setting reaction 6

Figure 1.2: Setting reaction of conventional glass ionomer cement 6

Figure 1.3: Fuji II LC® CAPSULE (GC, Japan). 17

Figure 1.4: Riva™ Light Cure (SDI, Australia). 20

Figure 1.5: Ketac™ N100 (3M ESPE, USA). 22

Figure 1.6: Vitremer™ (3M ESPE, USA). 25

Figure 1.7: Setting reactions of Vitremer™ Tri-Cure Glass Ionomer 26

Figure 1.8: ChemFil™ Rock (Dentsply, USA). 29

Figure 1.9: The Munsell Colour Tree…….....34

Figure 1.10: The CIELAB three dimensional colour space……...35

Figure 1.11: A spectrophotometer……..36

Figure 1.12: A typical SEM instrument……..42

Figure 1.13: Diagrammatic representation of (a) the functioning of an SEM……43

(b)Variety of signals produced during electron-sample interaction….....43

Figure 3.1: Perspex cast used to make sample discs of each material……48

Figure 3.2: The curing of a sample disc…….49

Figure 3.3: The Elipar DeepCure-S LED (3M ESPE, USA)……..50

Figure 3.4: Sof-Lex™ (3M ESPE, USA) discs……...51

Figure 3.5: The CM-2600d spectrophotometer (Konica Minolta, Japan)……..52

Figure 3.6: Suspension of a sample disc in a container without and with broth……52

Figure 3.7: A minitom diamond cut-off disc (Struers, Denmark)……..56

Figure 3.8: Visual inspection of cut sample discs……..57

Figure 3.9: Heraeus-Christ GmbH Centrifuge (Germany)…….59

Figure 3.10: Aluminium stub with aluminium base - side view (L), top view (R)……59

Figure 3.11: Dual-sided sticky tab……..60

Figure 3.12: Aluminium stubs prepared and numbered according to the material…....60

Figure 3.13: Specimens in the process of being attached to stubs…….61

Figure 3.14: Carbon rod used to sputter coat samples on aluminium stubs……...62

Figure 3.15: Sputter coated samples……...62

Figure 3.16: Emitech K950X Turbo Evaporator Sputter Coater (United Kingdom)….63

Figure 3.17: Quorum Q150T ES High Resolution Sputter Coater (United Kingdom)..64

Figure 3.18: Samples in the Quorum Q150T ES High Resolution Sputter Coater (United Kingdom)……65

Figure 3.19: Samples sputter coated in gold……...65

Figure 5.1: Fuji II LC®. Changes in L* scale over time polished versus unpolished surface with standard deviation..... 69

Figure 5.2: Fuji II LC®. Changes in a* scale over time for polished versus unpolished surface..... 70

Figure 5.3: Fuji II LC®. Changes in b* scale over time for polished versus unpolished surface showing standard deviation..... 71

Figure 5.4: Fuji II LC® changes in ΔE^*_{ab} scale over time for polished versus unpolished surface with standard deviation..... 72

Figure 5.5: Riva™ Light Cure changes in L* scale over time polished versus unpolished surface with standard deviation included. 73

Figure 5.6: Riva™ Light Cure changes in a* scale over time for polished versus unpolished surface with standard deviation included..... 74

Figure 5.7: Riva™ Light Cure changes in b* scale over time for polished versus unpolished surface showing standard deviation included. 75

Figure 5.8: Riva™ Light Cure changes in ΔE^*_{ab} scale over time for polished versus unpolished surface showing standard deviation with standard deviation. 76

Figure 5.9: Ketac™ N100 changes in L* scale over time polished versus unpolished surface with standard deviation. 77

Figure 5.10: Ketac™ N100 changes in a* scale over time for polished versus unpolished surface with standard deviation. 78

Figure 5.11: Ketac™ N100 changes in b* scale over time for polished versus unpolished surface showing standard deviation..... 79

Figure 5.12: Ketac™ N100 changes in ΔE^*_{ab} scale over time for polished versus unpolished surface showing standard deviation. 80

Figure 5.13: Vitremer™ changes in L* scale over time polished versus unpolished surface with standard deviation..... 81

Figure 5.14: Vitremer™ changes in a* scale over time for polished versus unpolished surface with standard deviation included. 82

Figure 5.15: Vitremer™ changes in b* scale over time for polished versus unpolished surface showing standard deviation..... 83

Figure 5.16: Vitremer™ changes in ΔE^*_{ab} scale over time for polished versus unpolished surface showing standard deviation..... 84

Figure 5.17: ChemFil™ Rock changes in L* scale over time polished versus unpolished surface with standard deviation. 85

Figure 5.18: ChemFil™ Rock changes in a* scale over time for polished versus unpolished surface with standard deviation..... 86

Figure 5.19: ChemFil™ Rock changes in b* scale over time for polished versus unpolished surface showing standard deviation. 87

Figure 5.20: ChemFil™ Rock changes in ΔE^*_{ab} scale over time for polished versus unpolished surface showing standard deviation. 88

Figure 5.21: Fuji II LC® CAPSULE Unpolished (a) and Polished (b) viewed under a light microscope..... 89

Figure 5.22: Riva™ LC Unpolished (a) and Polished (b) viewed under a light microscope. 89

Figure 5.23: Ketac™ N100 Unpolished (a) and Polished (b) viewed under a light microscope..... 90

Figure 5.24: Vitremer™ Unpolished (left) and Polished (right) viewed under a light microscope..... 91

Figure 5.25: ChemFil™ Rock Unpolished (left) and Polished (right) viewed under a light microscope..... 91

Figure 5.26: The polished surface of Fuji II LC® 92

Figure 5.27: The unpolished surface of Riva™ Light Cure 93

Figure 5.28: The unpolished surface of Ketac™ N100 93

Figure 5.29: The polished surface of Vitremer™ 94

Figure 5.30: The polished surface of ChemFil™ Rock 94

Figure 5.31: Fuji II LC® CAPSULE powder..... 95

Figure 5.32: Fuji II LC® CAPSULE sample disc 96

Figure 5.33: Riva™ LC powder 97

Figure 5.34: Riva™ LC sample disc 98

Figure 5.35: Ketac™ N100 paste 99

Figure 5.36: Ketac™ N100 sample disc 100

Figure 5.37: Vitremer™ powder 101

Figure 5.38: Vitremer™ sample disc 102

Figure 5.39: ChemFil™ Rock powder 103

Figure 5.40: ChemFil™ Rock sample disc. 104

List of Tables

Table 3.1: Glass Ionomers used to make sample discs..... 47

Table 3.2: Handling times of selected glass ionomers. 50

Table 3.3: Composition of Staining Broth..... 53

List of Abbreviations

i.e. - that is

°C - degrees Celcius

µm - micrometre

viz. - namely

HEMA - hydroxyethyl methacrylate

nm - nanometre

rpm - revolutions per minute

g - gram(s)

~ - approximately

wt - weight

vol - volume

mm - millimetres

SEM - Scanning Electron Microscope

cm - centimetre

ml - millilitres

X - times

Presentations and Awards

1. Winner of The Charles Valcke Award for the Best Poster Presentation in the Dental Materials Category at the SA IADR, September 2015, “The Colour Stability of Various Glass Ionomer Cements”.

Chapter 1

Literature Review

1.1 Introduction

Patients have become more aware of dental aesthetics. This awareness has a great influence on their decisions with respect to the chosen treatment modalities and their awareness of existing mismatched tooth-restoration colours. Resin-based restorative materials are used in anterior restorations and more frequently of late in posterior restorations too.

Glass ionomer cements are aesthetic materials with certain exclusive and unique properties which allows them to be used as a restorative material and as luting cements (Lohbauer, 2010). These unique properties include the ability to adhere to moist tooth structures, to chemically adhere to mineralised tissue, to release fluoride which makes them anticariogenic because fluorine is incorporated into the material, its thermal compatibility with tooth enamel, its biocompatibility and its low toxicity (Lohbauer, 2010). These unique properties, including the ability to modify the physical properties of the material by altering the powder : liquid ratio, lend glass ionomer cements the ability to be used in a wide array of clinical situations (Lohbauer, 2010). Similarly, due to these unique properties, the resin-modified glass ionomer cements are also used as restorative materials, luting cements, fixation of orthodontic brackets and core build-up for crowns (Francisconi *et al*., 2009). In spite of advancements in material sciences and the

improvement of many resin-based restorative materials and the resulting aesthetic outcome for patients, one of the main challenges remains the maintenance of these restorations over extended periods of time without requiring replacement.

1.2 Review of the Literature

In the 1960's the idea of a material which exhibited positive physico-chemical adhesion to tooth structure resulted in the development of polyacrylic acid based cements (Smith, 1998). At first there was zinc polycarboxylate and then there was glass ionomer cements (Smith, 1998).

The material commonly called 'glass ionomer' is referred to as glass polyalkenoate cement according to the International Standardisation Organisation and was developed at the Laboratory of the Government Chemist during the late 1960's (Sidhu and Nicholson, 2016; Walls, 1986). Technically, the term 'glass ionomer' is reserved for a material which consists of acid-decomposable glass and a water-soluble acid, *i.e.* a material which sets by an acid-base reaction, the simplest form being a conventional glass ionomer (Culbertson, 2001).

1.2.1 History of Glass Ionomers

In order to produce a material which was aesthetically acceptable as an adhesive restorative material, dental silicate and zinc polycarboxylate were combined to produce polyalkenoate cements, whilst maintaining and combining the advantages of these two materials (Chinelatti *et al.*, 2004). These components consist of an ion-leachable glass

powder and a polyalkenoic acid, which when mixed form a hard cement-like mass (Chinelatti *et al.*, 2004; Culbertson, 2001; Walls, 1986).

1.2.2 The Ion-Leachable Glass

The ion-leachable glass is the foundation of the powder in glass ionomer cements (Walls, 1986). It is an alumino-silicate glass with a high fluoride content and it is usually formed by the fusion of quartz, alumina, cryolite, fluorite, aluminium trifluoride and aluminium phosphate (Walls, 1986). The fusion process is performed in a silaminite crucible between 1100˚C and 1300˚C (Walls, 1986). The frit is cooled down until it has a dull glow, and is then quenched in water and finely ground to give particles which are less than 45 µm in size (Walls, 1986). Glass reactivity depends on the temperature to which the frit is raised during fusion (Walls, 1986). Glasses which form at temperatures of 1100˚C – 1200˚C are incompletely fused with large fluorite inclusions (Walls, 1986). Glasses which form at temperatures of 1300˚C – 1500˚C have more disseminated and smaller fluorite particles (Walls, 1986). They also have relatively more aluminium and less fluorine than the glass which melts at lower temperatures (Walls, 1986).

The incorporation of non-matrix inclusions into the glass improves the physical properties of the set cement (Walls, 1986). There are two types of inclusions, namely metallic inclusions and crystalline inclusions (Walls, 1986). Small metallic particles are incorporated in the glass during the fusion process to improve physical properties (Walls, 1986). These metal reinforced materials were referred to as cermet cements (Walls, 1986). They exhibit a metallic colour cast and titanium oxide has been admixed with the glass

for a more aesthetic result (Upadhya and Kishore, 2005; Walls, 1986). The inclusion of a variety of dispersed phase crystallites in the glass structure such as corundum, rutile, aluminium titinate and baddelyite were all found to enhance the flexural strength of the set cement (Walls, 1986).

1.2.3 The Polyalkenoic Acid

The first polyalkenoic acid used to form glass polyalkenoate was a 50% aqueous solution of polyacrylic acid which was unstable and underwent gelation when stored (Walls, 1986). This was postulated to be due to hydrogen bonding between the polyacid chains (Walls, 1986). This problem was overcome by methylation of some of the carboxyl groups but this resulted in a clinically unsatisfactory product (Walls, 1986). The most effective of the acrylic acid copolymers were those with itaconic acid and some alkenoic acids (maleic acid and fumaric acid) (Walls, 1986). These polyacids, together with vacuum-dried polyacrylic acid, now form the basis of the polyalkenoate cements (Walls, 1986).

A primary problem with the early cements was its inability to set quickly (Wilson *et al*., 1976), which resulted in the investigation of the effect of a host of chelating agents on the setting reaction. It was found that the addition of tiny quantities of the optically active isomers of tartaric acid increased the rate of setting (Sidhu and Nicholson, 2016; Prosser, Richards and Wilson, 1982; Wilson, Crisp and Ferner, 1976). This affected the compressive and tensile strengths of the material, while the working time was unaffected (Sidhu and Nicholson, 2016; Prosser, Richards and Wilson, 1982; Wilson, Crisp and

Ferner, 1976). This 'chelating co-monomer' is present in all of the commercially available forms of this material (Sidhu and Nicholson, 2016; Prosser, Richards and Wilson, 1982; Wilson, Crisp and Ferner, 1976).

The concept of mixing silicate and polycarboxylate cement was at first disregarded by Wilson in 1968 when faced with the unsuccessful attempt to form a cement by mixing a conventional silicate cement powder with an aqueous solution of polyacrylic acid. The development of ion-leachable glasses capable of reacting with polyalkenoic acid has resulted in the production of the glass polyalkenoate cements as a group of materials of its own (Walls, 1986). The biphasic nature of the interaction between glass and acid to produce cement is complicated. The modifications made to create a commercially feasible product have increased the complexity of the setting reaction of this material (Walls, 1986).

1.2.4 The Setting Reaction

All glass polyalkenoate cements set in the same manner: an acid-base reaction between ion-leachable glass and a polyalkenoic acid (Sidhu and Nicholson, 2016; Walls, 1986). The complexity of the reaction is increased by the presence of two very different cations in the glass *viz.* calcium and aluminium, which both play a pivotal role in the formation of the cement matrix (Figure 1.1 and Figure 1.2).

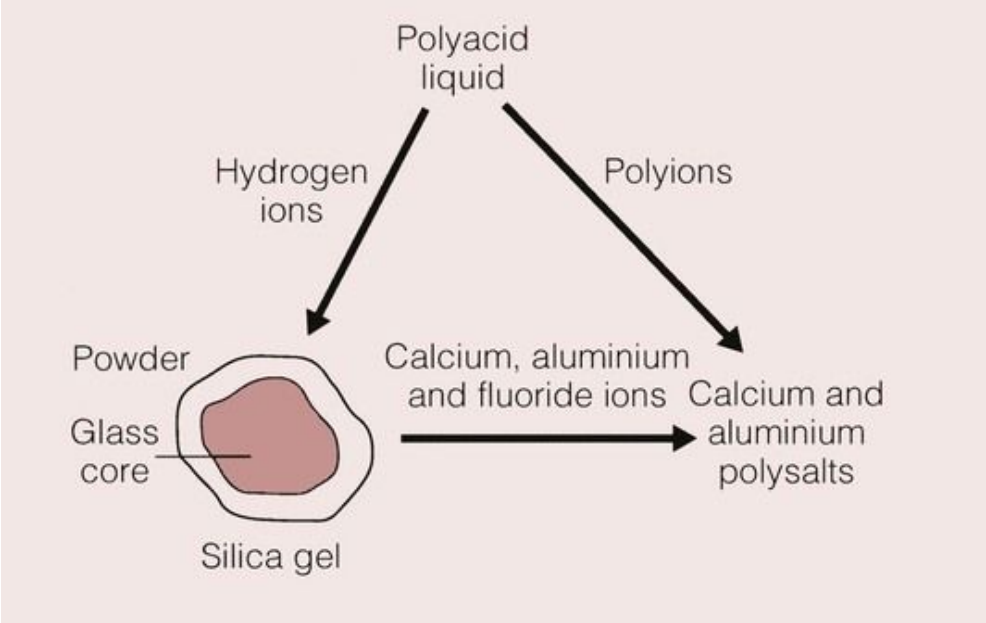

Figure 1.1: The initial stages of the glass ionomer setting reaction (https://pocketdentistry.com/2-3-glass-ionomer-cements-and-resin-modified-glass-ionomer-cements/n.d.).

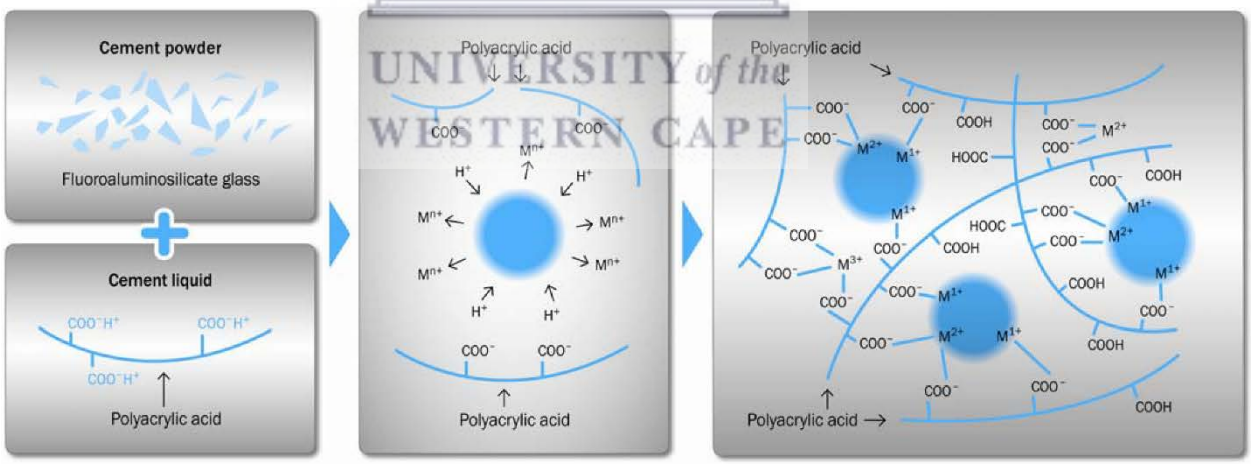

Figure 1.2: Setting reaction of conventional glass ionomer cement (Lohbauer, 2010).

Over a period of almost a decade, it was shown that there are two distinct phases in the setting reaction called dissolution and gelation (Prosser, Richards and Wilson, 1982;

Crisp and Wilson, 1976; Wilson, Crisp and Ferner, 1976; Crisp *et al.*, 1974; Crisp and Wilson, 1974).

1.2.4.1 The Dissolution Phase

The surface layer of the glass particles is attacked by the polyacid, which results in a limited amount of degradation of the glass with the release of calcium, aluminium and fluoride ions (Walls, 1986). The concentration of the calcium ion content rises much more rapidly than the aluminium ion concentration (Walls, 1986). During the early stages of the setting reaction, the polyacid spatial arrangement is altered (Walls, 1986). At the offset, the intermolecular forces cause the polymer chain to be coiled into a tight ball (Walls, 1986). As the ionisation process progresses, the molecule becomes more polar in nature and the polar forces developed during this stage result in the molecule adopting a more linear format, which in turn allows for better access to the carboxylic acid groups by the metallic ions, which then result in gelation and an increased setting rate (Walls, 1986).

1.2.4.2 The Gelation Phase

The moment calcium and aluminium ions are dissolved in the cement sol, the setting reaction starts (Wilson *et al.*, 1976). The initial chemical set occurs as a result of cross-linking with the more mobile and readily available calcium ions (Wilson *et al.*, 1976). Over the next 24 hours, a maturation phase occurs during which the less mobile trivalent aluminium ions become bound within the cement matrix resulting in more rigid cross-

linking between the polyalkenoic acid chains (Walls, 1986). The rate of the gelation reaction is influenced by four factors:

a. Temperature

The rate of gelation is influenced by the temperature of the reacting substances and the environment (Mount and Mackinson, 1978). In 1978, Mount and Mackinson found that, without affecting the physical properties of the materials, working time is increased when the mixing slab and powder for a glass polyalkenoate cement were cooled (Mount and Mackinson, 1978).

b. Physical presentation of the powder

The rate of gelation is influenced by the powder: liquid ratio and the surface area of the powder (Crisp *et al*., 1979). It was found that working and setting times were shorter and physical properties were improved for cements with finer glass powder (Crisp *et al*., 1979).

c. Availability of free fluoride ions

The large fluorite inclusions that are found in low fusion temperature glasses are readily attacked by the polyacid, resulting in the rapid release of large quantities of fluoride ions (Walls, 1986). This in turn results in metal cations binding to the polyanion chain (Walls, 1986). A release of hydrogen ions with a resulting maintenance of the low pH and a release of fluoride from the glass results in complexes being formed with aluminium ions (Walls, 1986).

d. The presence of tartaric acid

In 1976, Wilson *et al.* found that tartaric acid accelerated the setting reaction and that only the optically active isomers of tartaric acid were capable of eliciting this reaction. They also demonstrated that tartaric acid is incapable of forming a stable cement on its own, but the addition of tartaric acid is thus used to increase the rate of setting without affecting the working time (Wilson *et al*., 1976).

1.2.5 Structure of the Cement

The set cement is a composite structure consisting of particles of unreacted glass surrounded by a siliceous hydrogel (Walls, 1986). This is a residue of the glass particles formed after acid-mediated ion-leaching, which contains few aluminium ions and some residual fluorite droplets (Walls, 1986). These core particles are embedded in a matrix of cross-linked polyalkenoic molecules which are rich in calcium and a higher aluminium ion content (Brune and Smith, 1982; Barry, Clinton and Wilson, 1979). Some areas of the siliceous hydrogel without a glassy core are detectable in the matrix and represent small glass particles which have been degraded by the polyacid (Brune and Smith, 1982; Barry, Clinton and Wilson, 1979).

1.2.6 Water Content

By the end of the setting reaction, both the matrix and the siliceous hydrogel are hydrated, resulting in the cement being susceptible to desiccation if it is not protected by an appropriate surface coating (Walls, 1986). The chalky appearance on the surface layer of

a glass polyalkenoate after drying it is as a result of the desiccation (Walls, 1986). The degree of and the susceptibility to desiccation decreases with the maturation of the restoration *in situ* (Saito, 1978). Early contamination of the surface with water disrupts the surface structure with a change in the perceived colour and an increase in the surface roughness (Phillips and Bishop, 1985; Saito, 1978). These materials are less aesthetic than resin composites and are susceptible to water loss and uptake in the first few hours after placement which results in dissolution, and this may compromise finishing and polishing (Chinelatti *et al*., 2004).

In an attempt to improve the qualities of conventional glass ionomer cements, water soluble polymers or monomer systems which were capable of ambient polymerisation were added, forming a hybrid (Bagheri, Burrow and Tyas, 2005; Kleverlaan, Van Duinen and Feilzer, 2004; Smith, 1998). With these actions properties such as toughness, resistance to dehydration and the setting process were improved (Bagheri, Burrow and Tyas, 2005; Kleverlaan, Van Duinen and Feilzer, 2004; Smith, 1998). Still other disadvantages of conventional glass ionomers such as low wear resistance, strength and brittleness were modified (Bagheri, Burrow and Tyas, 2005; Kleverlaan, Van Duinen and Feilzer, 2004; Smith, 1998). These products are considered to be dual cure cements if only one polymerisation technique is used. However, if both mechanisms are used, the materials are considered to be tri-cure cements (Upadhya and Kishore, 2005). This was the introduction of resin-modified glass ionomers.

1.2.7 Resin-Modified Glass Ionomer

Resin-modified glass ionomers combine all the advantages of glass ionomer cements with those of resin-based composites such as:

- ability to bond to enamel and dentine,
- biocompatibility,
- ability to take up and release fluoride,
- minimal shrinkage during setting,
- a coefficient of thermal expansion similar to that of the tooth structure,
- cariostatic ability of glass ionomer,
- faster setting,
- improved wear resistance and
- good strength of resin-based composites, (Upadhya and Kishore, 2005; Chinelatti *et al.*, 2004; Kleverlaan, Van Duinen and Feilzer, 2004; Nicholson, 1998).

The rapid setting of resin-modified glass ionomers is possible due to the incorporation of a photopolymerisable monomer, *viz.* hydroxyethyl methacrylate (HEMA) and appropriate photo-initiators which allow the resin-modified glass ionomer cement to be cured by exposure to blue light during a second curing process (Upadhya and Kishore, 2005; Chinelatti *et al.*, 2004; Kleverlaan, Van Duinen and Feilzer, 2004; Nicholson, 1998).

The interaction of a glass ionomer with the dental tissue is a chemical interaction between the material and the tooth tissue (Cardoso *et al*., 2010). If a conditioner is used, a second, micro-mechanical bonding action takes place (Cardoso *et al*., 2010). The micro-mechanical bond is achieved when organic glass ionomer components infiltrate the

partially demineralised dentine surface which results in the formation of a sub-micron hybrid layer (Cardoso *et al*., 2010). As mentioned before, glass ionomers have the physico-chemical capability of bonding to tooth structure, but in spite of improvements, still have shortcomings such as polishability and general aesthetics (Coutinho *et al*., 2009).

Mouthwashes with a high percentage of alcohol and emulsifiers, detergents and organic acids are also responsible for the degradation and softening of resin-based restorative materials (Soares *et al*., 2012). This results in the absorption of colourants and thus, internal discolouration of resin-based restorative materials (Soares *et al*., 2012). The resultant degradation leads to an increase in surface roughness which impacts on the aesthetics of these materials (Soares *et al*., 2012).

Similarly, diet plays a significant role in the degradation of resin-based restorative materials, especially the consumption of fizzy drinks with poor hygienic habits (Soares *et al.*, 2012; Bagheri, Burrow and Tyas, 2005). Furthermore, colourants in food and beverages such as tea and coffee, fizzy drinks and alcoholic beverages also cause staining and surface damage (Soares *et al.*, 2012; Bagheri, Burrow and Tyas, 2005).

Resin-based restorative materials need to be polished after polymerisation as rough, unpolished restorations increase the coefficient of friction and may result in an increased rate of wear (Ghinea *et al*., 2011). Unfinished restorations can also lead to increased plaque retention, which leads to gingival irritation, surface staining, patient discomfort and possible secondary caries (Ghinea *et al*., 2011). Once a resin-based restorative material has been polymerised, the resin matrix and filler particles have varying degrees

of hardness (Ghinea *et al*., 2011). This may cause variations in polishing efficiency, which in turn leads to differences in surface roughness (Ghinea *et al*., 2011). Generally, because of the difference in composition, various resin-based restorative materials display varying levels of surface roughness after polishing (Ghinea *et al*., 2011). Materials containing larger fillers tend to show more surface roughness than materials which have smaller fillers (Ghinea *et al.*, 2011; Endo *et al.*, 2010). Finishing and polishing of resin-based restorative materials is of importance in order to ensure a restoration displays high quality aesthetics and longevity (Ghinea *et al*., 2011). It also ensures that the restoration has improved mechanical properties and is less susceptible to plaque accumulation and extrinsic discolouration (Endo *et al*., 2010).

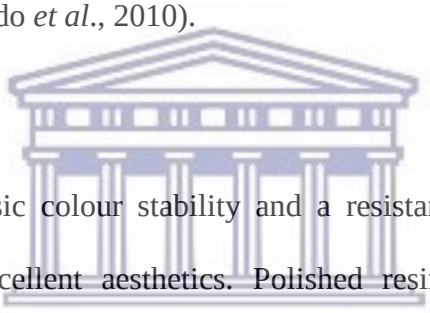

The maintenance of intrinsic colour stability and a resistance to surface staining is imperative in ensuring excellent aesthetics. Polished resin-based restorations with rougher and more irregular surfaces display a higher susceptibility to staining than those finished using a Mylar strip (Bagheri *et al*., 2005). Particle size and distribution have an influence on the optical properties of resin-based restorative materials (Bagheri *et al*., 2005). The colour depends on its surface spectral reflectance, which is a sensitive function of its roughness (Bagheri *et al*., 2005). As a result, the optical properties of a resin-based restorative material may be influenced by the surface changes which take place during finishing and polishing of a restoration (Ghinea *et al*., 2011).

In a further attempt to refine and improve the polishability of resin-based restorative materials, nano-sized filler particles have been incorporated into these materials (Endo *et al*., 2010). These include nanomers and nano-cluster filler particles (Endo *et al*., 2010).

These materials are purported to have reduced polymerisation shrinkage, enhanced mechanical characteristics and greatly improved aesthetics (Endo *et al*., 2010).

1.3 Nanotechnology

The term 'nanotechnology' was created by Professor Kerie E. Drexler, a lecturer, researcher, and writer in the field of nanotechnology (Jhaveri and Balaji, 2005). Nanotechnology is defined as the manipulation of matter at both an atomic and molecular level (Bhardwaj *et al*., 2014). Nanotechnology has applications in numerous industries, including dentistry (Khurshid *et al*., 2015; Bhardwaj *et al*., 2014). Nanotechnology has become one of the most sought after and researched technologies, and is one which will drastically alter the application of materials in different fields (Khurshid *et al*., 2015).

The quality of dental biomaterials has already been significantly improved due to the emergence of nanotechnology (Khurshid *et al*., 2015). This technology is used to manufacture materials which have better properties or by improving the properties of existing materials (Khurshid *et al*., 2015). Within the field of dentistry itself, the applications are vast (Khurshid *et al*., 2015). Nanoparticles can be used in nano-composites, nano-adhesives, nano light curing glass ionomers, in bone replacement materials and in dentine renaturalisation (Khurshid *et al*., 2015; Bhardwaj *et al*., 2014; Jhaveri and Balaji, 2005).

A trend in current research is to be able to operate on a scale so small that it is possible to interact with intracellular components (Saunders, 2009). With respect to advances in dental restorative materials, nanofillers ranging in size from 0.1 to 100 nm have been

developed (Saunders, 2009). Incorporating nanofillers in resin materials has many advantages which include: an increased filler load, increased continuity between the tooth and the restorative material and an increased material strength and durability (Park *et al.*, 2010; Saunders, 2009).

There are various nanostructures which have varying applications in dental use. These include nanoparticles used in resin-based materials; nanorods which are similar to enamel rods, nanotubes which have been used in bone growth applications, nanospheres, nanofibers and dendrimers and dentritic copolymers (Saunders, 2009).

1.4 Materials and Filler Particles

The size of filler particles of the glass powder in a glass ionomer cement is a key factor in its clinical performance, i.e. the finer the particle size (the greater surface area of the powder particles) the quicker the setting reaction (Iqbal, 2012).

In an attempt to improve the mechanical properties of conventional glass ionomers without negatively impacting the handling or biological properties thereof, various modifications to the inorganic component of glass ionomers have been tried (Moshaverinia *et al*., 2011). These attempts include the addition of metals, fibres and nonreactive fillers (Moshaverinia *et al*., 2011).

According to Moshaverinia *et al*., in 1983 the first attempt to strengthen a conventional glass ionomer was reported by a researcher named Simmons by adding amalgam alloy powder. However, it has subsequently been found that adding fibres or metal powders to conventional glass ionomers reduces its abrasion resistance (Moshaverinia *et al*., 2011).

Surface hardness of resin-modified glass ionomers is reported to be higher than that of conventional glass ionomers and is comparable to the surface hardness of composites (Kanchanavasita *et al.*, 1998).

Kanchanavasita *et al*. suggested that an improvement in the surface hardness may result in an improvement of the wear resistance of this group of materials. These researchers also found that another group of researchers had found that the surface roughness of resin-modified glass ionomers and conventional glass ionomers were in the same range after abrasion.

These are but a couple of changes made to fillers and particle size in conventional glass ionomers and resin-modified glass ionomers in attempts to improve properties and performances of the materials.

1.4.1 GC Fuji II LC® CAPSULE

GC Fuji II LC® capsule has smaller glass particles than GC Fuji II® (which is self-cured). This allows for a greater density within the material and assures a smoother, glossier, more attractive finish. As a result of the greater density, the material is harder and therefore offers higher abrasion resistance than GC Fuji II®. As a result, the restoration retains a brilliant, longer discoloration-free surface finish (GC, 2008) (Figure 1.3).

Figure 1.3: Fuji II LC® CAPSULE (GC, Japan).

Directions for use:

Directions given are as per the manufacturer's instructions on the package insert inside the product (GC Fuji II LC® Capsule, 2008).

Powder / Liquid Ratio (g/g)	0.33 / 0.10
Mixing Time (sec.)	10″
Working Time (min., sec.)	3′15″
Light Curing Time (sec.)	20″
Depth of Cure (A2) (mm)	1.8

Capsule Activation and Mixing:

a) Before activation, shake the capsule or tap its side on a hard surface to loosen the powder.

b) To activate the capsule, push the plunger until it is flush with main body.

c) Immediately place the capsule into a metal GC Capsule Applier and click the lever once. The capsule is now activated.

   Note: The capsule should be activated just before mixing and used immediately.

d) Immediately remove the capsule and set it into a mixer (an amalgamator) and mix for 10 seconds at high speed (+/-4,000 RPM).

Restorative Technique:

a) Immediately remove the mixed capsule from the mixer and load it into the GC Capsule Applier.

b) Make two clicks to prime the capsule then syringe. The working time is 3 minute 15 seconds from start of mixing at 23°C (73.4°F). Higher temperature will shorten working time.

Note:

1) To adjust the direction of the nozzle, hold the applier with the capsule towards you and turn the capsule body.

2) To remove the used capsule, push the applier release button. Twist the capsule and pull upwards.

c) Remove surface moisture but DO NOT DESICCATE.

d) Extrude cement directly into preparation. Avoid air bubbles.

e) Form the contour and place a matrix if required.

f) Light-cure for 20 seconds using a suitable visible light curing device (470nm wavelength). Place light source as closely as possible to the cement surface.

Note:

For cavities deeper than 1.8 mm, use a layering technique.

Finishing:

Finish under water spray using superfine diamond bur, silicone point and polishing strips.

Note:

Apply a final coat of GC Fuji VARNISH (blow dry) or GC Fuji COAT LC (light cure for 10 sec.) or G-COAT PLUS (light cure for 20 sec.) (GC, 2013).

1.4.2 RIVA™ LIGHT CURE (SDI)

Riva™ Light Cure is a light-cured, resin-reinforced glass ionomer restorative cement which, as a glass ionomer has the capability of releasing fluoride and bonding chemically to the tooth structure and is also aesthetic (SDI) (Figure 1.4). Riva™ Light Cure contains ionglass™ fillers which is a radiopaque, high ion releasing, bioactive glass used in SDI's range of glass ionomer products (SDI). The powder: liquid ratio in the capsule is 0.42 g: 0.14 g. The capsule is activated by pushing the plunger until it is flush with the body of the capsule.

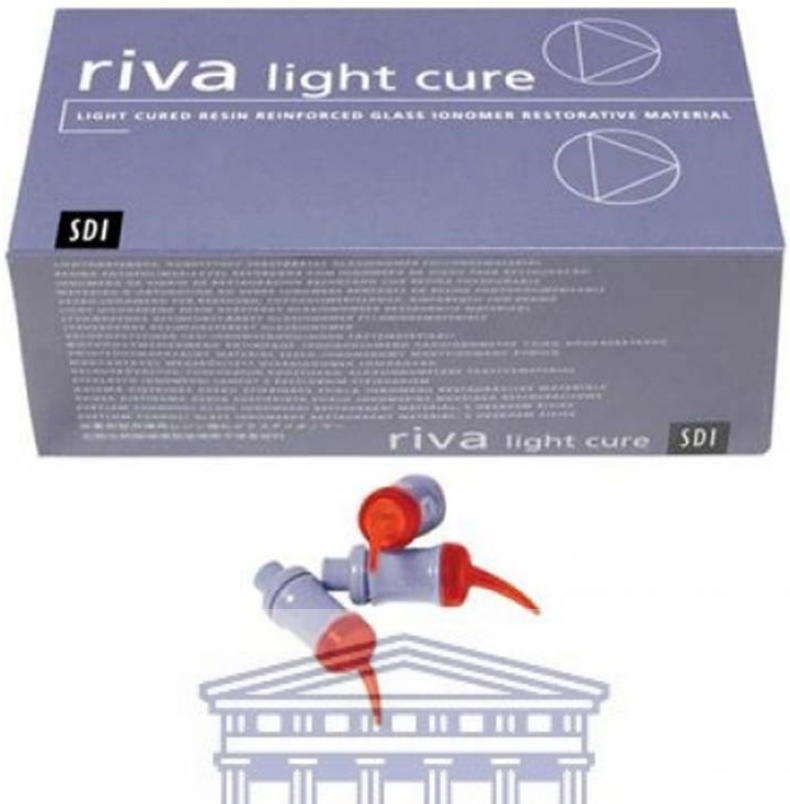

Figure 1.4: Riva™ Light Cure (SDI, Australia).

Directions for use:

Powder / Liquid Ratio (g/g)	0.42 / 0.14
Mixing Time (min., sec.)	10″
Working Time (min., sec.)	2′10″
Light Curing Time (sec.)	20″
Depth of Cure (A3) (mm)	1.8

1. Activate the capsule by pushing the plunger until it is flush with the body.

2. Immediately place the capsule into the Ultramat 2 amalgamator, or any other suitable mixer (4000-4800rpm), and triturate for 10 seconds.
3. Immediately remove the capsule and place into the Riva applicator.
4. Click the trigger of the Riva applicator until glass ionomer paste is seen through the clear nozzle.
5. Fill Riva Light Cure into the cavity, being careful not to trap air under the restoration.

   Note: At 23ºC/74ºF working time will be about 130 seconds (2'10'') from the start of mixing. In situations above this temperature, working times will shorten. Adhesion strength will decrease if material is manipulated after this time. Use a layering technique for cavities deeper than 2 mm.
6. Light cure for 20 seconds using the SDI Radii LED Curing Light or any other visible light-curing device (470 nm wavelength). Place light source as closely as possible to the cement surface.
7. Finish the restoration using standard techniques. Finishing may be commenced immediately after light curing.

8. Instruct patient not to eat for at least one hour after procedure (SDI, 2016).

1.4.3 Ketac™ N100 (3M ESPE)

Ketac™ N100 is a resin-modified glass ionomer which is available as a paste-paste system. 3M™ ESPE™ Ketac™ N100 Light-Curing Glass Ionomer Restorative uses the

science established with Vitrebond™ resin-modified glass ionomer, Vitremer™ Core Buildup Restorative as well as the nanofiller technology which was specifically developed for Filtek™ Supreme Plus Restorative (3M ESPE, 2007a) (Figure 1.5).

Figure 1.5: Ketac™ N100 (3M ESPE, USA).

The chemistry includes the components needed for a glass ionomer reaction; *i.e.* fluoroaluminosilicate glass, polyalkenoic acid, and water. The methacrylate component is fulfilled by the inclusion of hydrophilic and hydrophobic methacrylates and a light cure initiating system. Ketac™ N100 is also based on the polyalkenoic acid copolymer initially developed for Vitrebond™ light-cure ionomer liner base. The filler load is approximately 69% by weight (3M ESPE, 2007a; 3M ESPE, 2007b).

Directions for use:

Dispensing Clicker Dispenser:

Note:

Dispense and mix Ketac™ N100 restorative immediately prior to use to avoid water evaporation and drying out of the pastes. This product was designed to be dispensed and mixed with equal volumes of each paste. In the unlikely event the dispensed pastes appear to be of uneven volume, the dose should be discarded.

a. Remove cap from the Clicker dispenser by holding down the cap lever and sliding the cap off of the dispenser.
b. Dispense a small amount of material onto a mix pad to ensure even dispensing of both pastes. Discard this material.
c. Fully depress clicker lever to dispense Ketac™ N100 restorative onto a mix pad. Allow paste to fully extrude for 2-3 seconds, then release lever. Repeat dispensing process for additional material, most restorations will require approximately 2 clicks. The paste is automatically dispensed in equal volumes. The actual weight ratio dispensed is (1.3/1.0).
d. Wipe the dispenser tips clean with gauze to prevent cross contamination of the two pastes.
e. Replace cap by sliding onto dispenser until securely latched and an audible "click" is heard.

Mixing:

a. Using a plastic or metal cement spatula, mix the pastes together for 20 seconds until a uniform color is achieved. Avoid the incorporation of air bubbles.
b. Place material into preparation using conventional dental instruments, or back load a delivery tip by pressing it down over the mixed nano-ionomer, insert piston flush with the back of the tip and place tip into a 3M ESPE capsule dispenser or similar device.

Placement:

In a semi-dry to dry field incrementally syringe or place material in a depth of 2 mm or less. Wetting dental instruments used for shaping and contouring with Ketac™ N100 Primer can prevent nano-ionomer restorative from adhering to them. Working time is 3 minutes from start of mix at a room temperature of 23°C (73°F).

Curing:

Ketac™ N100 restorative will cure only by exposure to visible light. The maximum depth of material for light curing should not exceed 2 mm. Light cure the Ketac™ N100 restorative by exposing its entire surface area to a 3M ESPE visible light curing unit or other dental light curing unit of comparable intensity.

Finishing:

Immediately after curing, the Ketac™ N100 restoration can be contoured and polished using conventional finishing and polishing instruments, i.e. Sof-Lex™, under moist conditions (3M ESPE, 2007c).

1.4.4 Vitremer™ (3M ESPE)

The Vitremer™ Tri-Cure Glass Ionomer System overcomes the disadvantages of light cured glass ionomers while maintaining all their advantages as it has a third mode of cure (3M ESPE, 2012b) (Figure 1.6). This third mode is a dark cure of the methacrylate groups of the polymer system and HEMA. This reaction is initiated by water-activated redox catalysts which allow the methacrylate cure to proceed in the dark. This results in strong physical properties in areas where light access during curing is difficult.

Figure 1.6: Vitremer™ (3M ESPE, USA).

This dark methacrylate cure is a feature which is unique and exclusive to 3M tri-cure-based materials and ensures a uniform cure throughout the glass ionomer restorations which then results in improved physical properties (3M ESPE, 2012b). Thus, the cure process for the Vitremer™ Tri-Cure Glass Ionomer System is as follows:

1. An acid-base glass ionomer reaction which is initiated as soon as the powder and liquid are mixed and proceeds in the dark.

2. A photo-initiated free radical methacrylate cure which is initiated once the mixed material is exposed to light and only occurs in areas where the light is able to penetrate.

3. A dark cure free radical methacrylate cure which is initiated when the powder and liquid have been mixed and can proceed in the dark (Figure 1.7).

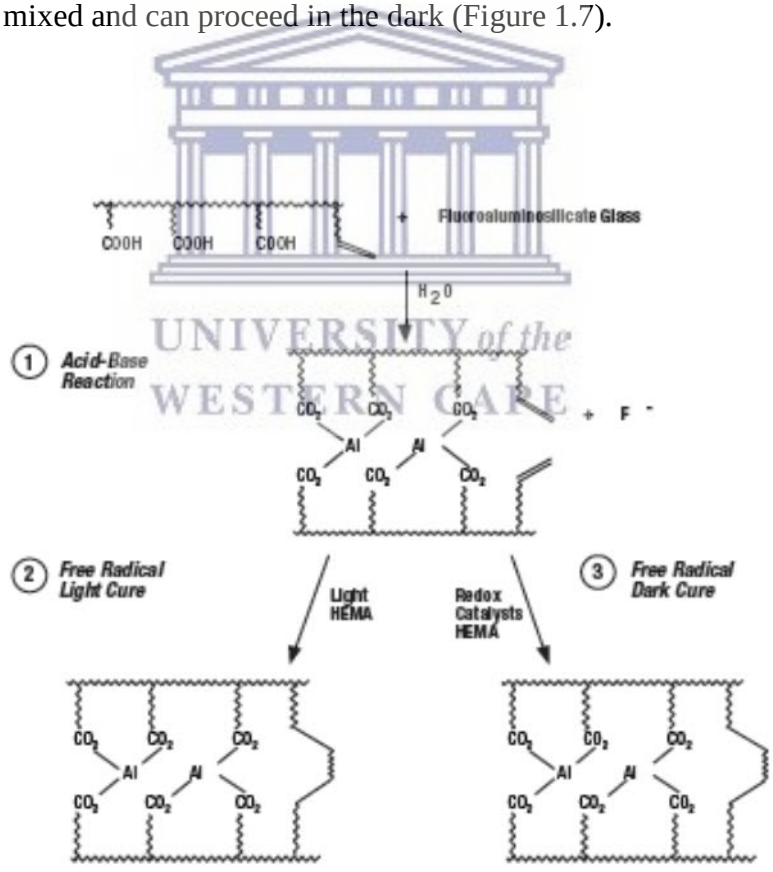

Figure 1.7: Setting reactions of Vitremer™ Tri-Cure Glass Ionomer (3M ESPE, 2012b).

Directions for use:

Dispensing powder and liquid:

The Vitremer powder jars contain protective seals. Remove seal completely before use. Unscrew cap, peel off seal and discard. Replace cap. The standard powder/liquid ratio of 2.5/1 by weight can be obtained with an equal number of level powder scoops and liquid drops. Additional powder may be incorporated to obtain a thicker consistency mix. Two scoops of powder and 2 drops of liquid will provide an adequate amount of material for most aesthetic restorations. Four scoops of powder and 4 drops of liquid will provide an adequate amount of material for most core build-ups.

Using a separate mix for each restoration to be placed is recommended. Shake the jar to fluff the powder before dispensing. Insert the scoop into the jar, overfill it with loosely packed powder and withdraw it against the plastic leveller to remove excess powder and obtain a level scoop. Dispense the desired number of powder scoops onto the mixing pad. To best obtain a proper liquid drop size, hold the Vitremer liquid vial vertically with the dropper tip down and without the tip contacting the mixing pad. Squeeze the vial to dispense the desired number of liquid drops onto the mixing pad.

Mixing:

Using a cement spatula, mix the powder into the liquid. All of the powder should be incorporated into the liquid within 45 seconds. Working time of the standard powder/liquid ratio is 3 minutes from the start of mix at a room temperature. Higher temperatures will shorten working time. Lower temperatures will lengthen working time. Back load a delivery tip by pressing it over the mixed glass ionomer, insert piston flush with the back of the tip and place tip into a 3M ESPE dispenser.

Curing:

Light cure the glass ionomer by exposing its entire surface area to 40 seconds of visible light from a 3M ESPE curing unit or other dental visible light curing unit of comparable intensity. The maximum depth of material for light curing should not exceed 2 mm. For core build-ups where a metal matrix band has been placed, light cure the glass ionomer from the occlusal for 40 seconds.

Self cure set time is 4 minutes from the start of mix at oral cavity.

Finishing:

Immediately after curing, the glass ionomer restoration can be contoured using conventional rotary instruments under water spray. The Sof-Lex™ disc system, manufactured by 3M ESPE, used wet and Sof-Lex strips, manufactured for 3M ESPE, are recommended for polishing. Immediately after curing, the glass ionomer core build-up can be prepared using conventional rotary instruments with water spray.

Finishing Gloss application:

To maximize aesthetics, apply the Vitremer finishing gloss to the polished restoration. Rinse and gently dry the restoration. Dispense a drop of the finishing gloss into a clean well or onto a clean mixing pad. Using a brush, apply a coating of the finishing gloss over the glass ionomer restoration and light cure for 20 seconds with a 3M curing unit.

For core build-ups, application of the finishing gloss is not necessary (3M ESPE, 2012b; 3M ESPE, 2012a).

1.4.5 ChemFil™ Rock (Dentsply)

ChemFil™ Rock contains novel reactive zinc-modified fluoroaluminosilicate glass fillers. This reactive zinc glass filler offers a unique ion release pattern leading to high strength of the material due to the immediate release of zinc ions during the setting reaction (Dentsply, 2011) (Figure 1.8).

Figure 1.8: ChemFil™ Rock (Dentsply, USA).

The released zinc ions form zinc-polyacid complexes which are stronger than complexes of strontium or calcium ions resulting in an accelerated build-up of flexural strength (Dentsply, 2011). The strength of zinc ion complexes is comparable to those of aluminium ions (Dentsply, 2011) . Aluminium ions are released from the zinc-fluoroaluminosilicate glass filler (Dentsply, 2011). According to the manufacturer, the final strength of ChemFil™ Rock is superior to glass ionomer restoratives that do not contain zinc (Dentsply, 2011). Similarly, there are other high viscocity conventional glass ionomer

cements such as Ketac Molar (3M ESPE), GC Fuji IX and GC Fuji Equia Forte, which all have equally superior properties such as higher compressive strengths and resistance to wear and erosion. However, these materials were not investigated.

The bimodal particle size distribution of the zinc glass filler has a mean particle size of about 3.5 μm and thus allows for a relatively high filler loading (~ 70 wt%, ~ 50 vol%) which contributes to the product's mechanical strength without compromising its handling properties (Dentsply, 2011).

Directions for use:

Time after activation

Mixing	15 seconds
Working time	1 minute 30 seconds
Waiting time before further manipulation/ finishing	6 minutes

Activation of the capsule:

Activate the capsule by pressing the capsule onto a stable surface and depressing the plunger to its limit (at this position the plunger will overlap by about 2 mm).

Mixing:

Immediately place the activated capsule in a capsule mixer (4000-4500 oscillations/ minute) and mix for 15 seconds

- or -

in a rotation mixer (e.g. RotoMix™) for 12 seconds of rotation and 3 seconds of centrifugation mixing.

Application of ChemFil™ Rock restorative:

1. Immediately remove the capsule from the capsule mixer and place into the Capsule Extruder 2. The capsule may be rotated 360° to gain the proper angle of entrance into the cavity. Do not apply excessive force.
2. Click the trigger of the Capsule Extruder 2 until glass ionomer paste is seen through the clear nozzle. Immediately start dispensing. Begin dispensing at the deepest part of the cavity, keeping tip close to cavity floor. Gradually withdraw tip as cavity is filled. Avoid lifting the tip out of dispensed material while dispensing to minimize air entrapment. At the completion of dispensing, wipe tip against cavity wall while withdrawing from the operative field.
3. Start packing, excess removal and contouring immediately after placement.
4. After application, press the release button of the Capsule Extruder 2 until the push rod releases. Slightly rotating the capsule, the empty capsule can easily be removed.

Working and setting time:

1. After activation the working time is 1 minute 30 seconds.
2. Wait at least 4 minutes 30 seconds after end of working time before further manipulation.

Finishing:

Start finishing no earlier than 4 minutes 30 seconds after end of working time (i.e. 6 minutes after activation) with cups, discs, and points (Enhance™ Finishing System) (Dentsply, 2011) .

The particles found in each of these glass ionomers are different, although they all contain fluoroaluminosilicate glass powder filler particles.

Recent advances in nanotechnology have led to the development of several nano-based products becoming available on the market. The progress in nanotechnology has yielded success in being able to produce nanofillers which range in size from 0.1 to 100 nm. The inclusion of nanofillers in resin-based materials result in an increased filler content which in turn results in fewer empty spaces within the resin matrix, improved material strength and durability. And as a result of nanofillers being much smaller than the wavelength of the incident blue light emitted from the light curing unit, nanofillers have a tendency to scatter or absorb less of the visible incident light which improves the translucency and aesthetics of nano-resins (Park *et al*., 2010).

In resin-based materials, the resin matrix and filler particles have varying levels of hardness which causes variations in polishing efficiency (Ghinea *et al*., 2011). It is this variation which leads to differences in surface roughness (Ghinea *et al*., 2011). Various resin-based restorative materials display varying levels of surface roughness after polishing purely as a result of the diversity in composition (Ghinea *et al*., 2011). Materials with larger fillers show more surface roughness than materials with smaller fillers (Ghinea *et al*., 2011). However, the smallest filler size does not guarantee the lowest

surface roughness and staining susceptibility (Berger *et al.*, 2011). Finishing and polishing of resin-based restorative materials should be done with the polishing agent recommended by the manufacturer.

1.5 Colour

The aim of specifying a shade in dentistry is the reproduction of the appearance of natural oral structures (Johnston, 2009). In Dentistry, the clinical measurement of colour is taken from an external curved surface without considering the layers beneath this surface (Johnston, 2009). The layers of teeth includes non-homogenous natural and prosthetic materials with varying colours and translucency, but as stated before, this is not measured separately but as a unit (Johnston, 2009). Munsell was the first to separate colour into the independent dimensions of hue, value and chroma and to systematically illustrate the colours in a three dimensional space (Johnston, 2009).

1.5.1 Munsell Colour Tree

Colours on the Munsell Tree are arranged according to their hue *i.e.* red, blue and green. The value of the colours are arranged on a vertical achromatic value axis with the darker colours at the bottom and the lighter colours on the top; whereas the chroma of the colours moves away from the vertical achromatic value axis as the saturation intensifies (Figure 1.9) (Chu *et al.*, 2004).

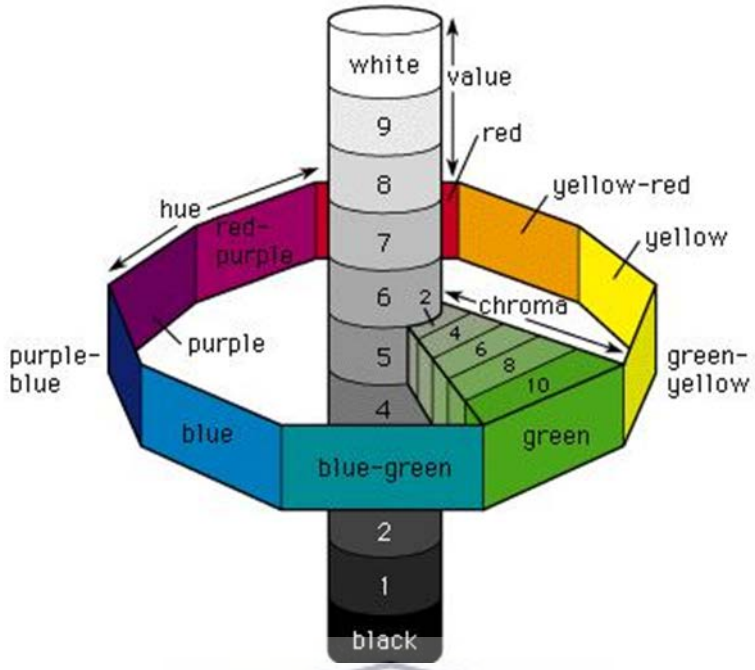

Figure 1.9: The Munsell Colour Tree (© 1994 Encyclopedia Britannica, Inc. http://www.conceptart.org/forums/showthread.php/325636-Why-isn-t-the-color-space-solid-a-cylinder).

This colour system is strictly based on the measurement of a human subject's visual response to colour and is therefore based on perception (Landa and Fairchild, 2005). This system is of extreme value in the field of dentistry where visual colour matching is regularly at the clinical chairside (Khashayar, 2013; Judd, 1968).

1.5.2 International Commission of Illumination (CIE) L*a*b* Colour System

The CIE L*a*b* colour system is a three dimensional colour model which describes colours that are visible to the human eye (Figure 1.10) (Commission Internationale de l'Eclairage (CIE), 1978) This colour system was established by the Commission

Internationale de l'Eclairage in 1976 (Minolta Co. Ltd., 1994; HunterLab, 1996; Commission Internationale de l'Eclairage (CIE), 1978).

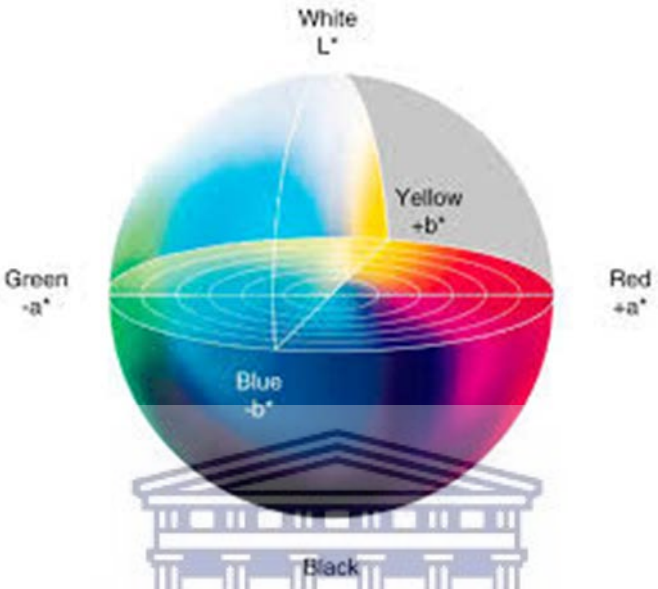

Figure 1.10: The CIELAB three dimensional colour space (HunterLab, 1996)

The intention behind the development of this colour scale was to provide a standard, almost uniform colour scale which could be used by everyone so that that the comparison of colour values was made easier (HunterLab, 1996).

Description of the colour system:

- Value or Lightness is represented by L* where minimum is 0 (black) and the maximum is 100 (white)
- Hue and Chroma are represented by a* and b* respectively (Burkinshaw, 2004).

Figure 1.10 a* and b* indicate the direction of colour:

- +a* is in the direction of red,
- -a* is in the direction of green,
- +b* is in the direction of yellow and
- –b* is in the direction of blue (Burkinshaw, 2004).

The centre of this model is achromatic and the a* and b* values increase in an outward direction from the centre. This means that as the a* and b* values increase, so too does the saturation.

In the L*a*b* colour space, colour difference is expressed as a single numerical value (ΔE_{ab}) which indicates the size of the difference in colour. The colour difference of an object between two measurements can be calculated using the colour components (L*, a* and b*). The colour difference between measurements is represented by ΔL*, Δa* and Δb*. Total colour change is calculated by using the following formula:

$$\Delta E^*_{ab} = [(\Delta L^*)^2 + (\Delta a^*)^2 + (\Delta b^*)^2]^{½}$$ (Minolta Co. Ltd., 1994)

The formula unfortunately, merely indicates the size of the colour difference and not the direction of movement (*i.e.* + or – signs). No indication is provided in which way the colours differ.

1.6 Spectrophotometry

Spectrophotometry is the science of using a computerised device called a spectrophotometer (Figure 1.11).

Figure 1.11: A spectrophotometer (Konica Minolta, Japan).

Spectrophotometers make use of multiple sensors (as many as 40) to measure the spectral reflectance of an object in each narrow wavelength range (Minolta Co. Ltd., 1994). The reflected light from the object under investigation is emitted by an intense gas-filled tungsten lamp which is integrated into the spectrophotometer unit (Minolta Co. Ltd., 1994). Spectrophotometers therefore do not rely on judgment of environmental conditions to evaluate a colour, but accomplish this by measuring the reflected emission of spectral colours (Horn *et al.*, 1998). In doing this, the surrounding light does not have an impact on the measurement being taken (Horn *et al*., 1998). Spectrophotometers have the ability to measure absolute colours and as result are considered highly accurate (Horn *et al*., 1998). This high accuracy rate makes it an ideal instrument for research studies and decreases the incidence of incorrect colour readings (Ishikawa-Nagai *et al*., 2005).

Studies by Horn *et al.* in 1998, Jarad *et al.* in 2005 and Kielbassa *et al.* in 2009, all show that colour assessment using a digital form of assessment compared to visual colour

assessment, was more reliable and predictable when a spectrophotometer was used (Jarad, Russell and Moss, 2005) (Kielbassa *et al*., 2009; (Jarad *et al*., 2005 Horn *et al*., 1998). Currently, computerised instrumentation for shade selection is available commercially. The aim in developing these instruments was to overcome inconsistencies and tooth colour mismatching as seen with visual tooth colour assessment methods (Kielbassa *et al*., 2009).

These developments are based on developments in industries such as paint, plastics, printing, ink and textile industries where spectrophotometry and computer calculations based on colour theory have utilised colour science in order to express colours numerically (Joiner, 2004).

1.7 Staining

Approximately a decade ago, the available aesthetic restorations had to be replaced relatively frequently since the staining or discolouration of these materials was common (Park *et al*., 2010). Discolouration or staining of any restorative material is an undesired effect, especially on resin-based restorative materials. Discolouration of resin-based aesthetic restorative materials, however, is an absolute eventuality as a result of the environment it has to survive in (Park *et al*., 2010).

The aetiology of discolouration is multifactorial *e.g.* dietary and smoking habits, patients' oral hygiene practices, exposure to pigment rich foods and moisture. Of the most common causes for discolouration are staining by food pigment and by beverages such as tea, coffee and red wine (Malhotra *et al*., 2011). Discolouration thus occurs as a result of both extrinsic and intrinsic factors (Soares *et al.*, 2012; Park *et al.*, 2010). Extrinsic staining is

usually due to surface roughness of a material or plaque on the restoration surface (Malhotra *et al*., 2011). Intrinsic staining is as a result of diffusion of the staining pigment into the material, followed by a chemical reaction with it (Malhotra *et al*., 2011). The propensity of a material to stain is related to the content and dimension of filler particles, the degree and depth of polymerisation, the curing time and efficacy of the curing unit used, adsorption and absorption of stains, the types of colourant and the interactions between resins and colouring agents (Malhotra *et al*., 2011; Topcu *et al*., 2009; Ayad, 2007; Abu-bakr *et al*., 2000).

If the polymerisation process of a resin-based restorative material is incomplete, unreacted monomers are left behind in the matrix, and these in turn can lead to discolouration by aging and reactions with other substances (Park *et al*., 2010). Other substances which make up resin-based restorative materials such as initiators, fillers and pigments also play a role in the stability of colour of the material (Park *et al*., 2010). The matrix of resin-based restorative materials is susceptible to the presence of organic acids which leads to the softening of the material. Park *et al*. (2010) rationalised that since polymerisation is achieved by light or heat, discolouration can occur as a result of exposure to these stimuli. Acidic erosion is an important factor clinically since acidic conditions occur within the oral environment due to either ingestion of acidic foods or as a result of the degradation of polysaccharides into acid in stagnant areas of the mouth (Soares *et al*., 2012; Park *et al*., 2010). Softening of the resin-based restorative material interferes with the lifespan of the material by increasing the chemical degradation which in turn decreases the physical properties (Soares *et al*., 2012).

Foods contain a host of colouring agents which can cause changes in the colour of resin-based restorative materials by absorbing the pigment over a long period of time (Park *et*

al., 2010). In addition to these factors, surface roughness also plays a role. Park *et al.* (2010) suggested that a roughened surface has different dimensions and thus have different contact rates with colouring agents. This will lead to discolouration of a resin-based restorative material.

Resin-modified glass ionomers were developed in an attempt to improve some of the mechanical properties of conventional glass ionomers (Khoroushi and Keshani, 2013). By adding hydroxyethyl methacrylate (HEMA), the flexural strength was improved and a different type was glass ionomer was developed (Khoroushi and Keshani, 2013). Most resin-modified glass ionomers are light cured, while still maintaining the acid-base set reaction which is found in conventional glass ionomers (Khoroushi and Keshani 2013; McCabe 1998). Resin-modified glass ionomers release similar quantities of fluoride when compared to fluoride released from conventional glass ionomers according to Khoroushi and Keshani (2013) and McCabe (1998).

According to Bagheri, Burrow and Tyas (2005), resin-modified glass ionomers have a higher susceptibility to surface colour change when exposed to pigment-rich food or drinks due to the presence of resin. These authors further concluded that as a result of the higher water content in conventional glass ionomers than in resin-modified glass ionomers, they absorbed less water than resin-modified glass ionomers, and thus stained less (Bagheri, Burrow and Tyas, 2005).

1.8 Scanning Electron Microscopy (SEM)

1.8.1 Description of the SEM

Scanning Electron Microscopes were first developed in the early 1950's. The Scanning Electron Microscope (SEM) (Figure 1.12) is a microscope which uses a focused beam of high energy electrons to form an image instead of light (*Purdue University Radiological & Environmental Management Division Of Environmental Health And Public Safety;* Swapp, 2017). The signals that are received from electron-sample interactions provide information about the sample texture, chemical composition, crystalline structure and orientation of materials which constitute the sample (Swapp, 2017). The uses of the SEM have expanded considerably since its development to include the medical and physical science fraternities and as a result, a much broader spectrum of samples are examinable with this technology (*Purdue University Radiological & Environmental Management Division Of Environmental Health And Public Safety).* The use of an SEM is more advantageous than that of a traditional light microscope. The SEM has a larger depth of field and as a result, allows for a larger area of a specimen to be in focus at a time. The SEM uses electromagnets instead of lenses and the operator has a much better control over the degree of magnification. As a result, the SEM has a much higher resolution (Swapp, 2017).

Figure 1.12: A typical SEM instrument, showing the electron column, sample chamber, EDS detector, electronics console, and visual display monitors.

In most cases, a specific area of a sample is selected in order to collect data. A two dimensional image is then generated which shows the spatial variations in the samples. Areas ranging from an approximately relatively large 1 cm to a very small 5 microns in width can be imaged in a scanning mode using conventional SEM techniques where magnification ranging from 20 X to approximately 30 000 X and a spatial resolution of 50 to 100 nm can be used. Using the SEM, it is also possible to analyse selected points on a sample. This is very useful when determining chemical compositions using energy-dispersive x-ray spectroscopy (EDS), crystalline structure and crystal orientations using electron backscatter diffraction (EBSD) (Swapp, 2017).

1.8.2 How the SEM Works

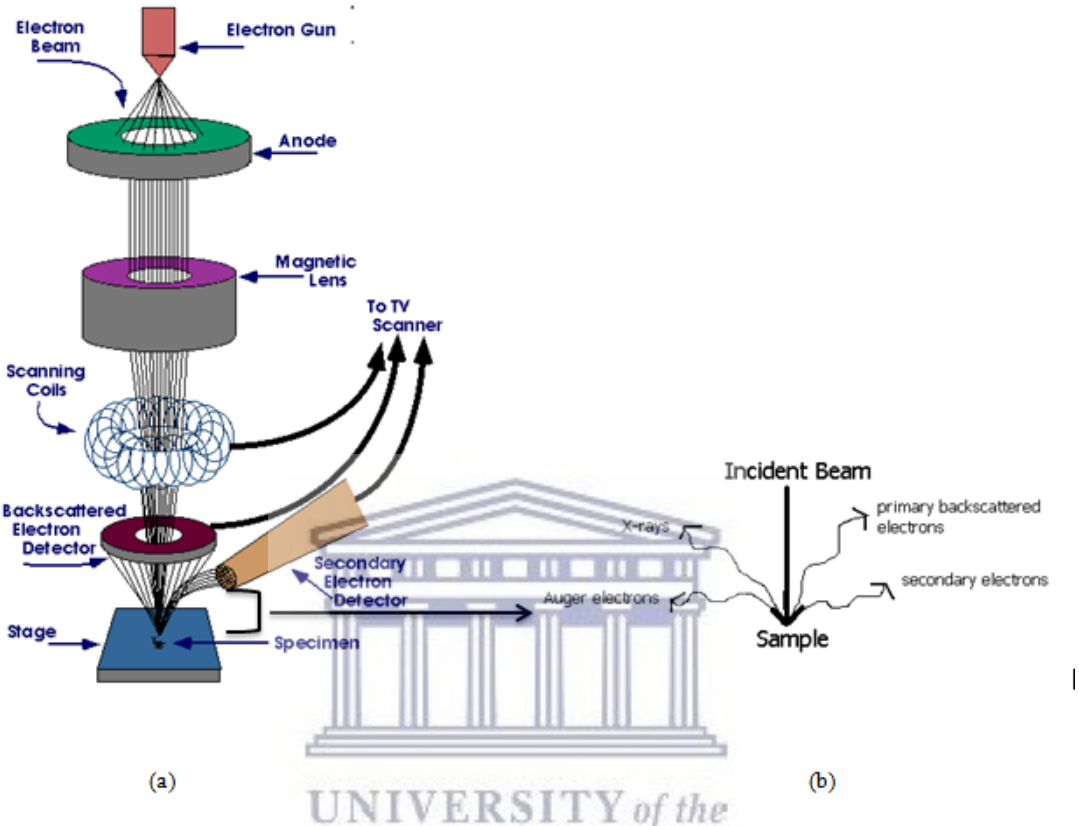

Figure 1.13: Diagrammatic representation of (a) the functioning of an SEM (*Purdue University Radiological & Environmental Management Division Of Environmental Health And Public Safety*) (b) Variety of signals produced during electron-sample interaction.

Accelerated electrons are produced at the top of the microscope by an electron gun. The electron beam then follows a vertical path in a vacuum, through the microscope. The beam passes through electromagnetic fields and lenses, which focus the beam down toward the sample. When the beam hits the sample, electrons and X-rays are ejected from the sample (Figure 1.13) (*Purdue University Radiological & Environmental Management Division Of Environmental Health And Public Safety*).

Detectors collect these X-rays, backscattered electrons, and secondary electrons and convert them into a signal that is sent to a screen similar to a television screen which then creates the final image (*Purdue University Radiological & Environmental Management Division Of Environmental Health And Public Safety*).

1.8.3 SEM Sample Preparation

Samples for the SEM have to be specially prepared. The SEM utilises vacuum conditions and uses electrons to form an image. All water has to be removed from samples as water vaporises in the vacuum. All metals require no preparation as they are conductive. All non-metals have to be made conductive by coating the sample with a thin layer of conductive material, often carbon, gold or some other metal or alloy. This is done in a device called a "sputter coater" (Swapp, 2017).

The sputter coater uses an electric field together with argon gas. The combination of the electric field and argon gas cause a single electron to be removed from the argon, making the atoms positively charged. The argon ions are then attracted to a negatively charged gold foil. The argon ion knocks out gold atoms from the surface of the gold foil. These gold atoms fall and settle on the surface of the sample, resulting in a thin gold coating (*Purdue University Radiological & Environmental Management Division Of Environmental Health And Public Safety*).

The material used for conductive coatings depends on the type of data that needs to be collected. If elemental analysis is required, then carbon is the most suited conductive coating. If, however, high resolution electron imaging applications are required, then

metal coatings are the most effective. An electrically insulating sample can be examined without a conductive coating. This then has got to be done in an instrument capable of “low vacuum” operation (Swapp, 2017).

Chapter 2
Aims and Objectives

2.1 Aim

The aim of this study was to determine the stainability of four resin-modified glass ionomers and one glass ionomer cement when exposed to a staining broth.

2.2 Objectives

1. To record any change in colour before and after exposing the samples of the four resin-modified glass ionomer cements and one glass ionomer cement to the staining broth using a spectrophotometer
2. To compare the stainability of the four resin-modified glass ionomer cements and one glass ionomer cement.
3. To examine the depth of staining of the four resin-modified glass ionomer cements and one glass ionomer cement using a light microscope and
4. To observe the particle size of the powder and the surface texture using Scanning Electron Microscopy of the four resin-modified glass ionomer cements and one glass ionomer cement.

2.3 Null Hypothesis

There is no difference in stainability amongst the four resin-modified glass ionomer cements and one glass ionomer cement when viewed using different media (Spectrophotometer, light microscope and SEM).

Chapter 3

Materials and Methods

The materials tested are a conventional glass ionomer, resin-modified glass ionomers and a nano-filled resin-modified glass ionomer which reflect the materials available and used clinically in the Restorative Department at the Dental Faculty of the University of the Western Cape at the time the study was conducted. These materials were also chosen to help decide which ones would not negatively impact on the aesthetics for patients, based on the evidence found in the literature and the outcomes of this study.

Five glass ionomer restorative materials were used in this study, four resin-modified and one conventional zinc-reinforced cement were used. Of the four true resin-modified glass ionomers, one is a nano-filled ionomer (Table 3.1).

Table 3.1: Glass Ionomers used to make sample discs.

MATERIAL	MANUFACTURER	MATERIAL TYPE
Fuji II LC® Capsule	GC	Resin-modified glass ionomer
Riva™ Light Cure	SDI	Resin-modified glass ionomer
Ketac™ N100	3M ESPE	Resin-modified glass ionomer (Nano-filled)
Vitremer™	3M ESPE	Resin-modified glass ionomer
ChemFil™ Rock	Dentsply	Zinc-reinforced glass ionomer

3.1 Sample Disc Preparation

A total of 75 discs, each with a 15 mm diameter and 2 mm in thickness were prepared. Fifteen disc-shaped samples were made from each material by filling a Perspex cast (Figure 3.1) and pressing it between a transparent plastic sheet and a glass slab to ensure extrusion of any excess material. Shade A2 was used for all materials (besides 3M ESPE's Vitremer™ where B2 was used as the closest shade as Vitremer™ is not available in Shade A2) in order to standardise the experiment. Each material had its own Perspex cast.

Figure 3.1: Perspex cast used to make sample discs of each material.

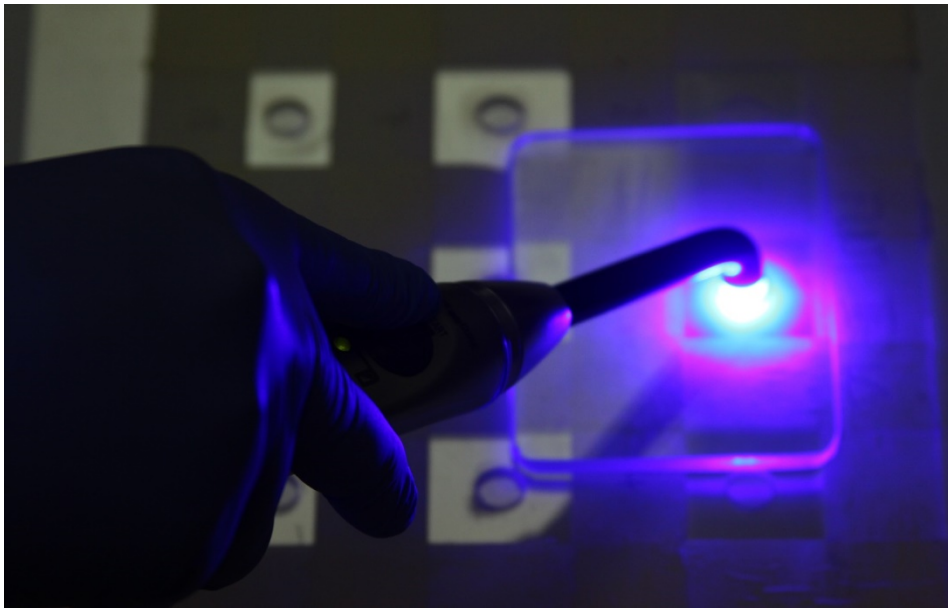

Figure 3.2: The curing of a sample disc whilst being compressed between a plastic cellophane sheet and a glass slab to ensure extrusion of any excess.

The selected materials were all light-cured using an Elipar™ DeepCure-S LED curing light (3M ESPE, USA) (Figure 3.2 and Figure 3.3) according to the manufacturers' instructions for each material except for ChemFil™ Rock which autopolymerises. The materials were all manipulated and polymerised according to each manufacturer's instructions (Table 3.2).

The light source was checked for light output using a CureRite Light Meter (Dentsply, USA) and found to be operating at 1200 mW/cm^2. This was checked after every group of 15 samples.

Figure 3.3: The Elipar DeepCure-S LED (3M ESPE, USA).

Table 3.2: Handling times of selected glass ionomers.

Resin-Modified Glass Ionomer	Mixing Time	Working Time	Curing Time	Max increment size
Fuji II LC® CAPSULE	10 sec	3 min 15 sec	20 sec	1.8 mm
Riva™ Light Cure	10 sec	2 min 10 sec	20 sec	2 mm
Ketac™ N100	20 sec	3 min	20 sec	2 mm
Vitremer™	45 sec	3 min	40 sec	2 mm
ChemFil™ Rock	15 sec	1 min 30 sec	6 min	Bulk fill

Following curing, only one side of each sample disc was polished with Sof-Lex™ discs (3M ESPE, USA) (Figure 3.4). The discs were used from a coarser grit to a progressively finer grit - medium, fine and lastly superfine.

Figure 3.4: Sof-Lex™ (3M ESPE, USA) discs used from a coarser grit to a finer grit to polish restorations.

The Sof-Lex™ discs are coated with aluminium oxide of varying grit and the normal thickness Sof-Lex™ discs were used. The sample discs were rinsed briefly with distilled water using a squeeze bottle after they were polished. The opposite side of each sample disc (the unpolished side) was designated as "matrix finish". The polished surface of each sample disc was assessed visually to ensure a smooth polish. All the sample discs were assessed without being viewed under any magnification and appeared to show good polish without any scratches.

A baseline colour measurement was recorded immediately after curing using a spectrophotometer (CM-2600d, Konica Minolta, Japan) (Figure 3.5).

Figure 3.5: The CM-2600d spectrophotometer (Konica Minolta, Japan)

An orthodontic rubber band was placed around each sample disc. Floss was then tied to the rubber band on each sample disc for suspension in a broth during the staining process.

Figure 3.6: Suspension of a sample disc in a container without and with broth

All sample discs were then immersed in distilled water in a 40 ml specimen jar (Figure 3.6) and stored for one week at 37°C in an incubator (Memmert, Germany) to evaluate for any potential colour changes after baseline measurements (Bagheri *et al*., 2005). The sample discs, once removed, were first rinsed with distilled water and then dried using 1 ply regular folded hand towels (Kimberly-Clark Professional, Scott Brand®, Kimdri*, RSA). A second set of colour measurements were recorded again on either side of each sample disc using a spectrophotometer (Figure 3.5) (Bagheri *et al*., 2005). This was done to ascertain whether the immersion in distilled water had any effect on the colour of the sample discs. Each sample disc was then suspended in a new 40 ml specimen jar containing 25 ml of a staining broth prepared as described by the American Dental Association (American Dental Association, 2008) (Table 3.3) at 37°C in an incubator (Bagheri *et al*., 2005). The pH was measured and recorded as 5.4.

Table 3.3: Composition of Staining Broth.

Instant coffee	27g
Instant tea	27g
Gastric mucin dissolved into 9 L of sterilised trypticase soy broth	20g
FD&C Red 40	6ml
FD&C Yellow 5	6ml
24-hour Micrococcus luteus culture	325 ml
Red wine	750 ml

Readings were taken after a 2-hour, 4-hour, 8-hour, 24-hour and then after a 7 day immersion period in the staining broth. At the time of taking the readings, each sample disc was rinsed with distilled water for 10 seconds on each side using a squeeze bottle and then gently blotted dry with 1 ply regular folded hand towels (Kimberly-Clark Professional, Scott Brand®, Kimdri*, RSA).

3.2 Colour (Spectrophotometer) Analysis

Prior to each session of colour measurements, the spectrophotometer was calibrated as suggested by the manufacturer; it was first zero calibrated and then calibrated for a white background (Minolta Co. Ltd., 1994). The sample discs were placed in the spectrophotometer (Figure 3.5) and colour readings on each side of each sample disc were recorded in the L*, a* and b* scale. Each reading was repeated three times. The baseline colour measurement was recorded immediately after curing using the spectrophotometer, but one week later and after immersion in distilled water, the readings were the same. Subsequently, the sample discs were then immersed in a staining broth (Table 3.3) and colour changes recorded periodically as stated.

The spectrophotometer was set on the L*a*b* scale. Multiple factors were analysed in terms of the colour matching process using the CIELAB (Commission Internationale de l'Eclairage colour co-ordinates as described below:

1. $\Delta L^* = L^*_{after} - L^*_{before}$
   (L*: lightness) difference in lightness/darkness value + = lighter and - = darker

2. $\Delta a^* = a^*_{after} - a^*_{before}$
   (a*: green-red) difference on red/green axis + + redder and - = greener

3. $\Delta b^* = b^*_{after} - b^*_{before}$
   (b*: yellow-blue) difference on yellow/blue axis + = yellower and - = bluer

4. $\Delta E_{*(L^*a^*b^*)} = [(\Delta L^*)^2 + (\Delta a^*)^2 + (\Delta b^*)^2]^{½}$
   (total colour difference value)

The colour differences in the individual components *i.e.* ΔL*, Δa* and Δb* were calculated using the formulae stated above. The total colour difference ($\Delta E^*_{a^*b^*}$) for each group before (baseline) and after staining (7 days) were compared.

3.2.1 Surface Examination Following Staining

After the sample discs were manufactured, the surfaces, as per protocol, was polished and finished using a matrix. These were placed in distilled water for 7 days as explained previously, then removed, dried and placed in a staining broth for a further 7 days. After removal from the staining broth, each side of the sample discs was rinsed with distilled water using a squeeze bottle for approximately 10 seconds and then gently blotted dry with 1 ply regular folded hand towels (Kimberly-Clark Professional, Scott Brand®, Kimdri*, RSA). These were then visually assessed and examined under the light microscope (Stemi 508, Zeiss, Germany) at a magnification of 40X to establish if there was any breakdown of the sample. The extended period in the broth meant prolonged exposure to a low pH environment and the bacteria present. Under the light microscope, the effects of this environment, such as, porosities or defects on the surface which formed as a result of exposure to the broth, would be visible.

3.3 Visual Assessment of Depth Penetration Using A Light Microscope

The specimens were sectioned using a minitom diamond cut-off disc (Struers, Denmark) (Figure 3.7) in an attempt to determine the depth of the stain.

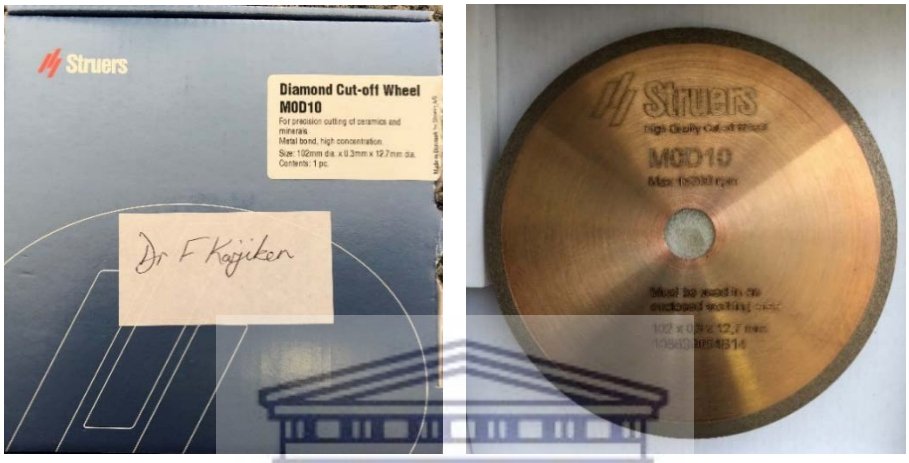

Figure 3.7: A minitom diamond cut-off disc (Struers, Denmark).

The cut discs were then visually inspected under a light microscope (Magnification 40X) by two investigators (Figure 3.8) to establish whether staining had penetrated beyond the surface of the disc.

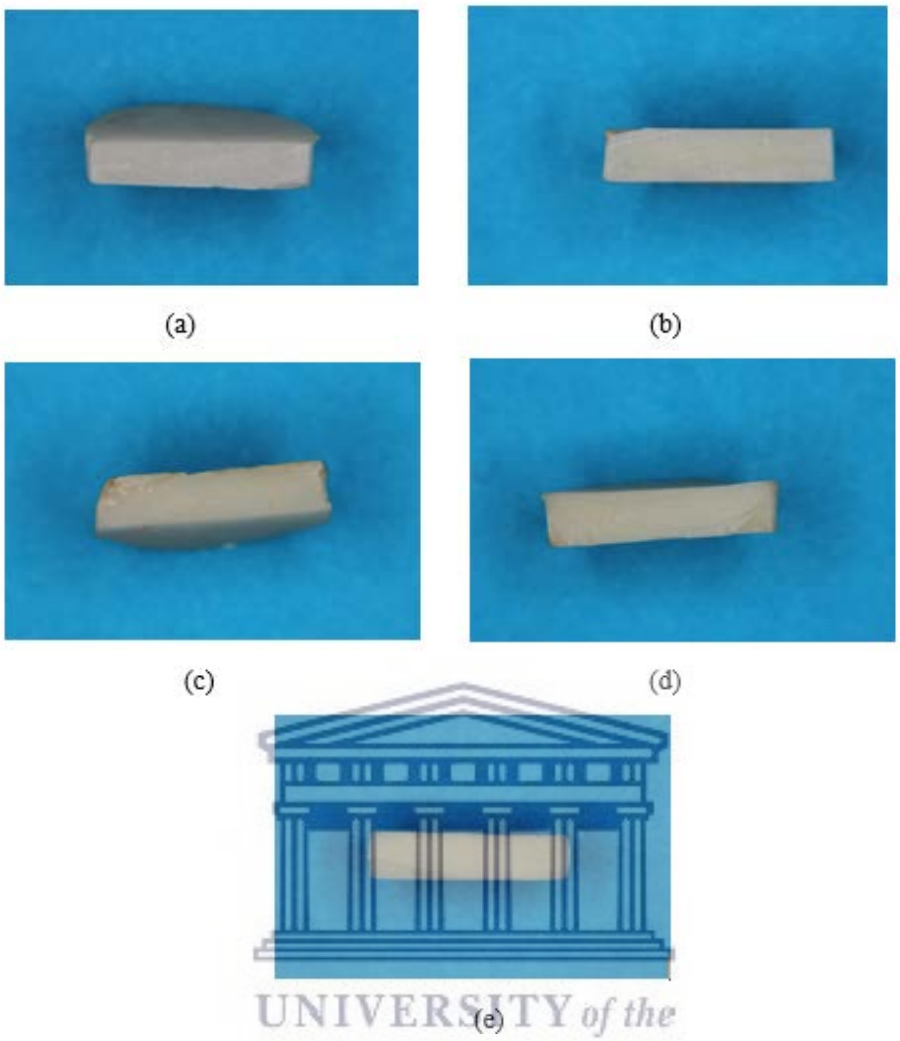

Figure 3.8: Visual inspection of cut sample discs after completion of the staining procedure to assess the penetration of staining within the respective materials.

(a) Fuji II LC® CAPSULE disc sectioned with the polished side at the top of the picture,

(b) Riva™ Light Cure disc sectioned with the polished side at the top of the picture,

(c) Ketac™ N100 disc sectioned with the polished side at the top of the picture,

(d) Vitremer™ disc sectioned with the polished side at the top of the picture,

(e) ChemFil™ Rock disc sectioned with the polished side at the top of the picture.

3.4 Scanning Electron Microscope Analysis

3.4.1 Analysis of Glass Ionomer Powder / Paste

A mass of 0.5g of powder of each of the selected materials (except for Ketac™ N100 which does not have a powder component) was measured on a scale (Ohaus TS400D Precision Standard Balance, USA). This was placed in 5.0 ml of acetone solvent (Merck, RSA) in an 8 ml test-tube and centrifuged (Heraeus-Christ GmbH, Germany) (Figure 3.9) for 2 minutes at 1000 revolutions per minute (rpm) to separate the solvent and matrix substance from the filler particles. The remaining material mass was removed from the test tube by tipping the contents into a clean test tube so that the mass was not handled and the acetone washing process was repeated two more times.

Subsequently, the remaining material mass, which had aggregated as a result of the dissolution in acetone, was then placed in 5.0 ml of chloroform (Merck, RSA) for further washing and separation of the filler particles. This extracted material mass together with the chloroform was then centrifuged again for 2 minutes at 1000 rpm. The remaining residual matrix substance and chloroform were discarded. Using fresh chloroform, the remaining aggregated material mass was put through the washing process two more times as previously done. The remaining filler particles were then suspended in 5.0 ml of absolute ethanol (Merck, RSA) to ensure their preservation. The ethanol solution with filler particles were then smeared onto a glass slab, where the ethanol was then allowed to evaporate leaving behind a dehydrated mass (Lang et al., 1992).

Figure 3.9: Heraeus-Christ GmbH Centrifuge (Germany).

Following onto the previous step, the dehydrated mass was scraped off the glass slab onto an aluminium stub which in turn is placed onto an aluminium base (Figure 3.10).

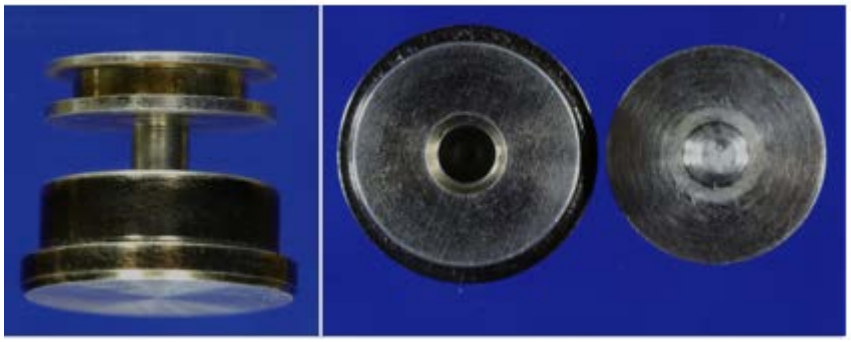

Figure 3.10: Aluminium stub with aluminium base - side view (L), top view (R).

The aluminium stub is a sample holder onto which samples are mounted. These aluminium stubs are prepared to receive the dehydrated samples by placing a carbon adhesive tab, which serves as a dual sided sticky tape, on it (Figure 3.11).

Figure 3.11: Dual-sided sticky tab

The stub with sample is then placed into the aluminium base where it is held upright so that it does not move around when placed in the sputter coater, where samples are coated with a conductive material. This entire sample is also later viewed in the SEM in this upright position. Each stub is numbered for each specific material (Figure 3.12) before the dehydrated samples are scraped onto the stub with the carbon tab on it (Figure 3.13)

Figure 3.12: Aluminium stubs are prepared and numbered according to the material used.

Figure 3.13: Specimens in the process of being attached to stubs.

Within the sputter coater, each prepared stub was then sputter coated with carbon and subsequently viewed under SEM. The process within the sputter coater can take one of two directions, coating the stub either with carbon or with gold. As stated above, the carbon route was chosen as the dehydrated samples were considered to be micro-samples. If the gold route was chosen, the SEM view of the micro-sample would display gold particles, which would not be seen with the carbon route. In addition, the gold route would include a number of artefacts when viewed with the SEM. If it was a macro-sample instead, either route (carbon or gold) would show similar pictures with SEM. This normally would happen if the gold route was chosen for a dehydrated sample instead.

In the sputter coater, a high current is passed through a pure carbon rod (Figure 3.14) which then sputters carbon onto the sample (Figure 3.15). The tip of the carbon rod is sharpened to approximately 4 mm and when the current passes through the rod, the sharpened tip evaporates and carbon is released onto the sample. This is done once a

vacuum has been created in the chamber of the Emitech K950X Turbo Evaporator Sputter Coater (United Kingdom) (Figure 3.16).

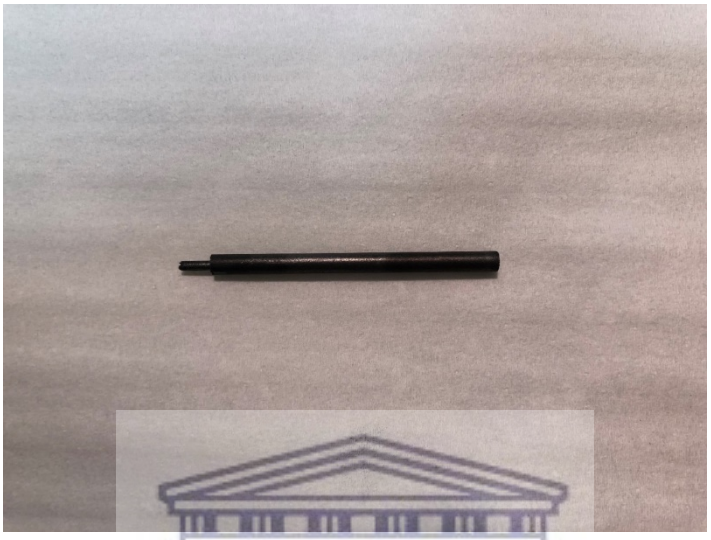

Figure 3.14: Carbon rod used to sputter coat samples on aluminium stubs.

Figure 3.15: Sputter coated samples.

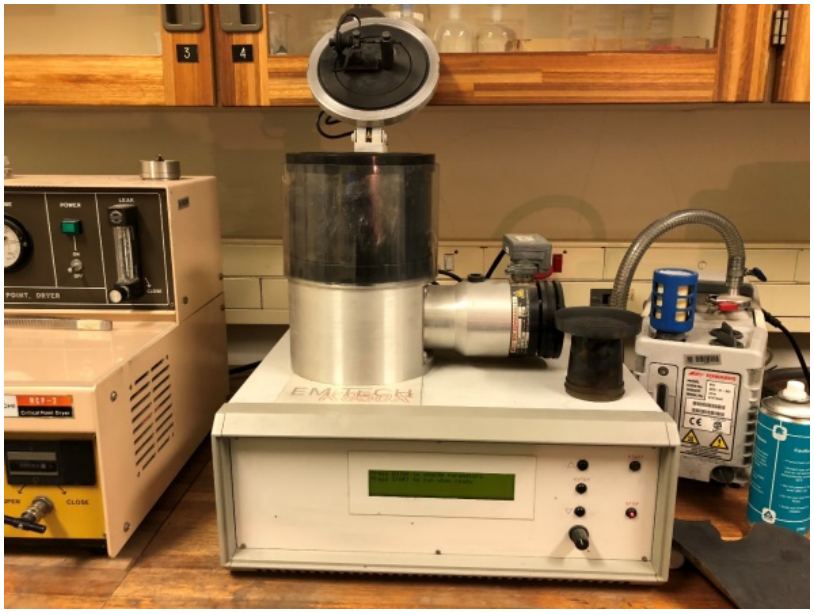

Figure 3.16: Emitech K950X Turbo Evaporator Sputter Coater (United Kingdom).

In the SEM, an electron gun is the source of electrons which are then transmitted down a lead column onto the particles on the stub at an atomic level. Electrons that are knocked out of the sample, are collected by a secondary electron detector which then creates the image seen on the computer screen, via the integrated software. The samples were viewed at various magnifications of 5000X, 50 000X, 100 000X and 150 000X. It was attempted to view the samples at these standard magnifications so that the best images with the least distortion could be reported.

3.4.2 Analysis of Surface Structure

In addition to the above processes, two new sample discs (macro-samples) of each of the selected materials were prepared in the same manner for examination under the SEM. One of each of these samples were cut with a minitom diamond cut-off disc (Struers,

Denmark) and mounted on an aluminium stub and secured using carbon adhesive tabs, the other samples were mounted whole onto the aluminium stub.

These samples were then placed in the Quorum Q150T ES High Resolution Sputter Coater (United Kingdom) (Figure 3.17 and Figure 3.18) and were sputter coated with gold in order to make them conductive for the electrons emitted by the SEM. Gold was chosen over carbon as these samples were macro-samples and gold particulates would not have an impact on the visualisation of the surface by the SEM.

Figure 3.17: Quorum Q150T ES High Resolution Sputter Coater (United Kingdom).

Figure 3.18: Samples in the Quorum Q150T ES High Resolution Sputter Coater (United Kingdom).

The chamber is filled with argon gas under high vacuum. The argon gas ionises with the gold target and releases gold particles on to the sample. The gold particles are deposited onto the samples by means of an ionisation process between the Argon gas and the gold target in the Sputter Coater (Figure 3.17). This is how the sputter process is conducted. The sputter process takes about 60 seconds (Figure 3.19). These samples were viewed at different magnifications as previously stipulated.

Figure 3.19: Samples sputter coated in gold.

Chapter 4

Data Analysis

After collecting data related to several testing methods such as:

1. Colour readings using spectrophotometry,
2. Visual assessment of the surfaces of the sample discs to determine if there was any breakdown of the surface,
3. Cutting of the sample discs and viewing it under a light microscope to see if staining penetrated beyond the surface,
4. Evaluating the glass ionomer filler particles with an SEM, and
5. Evaluating the surface structure of the sample discs with an SEM

The colour readings, which were taken at the indicated intervals, were transferred to an Excel spreadsheet (Microsoft Corporation 2010, USA) and then analysed using IBM SPSS ver21 statistics program (SPSS Inc., Chicago IL, USA).

For the analysis, tests included multiple comparisons between the groups which were analysed using the ANOVA. All non-parametric statistical analyses were performed at a 95% confidence interval (CI) with the level of probability set at alpha = 0.05.

The colour readings were taken at baseline and compared to readings at 2, 4, 8 and 24 hours and 7 days for statistical differences in the colour change. Colour changes were first recorded in the L* scale (lightness/brightness scale), a* scale (red-green chroma) and b* (yellow-blue chroma). Colour difference ($\Delta E^*_{a^*b^*}$) quantifies the colour difference

between the two objects.

Mean colour differences ($\Delta E^*_{a^*b^*}$) between the various time periods of the spectrophotometer readings were then analysed using the Commission Internationale de l'Eclairage (Commission Internationale de l'Eclairage (CIE), 1978) colour coordinates and described using the following calculations.

1. $\Delta L^* = L^*_2 - L^*_1$

   ΔL^*: lightness-brightness (difference in lightness/darkness value) where + = lighter and – = darker

2. $\Delta a^* = a^*_2 - a^*_1$

   Δa^*: green-red (difference on red/green axis) where + = redder and – = greener

3. $\Delta b^* = b^*_2 - b^*_1$

   Δb^*: yellow-blue (difference on yellow/blue axis) where + = yellower and – = bluer

Chapter 5

Results

5.1 Colour (Spectrophotometer) Analysis

The results for colour changes were completed for each individual material and discussed with regards to lightness / brightness, red-green chroma scale, yellow-blue chroma scale and colour difference.

5.1.1 Fuji II LC® CAPSULE Colour Changes

i. Lightness/Brightness (L* scale)

There was a progressive decrease in the lightness/brightness (L* scale) mean values taken from baseline, 4 hours, 8 hours, 24 hours and final reading at 7 days for both polished and unpolished surfaces after immersion in the staining broth (Figure 5.1). The lightness decreased from 83.60 to 77.61 for the unpolished surface and from 83.07 to 77.50 for the polished surface. There was a statistically significant difference between baseline and 7 days in immersion broth in the L* scale for both polished and unpolished surfaces (ANOVA, p=0.000).

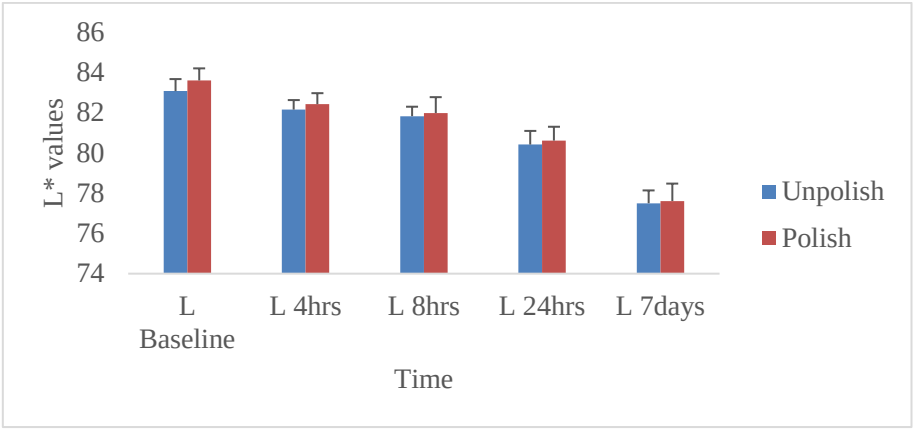

Figure 5.1: Fuji II LC®. Changes in L* scale over time polished versus unpolished surface with standard deviation.

ii. Red-Green Chroma Scale (a*scale)

In the a* scale, there was an increase in the red-green chroma scale mean values taken from baseline, 4 hours, 8 hours, 24 hours and final reading at 7 days for both polished and unpolished surfaces after immersion in the staining broth (Figure 5.2). The red/green colour change decreased from 5.70 to 4.11 for the unpolished surface and from 5.77 to 4.11 for the polished surface. There was a statistically significant difference between baseline and 7 days in immersion broth in the a* scale (ANOVA, p=0.000).

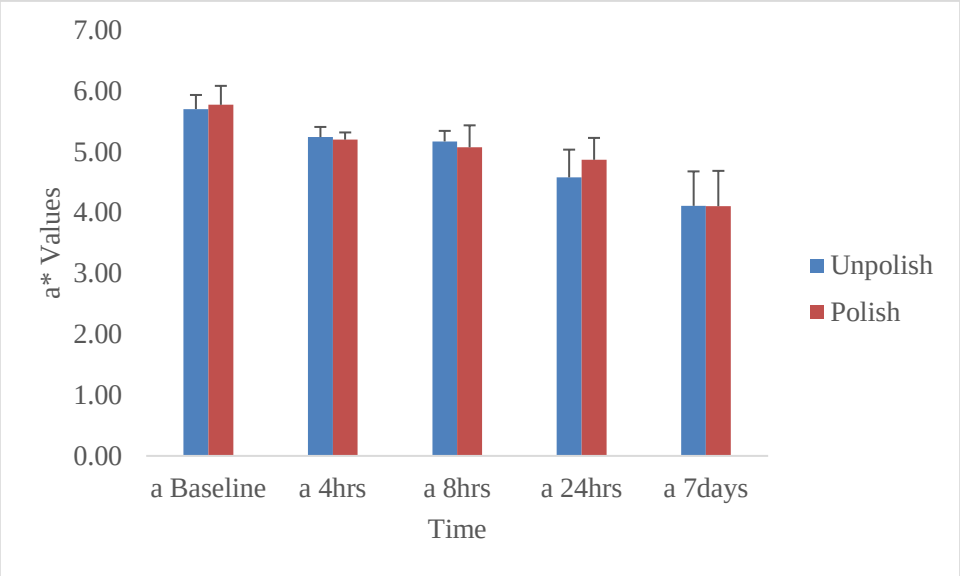

Figure 5.2: Fuji II LC®. Changes in a* scale over time for polished versus unpolished surface

iii. Yellow-Blue Chroma Scale (b* scale)

In the b* scale, there was an increase in the yellow/blue chroma scale mean values taken from baseline, 4 hours, 8 hours, 24 hours and final reading at 7 days for both polished and unpolished surfaces after immersion in the staining broth (Figure 5.3). The yellow/blue colour change increased from 21.95 to 49.50 for the unpolished surface and from 20.23 to 45.17 for the polished surface. There was a statistically significant difference between baseline and 7 days in immersion broth in the b* scale (ANOVA, p=0.000)

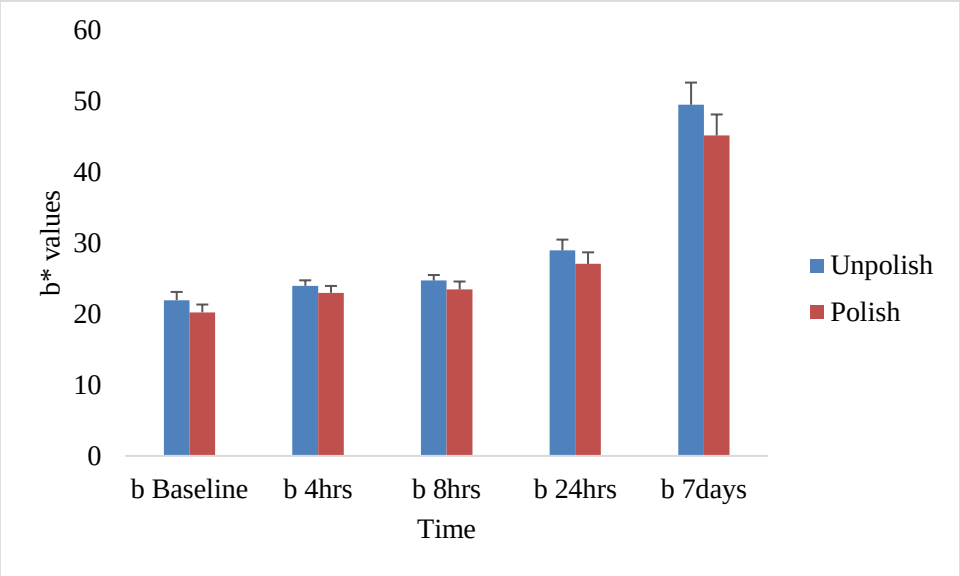

Figure 5.3: Fuji II LC®. Changes in b* scale over time for polished versus unpolished surface showing standard deviation

iv. Total Colour Change (ΔE^*_{ab} scale)

ΔE^*_{ab} scale mean values taken from baseline, 4 hours, 8 hours, 24 hours and final reading at 7 days for both polished and unpolished surfaces after immersion in the staining broth are shown in Figure 5.4. The total colour change increased from 2.30 to 28.16 for the unpolished surface and from 3.09 to 25.72 for the polished surface. There was a statistically significant difference for both between baseline and 7 days in immersion broth in the ΔE^*_{ab} scale (ANOVA, p=0.000). As there was no change in colour at 2 hours it was not included on the graphs.

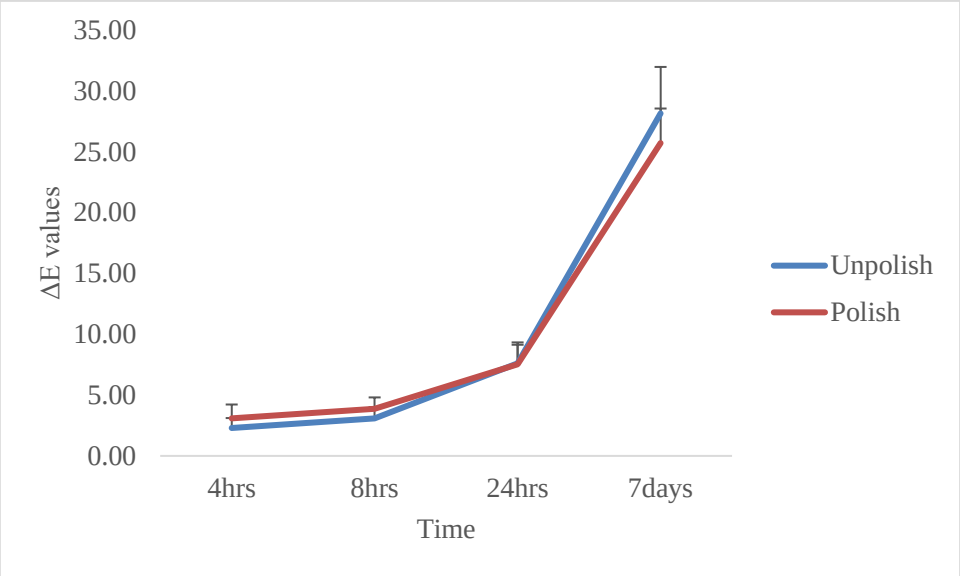

Figure 5.4: Fuji II LC® changes in ΔE^*_{ab} scale over time for polished versus unpolished surface with standard deviation

5.1.2 RIVA™ Light Cure Colour Changes

i. Lightness/Brightness (L* scale)

There was a progressive decrease in the lightness/brightness (L* scale) mean values taken from baseline, 4 hours, 8 hours, 24 hours and final reading at 7 days for both polished and unpolished surfaces after immersion in the staining broth (Figure 5.5). The lightness decreased from 84.89 to 75.11 for the unpolished surface and from 85.11 to 76.58 for the polished surface. There was a statistically significant difference between baseline and 7 days in immersion broth in the L* scale for both polished and unpolished surfaces (ANOVA, p=0.000).

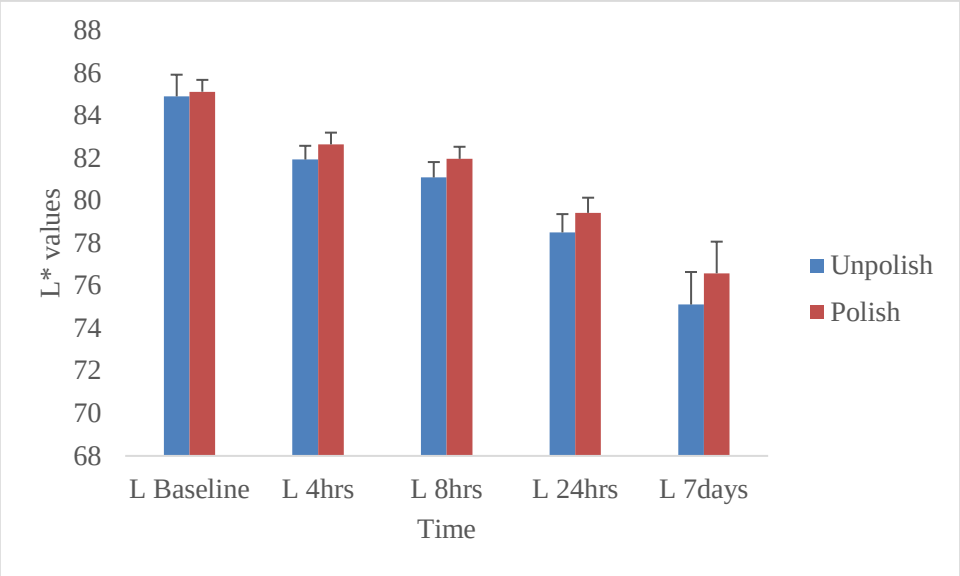

Figure 5.5: Riva™ Light Cure changes in L* scale over time polished versus unpolished surface with standard deviation included.

ii. Red-Green Chroma Scale (a*scale)

In the a* scale, there was a colour change in the red-green chroma scale mean values taken from baseline, 4 hours, 8 hours, 24 hours and final reading at 7 days for both polished and unpolished surfaces after immersion in the staining broth (Figure 5.6). The red/green colour change increased from 4.50 to 5.92 for the unpolished surface and decreased from 4.75 to 4.49 for the polished surface. There was a statistically significant difference between baseline and 7 days in immersion broth in the a* scale (ANOVA, p=0.000).

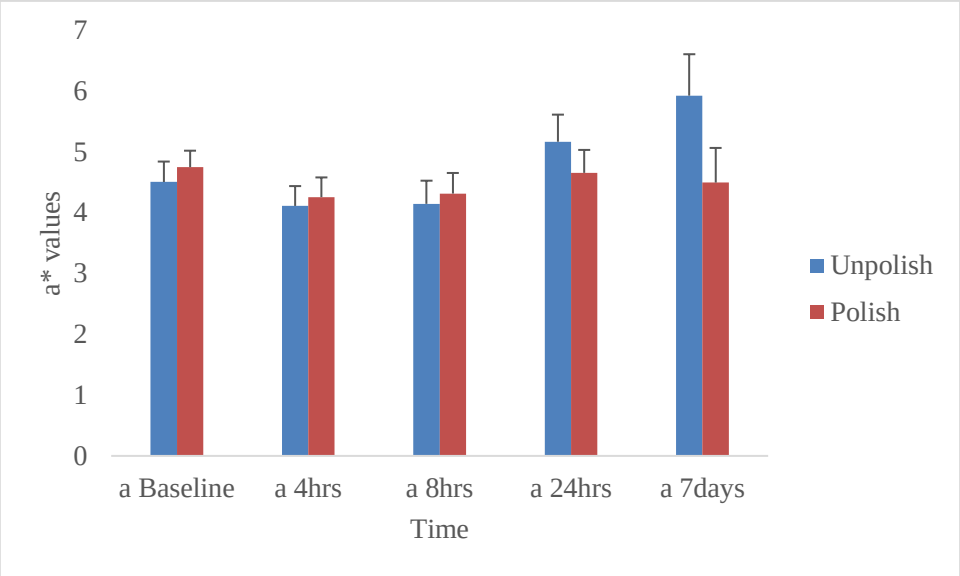

Figure 5.6: Riva™ Light Cure changes in a* scale over time for polished versus unpolished surface with standard deviation included

iii. Yellow-Blue Chroma Scale (b* scale)

In the b* scale, there was an increase in the yellow/blue chroma scale mean values taken from baseline, 4 hours, 8 hours, 24 hours and final reading at 7 days for both polished and unpolished surfaces after immersion in the staining broth (Figure 5.7). The yellow/blue colour change increased from 29.07 to 55.80 for the unpolished surface and from 28.60 to 49.30 for the polished surface. There was a statistically significant difference between baseline and 7 days in immersion broth in the b* scale (ANOVA, p=0.000).

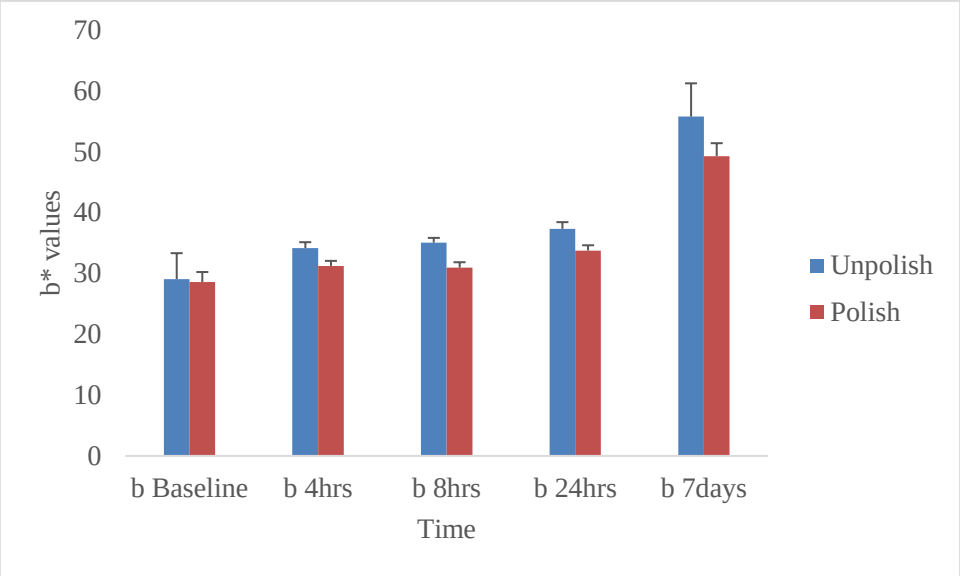

Figure 5.7: Riva™ Light Cure changes in b* scale over time for polished versus unpolished surface showing standard deviation included.

iv. Total Colour Change (ΔE^*_{ab} scale)

ΔE^*_{ab} scale mean values taken from baseline, 4 hours, 8 hours, 24 hours and final reading at 7 days for both polished and unpolished surfaces after immersion in the staining broth are shown in (Figure 5.8). The total colour change increased from 6.00 to 28.55 for the unpolished surface and from 3.87 to 22.44 for the polished surface. There was a statistically significant difference for both between baseline and 7 days in immersion broth in the ΔE scale (ANOVA, p=0.000).

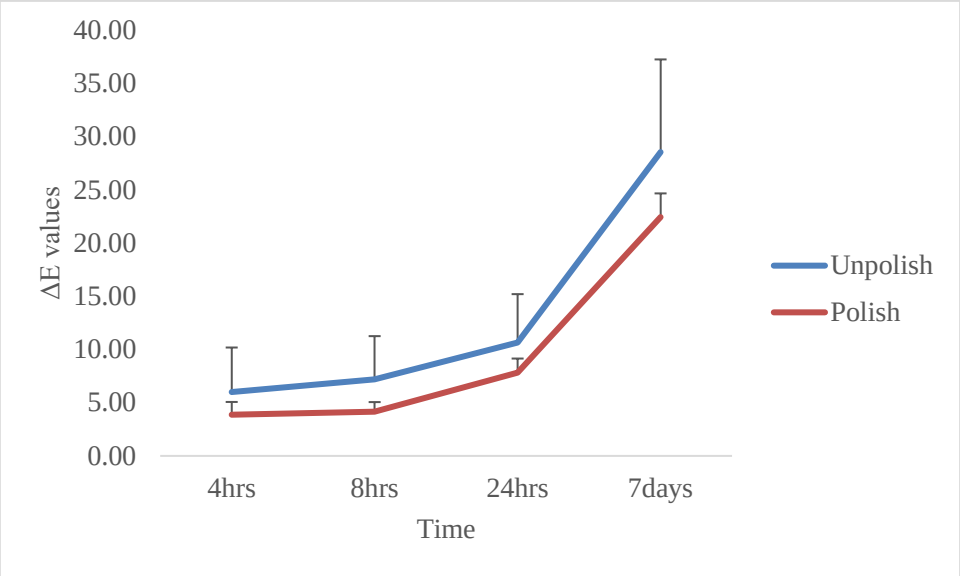

Figure 5.8: Riva™ Light Cure changes in ΔE^*_{ab} scale over time for polished versus unpolished surface showing standard deviation with standard deviation.

5.1.3 Ketac™ N100 Colour Changes

i. Lightness/Brightness (L* scale)

There was a progressive decrease in the lightness/brightness (L* scale) mean values taken from baseline, 4 hours, 8 hours, 24 hours and final reading at 7 days for both polished and unpolished surfaces after immersion in the staining broth (Figure 5.9). The lightness decreased from 81.28 to 70.33 for the unpolished surface and from 80.97 to 76.17 for the polished surface. There was a statistically significant difference between baseline and 7 days in immersion broth in the L* scale for both polished and unpolished surfaces (ANOVA, p=0.000).

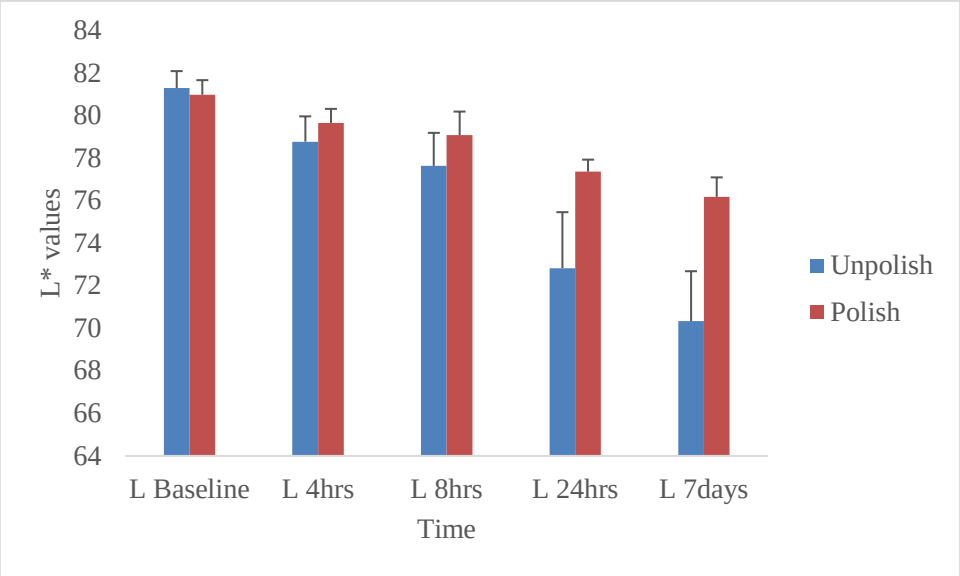

Figure 5.9: Ketac™ N100 changes in L* scale over time polished versus unpolished surface with standard deviation.

ii. Red-Green Chroma Scale (a*scale)

In the a* scale, there was an increase in the red-green chroma scale mean values taken from baseline, 4 hours, 8 hours, 24 hours and final reading at 7 days for both polished and unpolished surfaces after immersion in the staining broth (Figure 5.10). The red/green colour change increased from 3.01 to 5.04 for the unpolished surface and decreased from 3.18 to -0.08 for the polished surface. There was a statistically significant difference between baseline and 7 days in immersion broth in the a* scale (ANOVA, p=0.000).

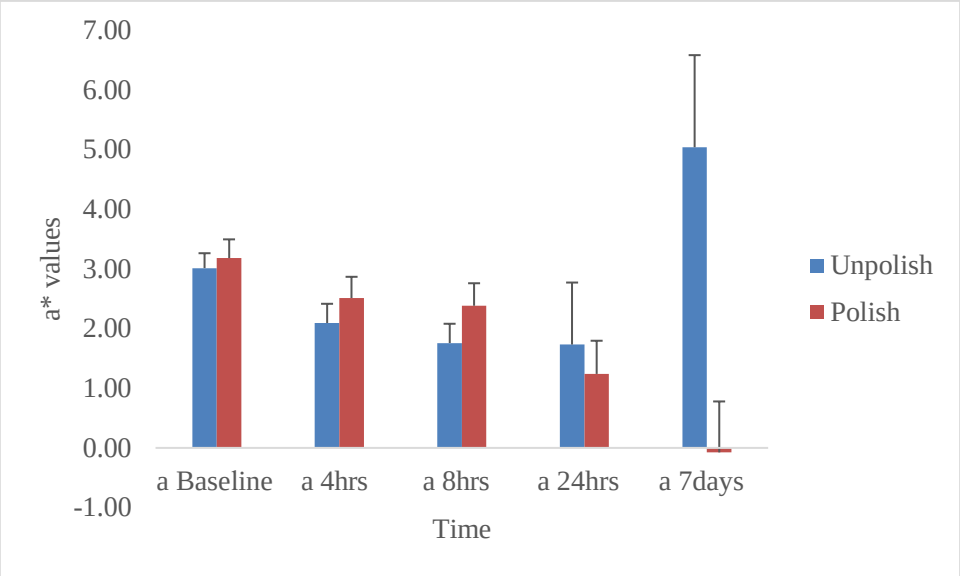

Figure 5.10: Ketac™ N100 changes in a* scale over time for polished versus unpolished surface with standard deviation.

iii. Yellow-Blue Chroma Scale (b* scale)

In the b* scale, there was a change in the yellow/blue chroma scale mean values taken from baseline, 4 hours, 8 hours, 24 hours and final reading at 7 days for both polished and unpolished surfaces after immersion in the staining broth (Figure 5.11). The yellow/blue colour change increased from 22.43 to 64.71 for the unpolished surface and from 22.40 to 44.40 for the polished surface. There was a statistically significant difference between baseline and 7 days in immersion broth in the b* scale (ANOVA, p=0.000).

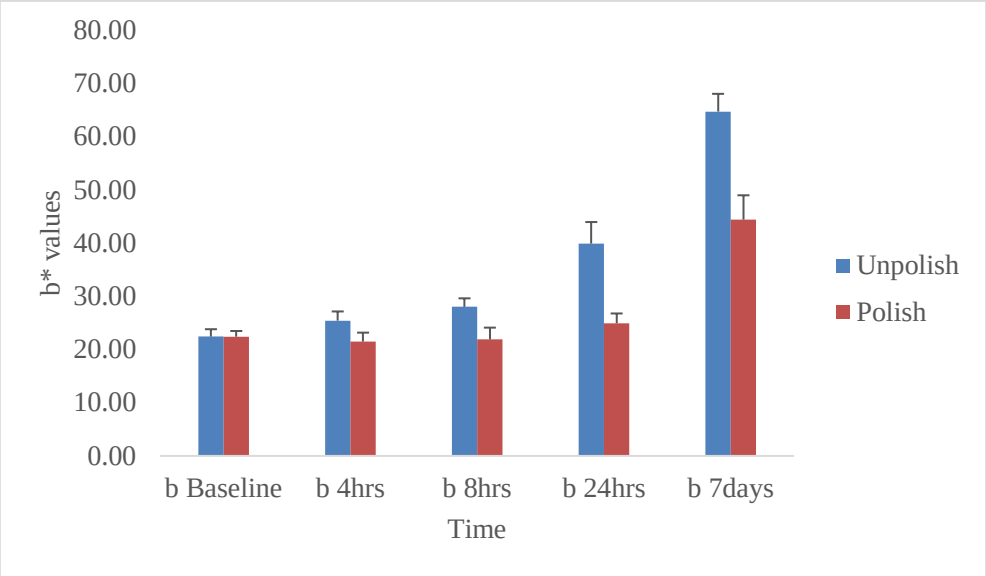

Figure 5.11: Ketac™ N100 changes in b* scale over time for polished versus unpolished surface showing standard deviation.

iv. Total Colour Change (ΔE^*_{ab} scale)

ΔE^*_{ab} scale mean values taken from baseline, 4 hours, 8 hours, 24 hours and final reading at 7 days for both polished and unpolished surfaces after immersion in the staining broth are shown in (Figure 5.12). The total colour change increased from 4.19 to 43.84 for the unpolished surface and from 2.30 to 22.79 for the polished surface. There was a statistically significant difference for both between baseline and 7 days in immersion broth in the ΔE^*_{ab} scale (ANOVA, p=0.000).

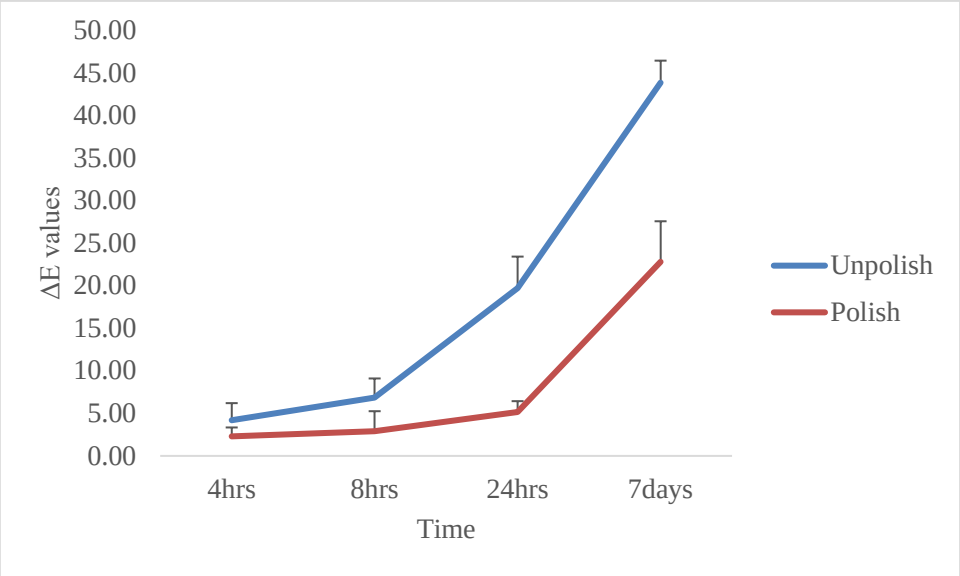

Figure 5.12: Ketac™ N100 changes in ΔE^*_{ab} scale over time for polished versus unpolished surface showing standard deviation.

5.1.4 Vitremer™ Colour Changes

i. Lightness/Brightness (L* scale)

There was a progressive decrease in the lightness/brightness (L* scale) mean values taken from baseline, 4 hours, 8 hours, 24 hours and final reading at 7 days for both polished and unpolished surfaces after immersion in the staining broth (Figure 5.13). The lightness decreased from 85.59 to 78.24 for the unpolished surface and from 85.95 to 78.05 for the polished surface. There was a statistically significant difference between baseline and 7 days in immersion broth in the L* scale for both polished and unpolished surfaces (ANOVA, p=0.000).

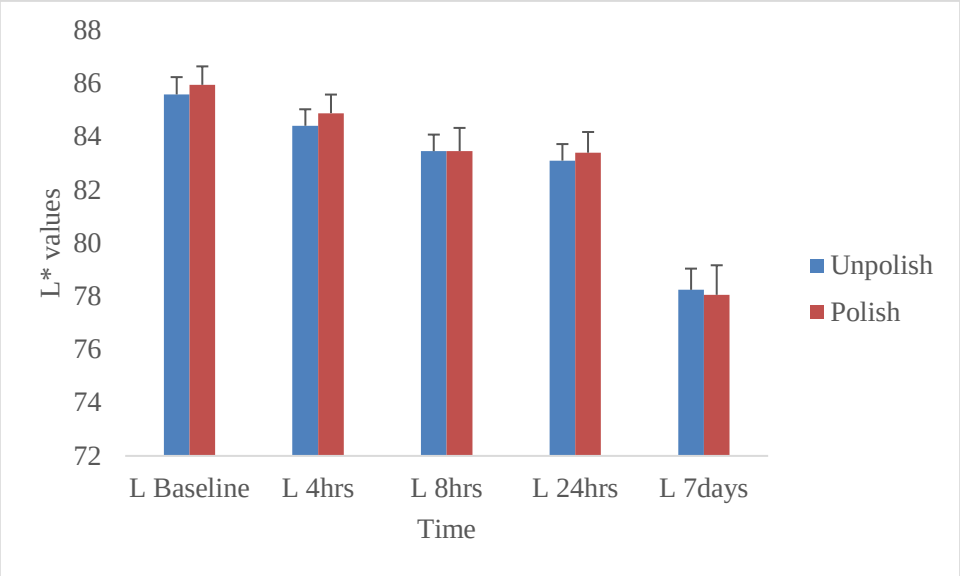

Figure 5.13: Vitremer™ changes in L* scale over time polished versus unpolished surface with standard deviation.

ii. Red-Green Chroma Scale (a*scale)

In the a* scale, there was a change in the red-green chroma scale mean values taken from baseline, 4 hours, 8 hours, 24 hours and final reading at 7 days for both polished and unpolished surfaces after immersion in the staining broth (Figure 5.14). The red/green colour change decreased from 1.31 to 1.02 for the unpolished surface and decreased from 1.44 to – 0.70 for the polished surface. There was a statistically significant difference between baseline and 7 days in immersion broth in the a* scale (ANOVA, p=0.000).

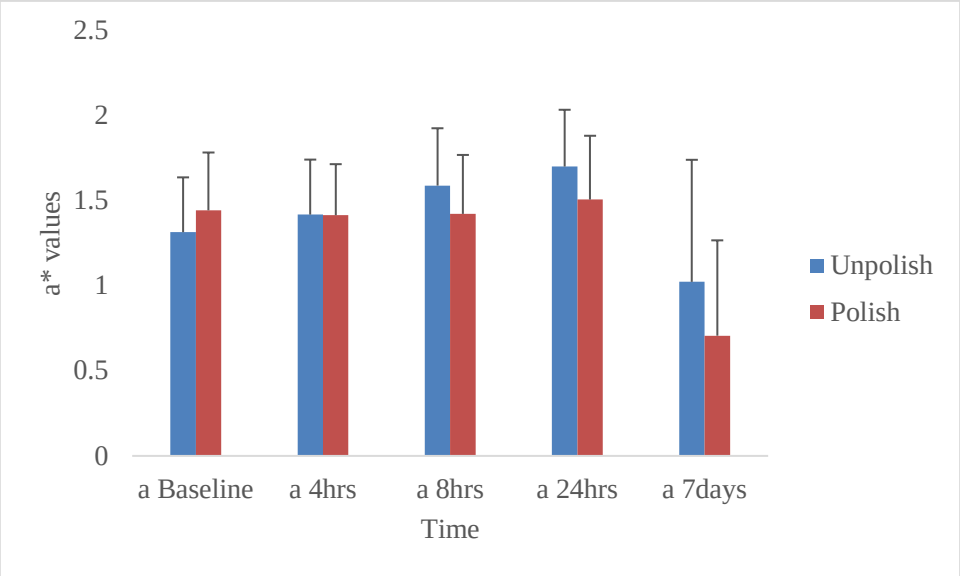

Figure 5.14: Vitremer™ changes in a* scale over time for polished versus unpolished surface with standard deviation included.

iii. Yellow-Blue Chroma Scale (b* scale)

In the b* scale, there was an increase in the yellow/blue chroma scale mean values taken from baseline, 4 hours, 8 hours, 24 hours and final reading at 7 days for both polished and unpolished surfaces after immersion in the staining broth (Figure 5.15). The yellow/blue colour change increased from 1.243 to 3.19 for the unpolished surface and from 1.23 to 4.75 for the polished surface. There was a statistically significant difference between baseline and 7 days in immersion broth in the b* scale (ANOVA, p=0.000).

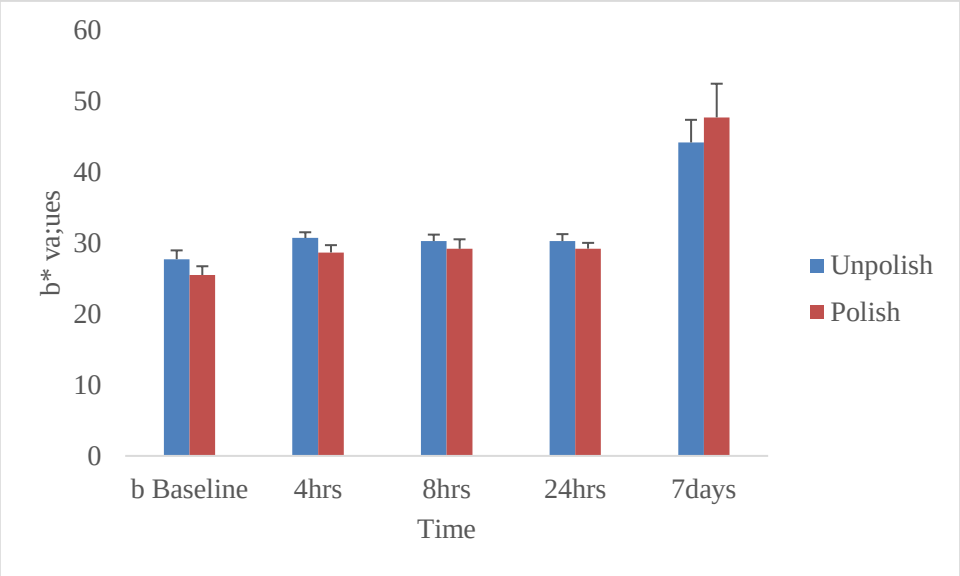

Figure 5.15: Vitremer™ changes in b* scale over time for polished versus unpolished surface showing standard deviation.

iv. Total Colour Change (ΔE^*_{ab} scale)

ΔE^*_{ab} scale mean values taken from baseline, 4 hours, 8 hours, 24 hours and final reading at 7 days for both polished and unpolished surfaces after immersion in the staining broth are shown in (Figure 5.16). The total colour change increased from 3.22 to 18.07 for the unpolished surface and from 3.36 to 23.63 for the polished surface. There was a statistically significant difference for both between baseline and 7 days in immersion broth in the ΔE^*_{ab} scale (ANOVA, p=0.000).

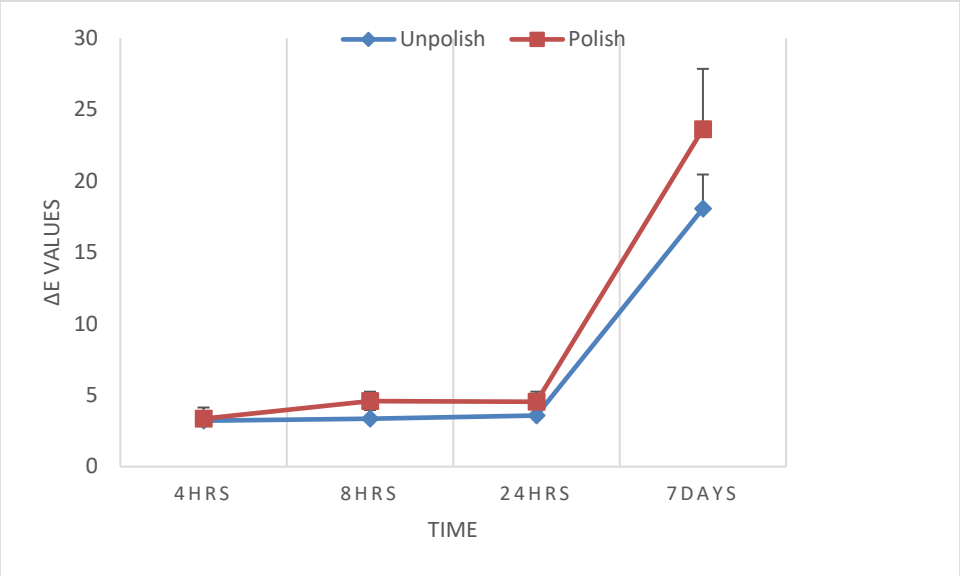

Figure 5.16: Vitremer™ changes in ΔE^*_{ab} scale over time for polished versus unpolished surface showing standard deviation.

5.1.5 ChemFil™ Rock Colour Changes

i. Lightness/Brightness (L* scale)

There was a progressive decrease in the lightness/brightness (L* scale) mean values taken from baseline, 4 hours, 8 hours, 24 hours and final reading at 7 days for both polished and unpolished surfaces after immersion in the staining broth (Figure 5.17). The lightness decreased from 83.38 to 78.06 for the unpolished surface and from 85.95 to 78.05 for the polished surface. There was a statistically significant difference between baseline and 7 days in immersion broth in the L* scale for both polished and unpolished surfaces (ANOVA, p=0.000).

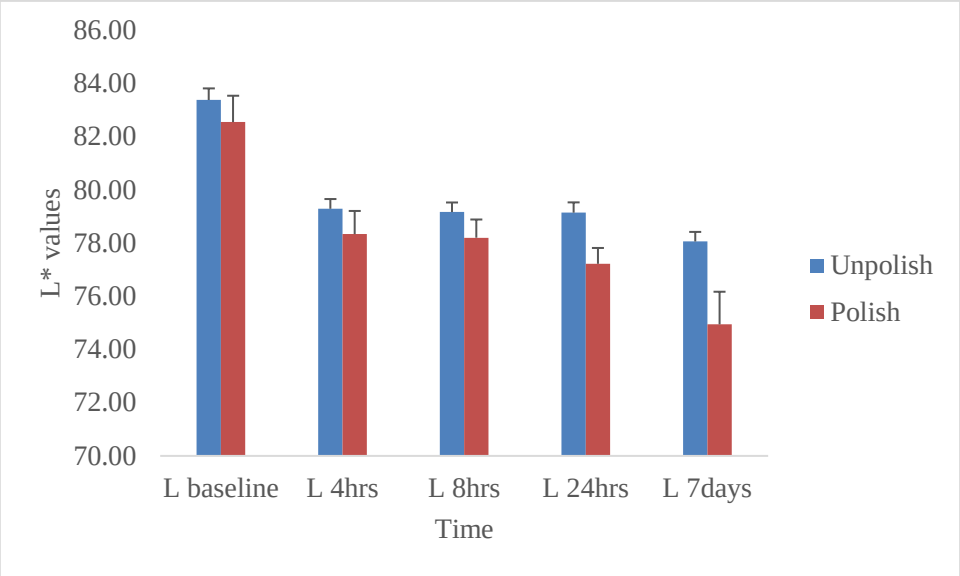

Figure 5.17: ChemFil™ Rock changes in L* scale over time polished versus unpolished surface with standard deviation.

ii. Red-Green Chroma Scale (a*scale)

In the a* scale, there was an change in the red-green chroma scale mean values taken from baseline, 4 hours, 8 hours, 24 hours and final reading at 7 days for both polished and unpolished surfaces after immersion in the staining broth (Figure 5.18). The red/green colour change decreased from 0.44 to 0.12 for the unpolished surface and increased from 0.55 to – 1.19 for the polished surface. There was a statistically significant difference between baseline and 7 days in immersion broth in the a* scale (ANOVA, p=0.000).

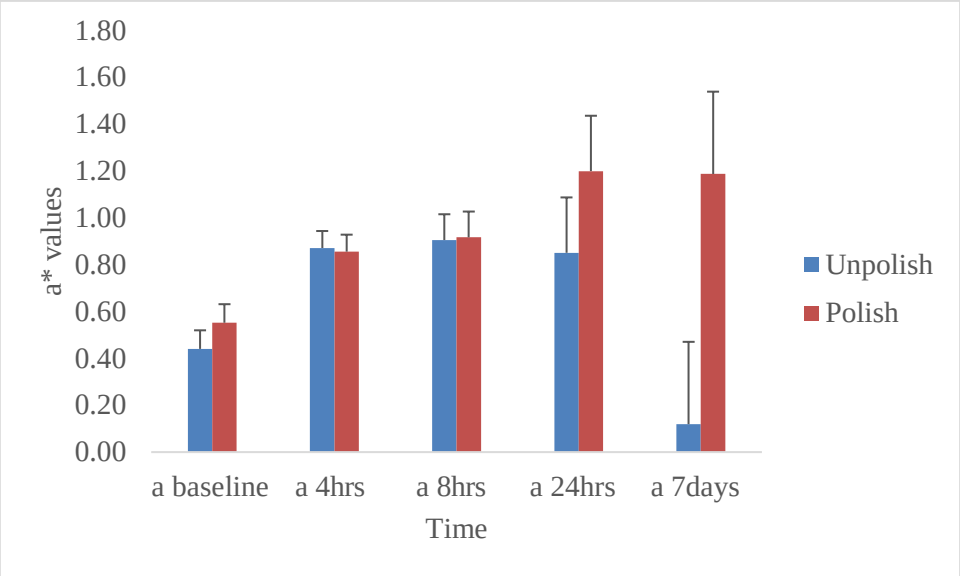

Figure 5.18: ChemFil™ Rock changes in a* scale over time for polished versus unpolished surface with standard deviation.

iii. Yellow-Blue Chroma Scale (b* scale)

In the b* scale, there was an increase in the yellow/blue chroma scale mean values taken from baseline, 4 hours, 8 hours, 24 hours and final reading at 7 days for both polished and unpolished surfaces after immersion in the staining broth (Figure 5.19). The yellow/blue colour change increased from 12.01 to 20.95 for the unpolished surface and from 12.35 to 28.27 for the polished surface. There was a statistically significant difference between baseline and 7 days in immersion broth in the b* scale (ANOVA, p=0.000).

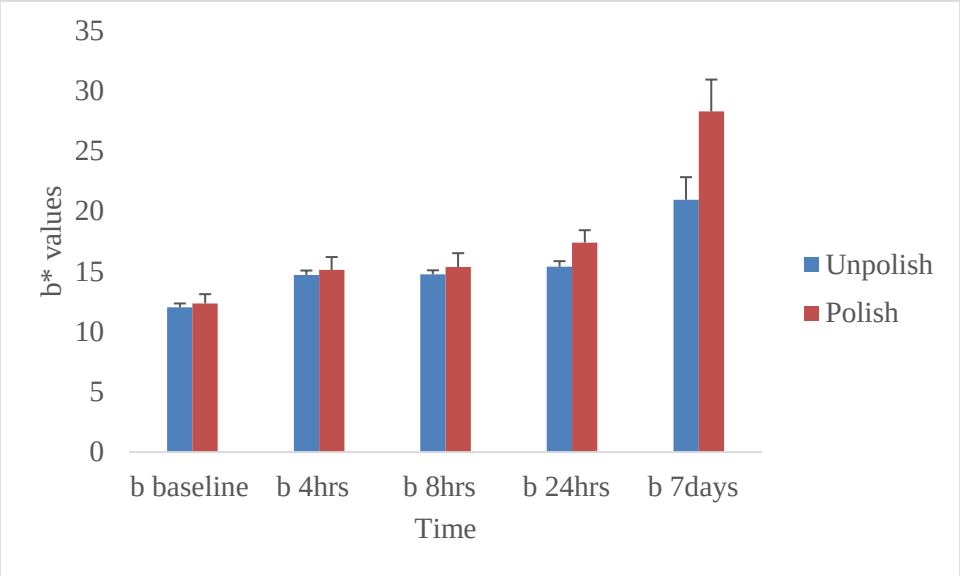

Figure 5.19: ChemFil™ Rock changes in b* scale over time for polished versus unpolished surface showing standard deviation.

iv. Total Colour Change (ΔE^*_{ab} scale)

ΔE^*_{ab} scale mean values taken from baseline, 4 hours, 8 hours, 24 hours and final reading at 7 days for both polished and unpolished surfaces after immersion in the staining broth are shown in (Figure 5.20). The total colour change increased from 4.92 to 10.45 for the unpolished surface and from 5.10 to 17.69 for the polished surface. There was a statistically significant difference for both between baseline and 7 days in immersion broth in the ΔE^*_{ab} scale (ANOVA, p=0.000).

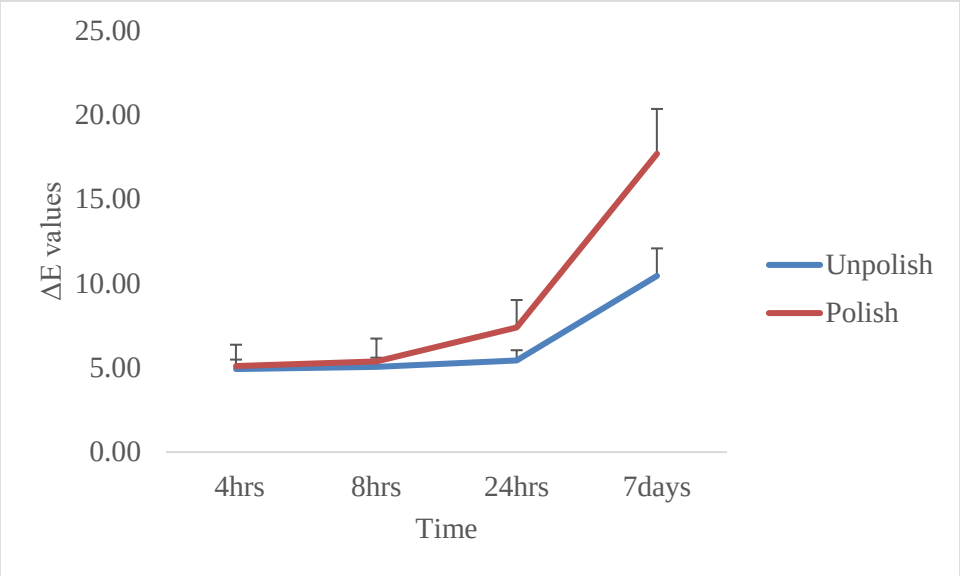

Figure 5.20: ChemFil™ Rock changes in ΔE^*_{ab} scale over time for polished versus unpolished surface showing standard deviation.

5.2. Examination of Staining (Light Microscopy)

5.2.1. Surface Staining

The surface staining of each material was determined using light microscopy analysis at a magnification of 40X. The results showed that staining was observed on the surface for all materials (Figure 5.21 - Figure 5.25).

i. **GC Fuji II LC® Capsule**

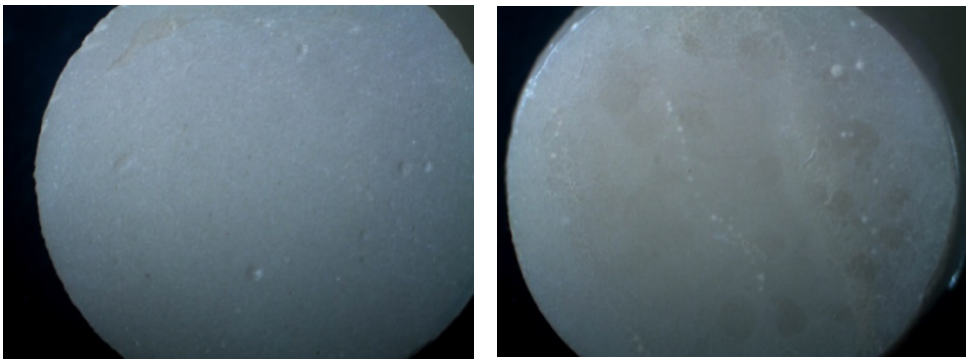

(a) (b)

Figure 5.21: Fuji II LC® CAPSULE Unpolished (a) and Polished (b) viewed under a light microscope.

Visually, from baseline to seven days following immersion in staining broth, along with the porosities which had formed on the surface, Fuji II LC® Capsule took on a very light brownish tinge.

ii. Riva™ Light Cure (SDI)

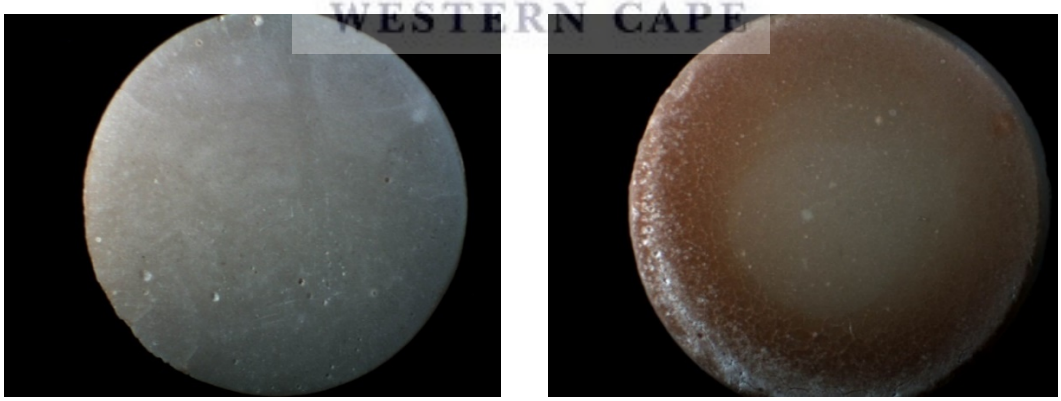

(a) (b)

Figure 5.22: Riva™ LC Unpolished (a) and Polished (b) viewed under a light microscope.

Visually, from baseline to seven days following immersion in staining broth, Riva™ Light Cure took on a reddish brown stain.

iii. Ketac™ N100 (3M ESPE)

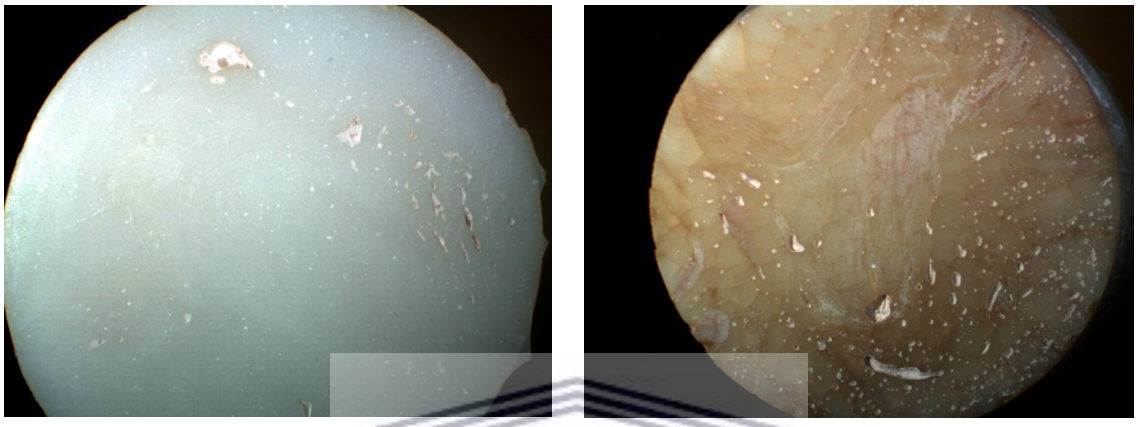

(a) (b)

Figure 5.23: Ketac™ N100 Unpolished (a) and Polished (b) viewed under a light microscope.

Visually, from baseline to seven days following immersion in staining broth, together with porosities which had formed, Ketac™ N100 took on a reddish brown stain.

iv. Vitremer™ (3M ESPE)

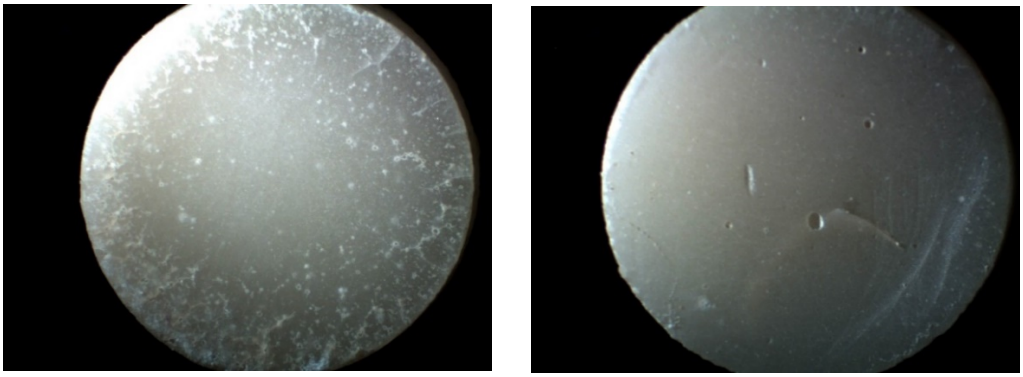

(a) (b)

Figure 5.24: Vitremer™ Unpolished (left) and Polished (right) viewed under a light microscope.

Visually, from baseline to seven days following immersion in staining broth, Vitremer™ took on a very light greyish tinge.

v. ChemFil™ Rock (Dentsply)

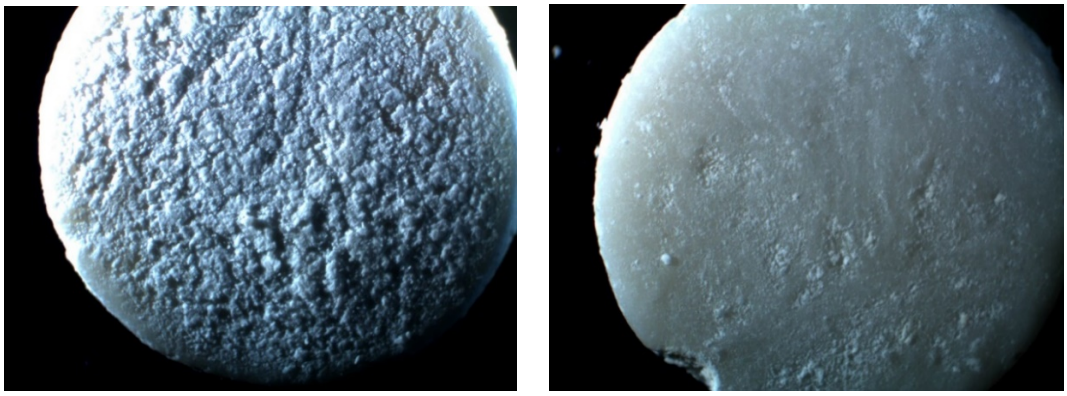

(a) (b)

Figure 5.25: ChemFil™ Rock Unpolished (left) and Polished (right) viewed under a light microscope.

Visually, from baseline to seven days following immersion in staining broth, ChemFil™ Rock displayed porosities.

5.2.2. Depth of Staining

i. **GC Fuji II LC® Capsule**

The depth of staining of each material was viewed and determined using light microscopy. The results showed that staining was observed on the surface for all materials with some penetration (Figure 5.26, Figure 5.27, Figure 5.29 and Figure 5.30). Ketac™ N100 (Figure 5.28) showed surface staining with some stains penetrating into voids and crevices which formed during the staining process, in all likelihood due to the low pH of the staining broth.

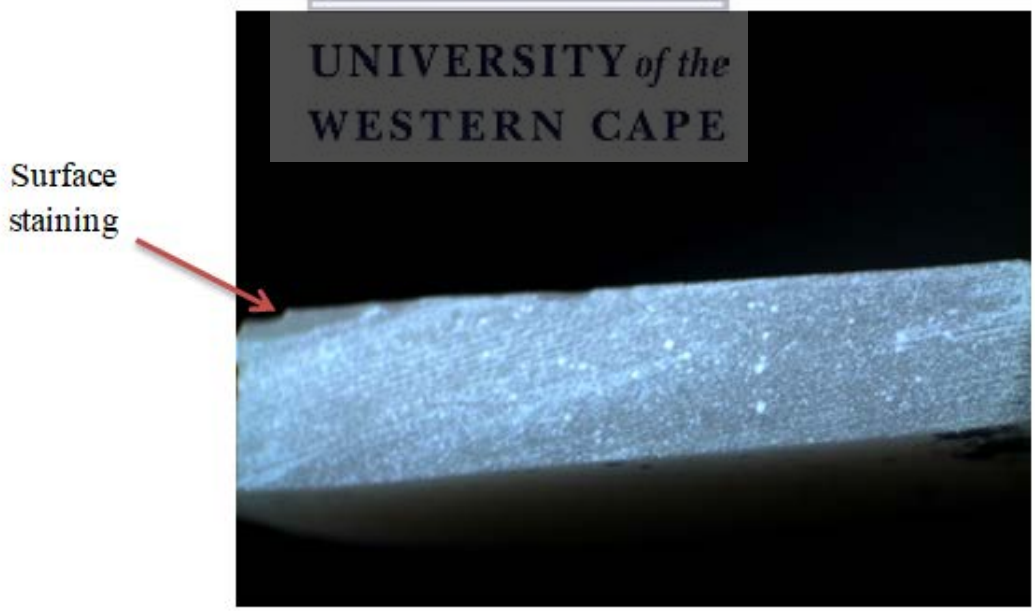

Figure 5.26: The polished surface of Fuji II LC® (top) showing superficial stain on its surface with some degree of penetration.

ii. Riva™ Light Cure (SDI)

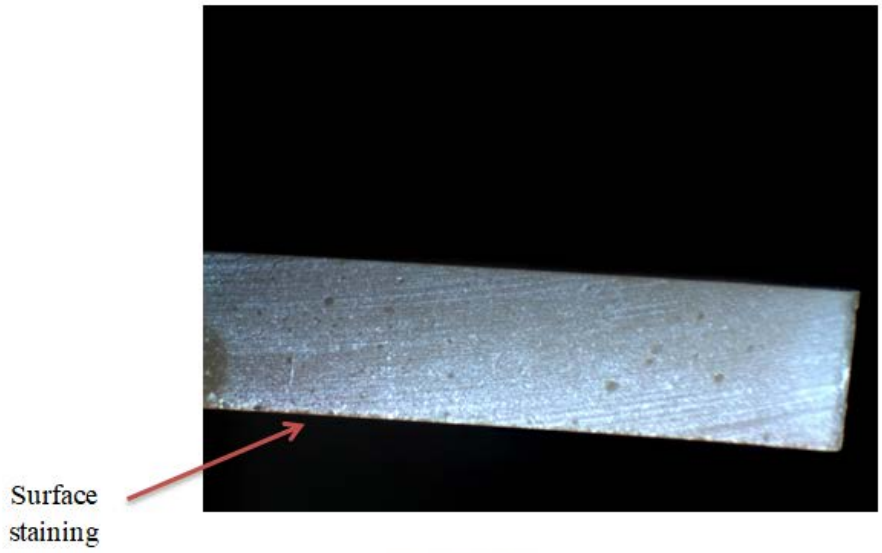

Figure 5.27: The unpolished surface of Riva™ Light Cure (bottom) showing superficial stain on its surface along with mild penetration of colour.

iii. Ketac N100™ (3M ESPE)

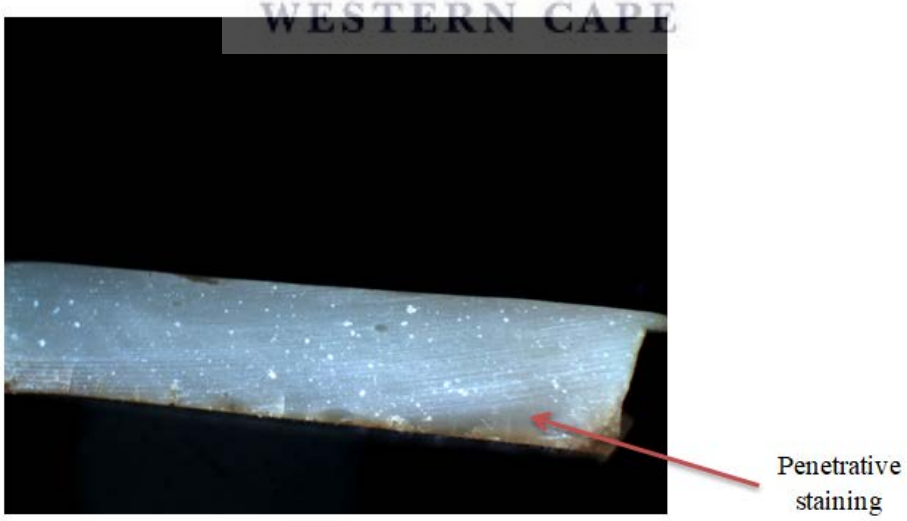

Figure 5.28: The unpolished surface of Ketac™ N100 (bottom) showing penetrative staining.

iv. Vitremer™ (3M ESPE)

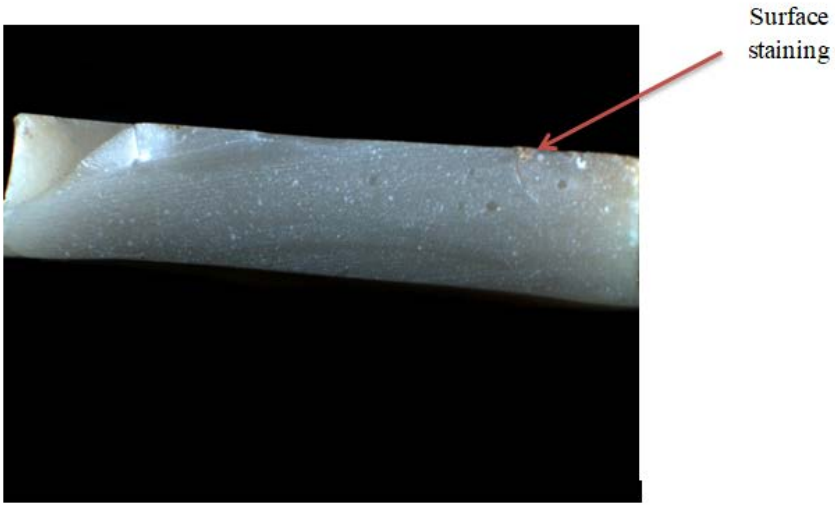

Figure 5.29: The polished surface of Vitremer™ (top) showing superficial stain on its surface with light penetration of colour.

v. **ChemFil™ Rock (Dentsply)**

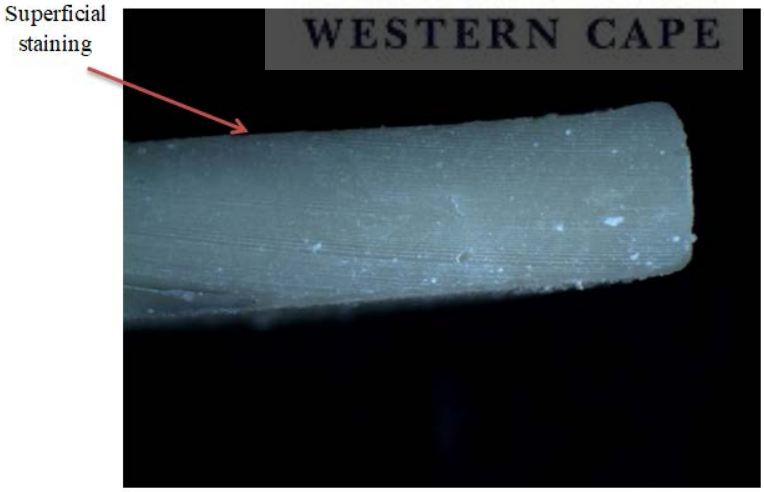

Figure 5.30: The polished surface of ChemFil™ Rock (top) showing superficial stain on its surface with mild penetrative staining.

5.3.Scanning Electron Microscopy

5.3.1. Fuji II LC® CAPSULE

The scanning electron microscopy analysis of Fuji II LC® CAPSULE powder showed a wide array of differently sized filler particles when scanned at 1000 X magnification (Figure 5.31 (a)). This observation was confirmed when the prepared powder particles were viewed at a higher magnification of 15 000 X (Figure 5.31(b)).

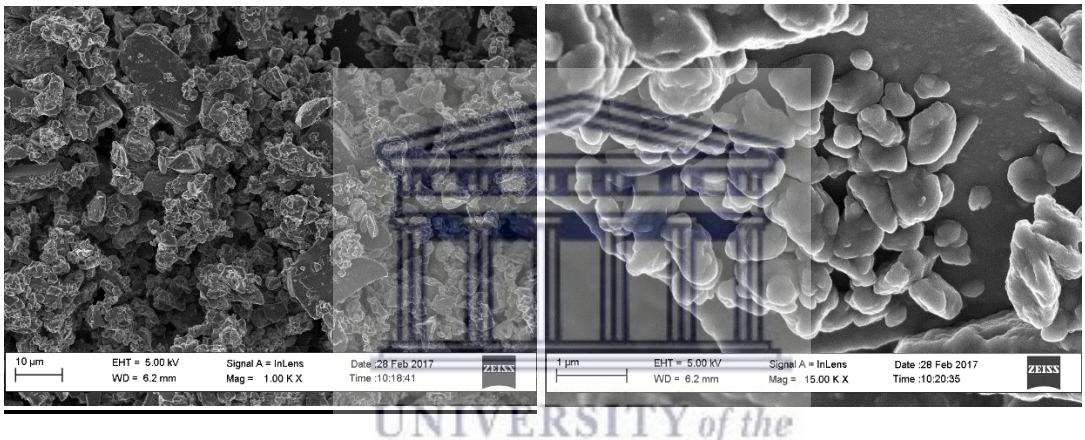

(a) (b)

Figure 5.31: Fuji II LC® CAPSULE powder viewed at (a) 1000 X magnification showing a wide array of differently sized filler particles, (b) at 15 000 X magnification showing smaller filler particles attached to larger filler particles.

Scanning electron microscopy analysis of Fuji II LC® CAPSULE showed roughness in the polished surfaces demonstrating insufficient polishing (Figure 5.32(a)). This was also confirmed when the magnification of the SEM was increased to 100 000 X (Figure 5.32(b)).

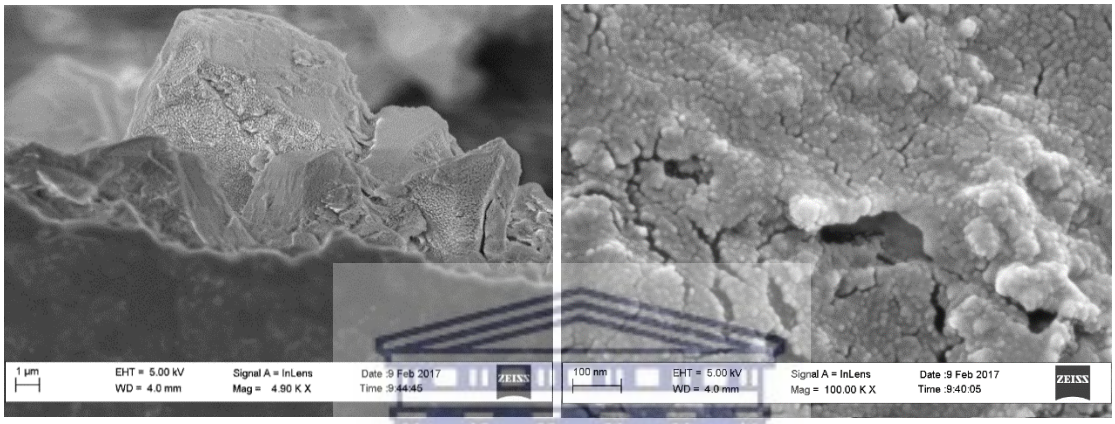

(a) (b)

Figure 5.32: Fuji II LC® CAPSULE sample disc viewed at (a) a magnification of 5000 X, (b) a magnification of 100 000 X. showing the surface roughness of the polished surface.

5.3.2. Riva™ Light Cure

The scanning electron microscopy analysis of Riva™ Light Cure powder showed numerously different sized filler particles, as can be seen at 1000 X magnification in (Figure 5.33 (a)). This becomes more apparent when viewing the prepared powder particles at a higher magnification of 15 000 X (Figure 5.33 (b)).

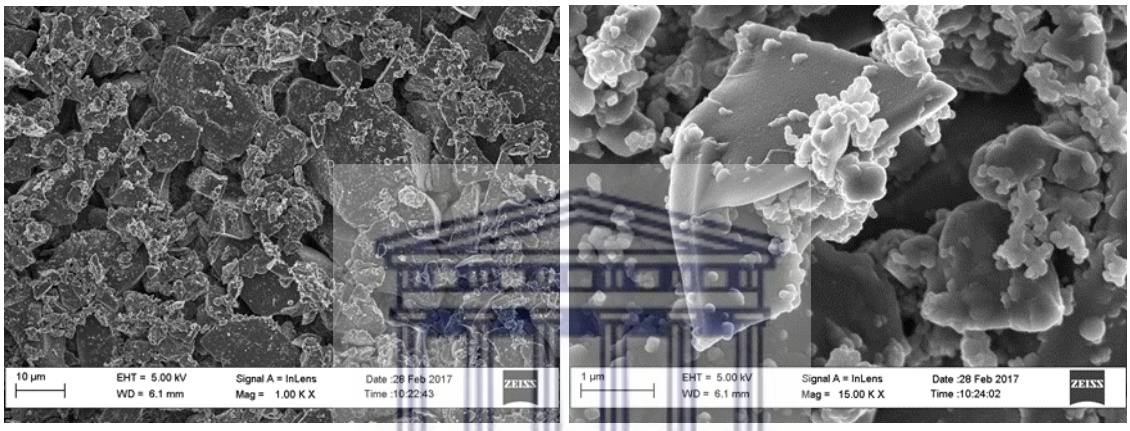

(a) (b)

Figure 5.33: Riva™ LC powder viewed at (a) 1000 X magnification (b) 15000 X. The two photos show varying filler particle size.

The scanning electron microscopy analysis for the surface of a Riva™ Light Cure sample disc at a lower magnification (Figure 5.34 (a)) showed that despite polishing, cracks were evident. At a higher magnification (Figure 5.34 (b)) it became apparent that the cracks were deep cracks and not superficial.

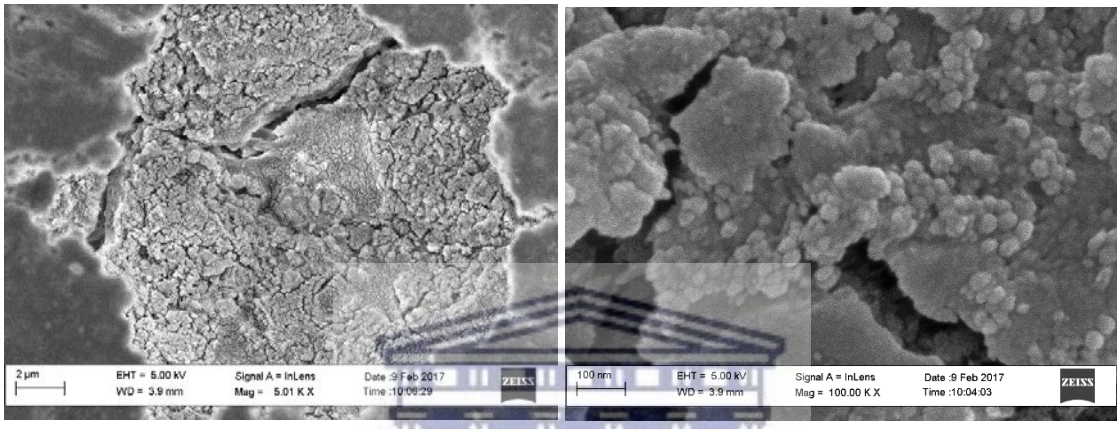

(a) (b)

Figure 5.34: Riva™ LC sample disc viewed at (a) a magnification of 5000 X, (b) a magnification of 100 000 X. showing cracks that extend deep into the sample.

5.3.3. Ketac™ N100

The scanning electron microscope analysis of the prepared paste of Ketac™ N100 at a 1000 X magnification (Figure 5.35 (a)) showed much smaller filler particles that are close to each other. At 15 000 X magnification (Figure 5.35 (b)), the filler particles appeared as clusters.

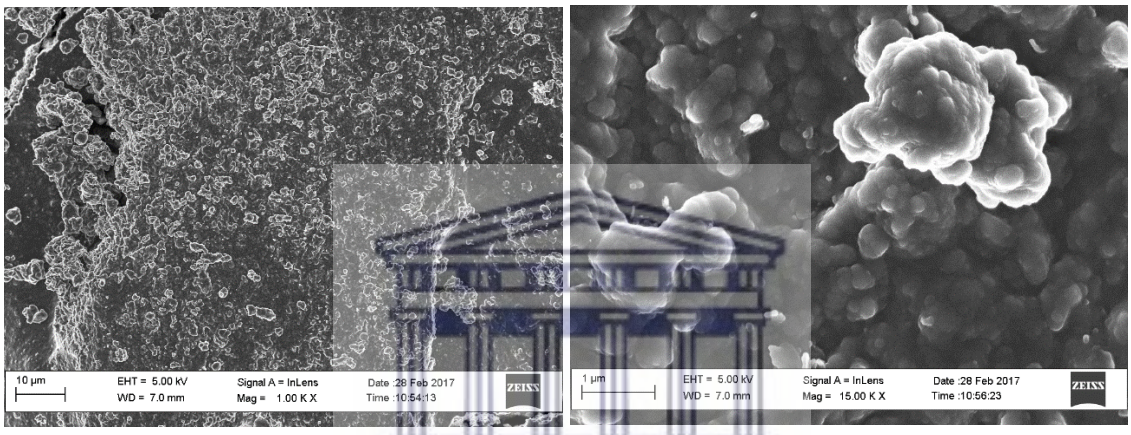

(a) (b)

Figure 5.35: Ketac™ N100 paste viewed at (a) 1000 X magnification showed glass filler particles appear to be ground very finely, with very few large particles visible, (b) 15 000 X magnification showing even smaller particles in the paste mix.

The scanning electron microscopy analysis for the surface of the Ketac™ N100 sample disc at 5000 X magnification shows lots of smaller fillers closer together on the surface (Figure 5.36 (a)). At 100 000 X magnification in (Figure 5.36 (b)), the fillers appear to coalesce, leaving very little room in the matrix.

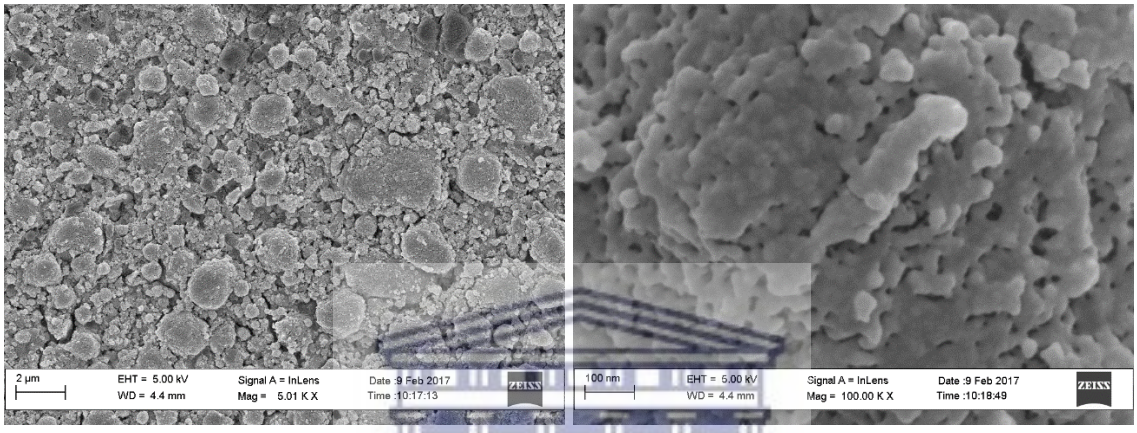

(a) (b)

Figure 5.36: Ketac™ N100 sample disc viewed at (a) a magnification of 5000 X showing Large number of smaller fillers visible on the surface of this sample disc, (b) a magnification of 100 000 X. showing coalesce of the filler particles.

5.3.4. Vitremer™

The scanning electron microscope analysis of the prepared powder of Vitremer™ at 1000 X magnification (Figure 5.37 (a)) showed many filler particles of varying size. At 15 000 X magnification (Figure 5.37 (b)) the difference in particle size is more apparent.

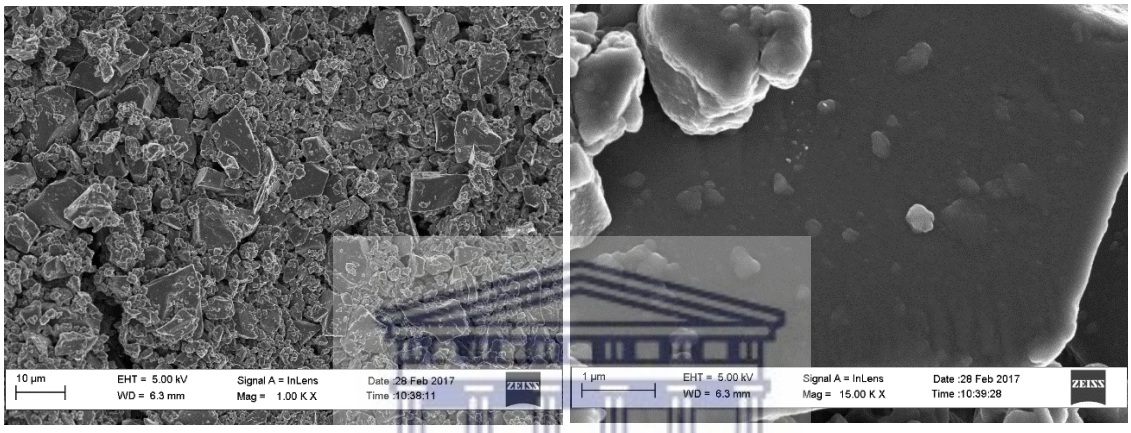

(a) (b)

Figure 5.37: Vitremer™ powder viewed at (a) 1000 X magnification showing glass filler particles of varying sizes, (b) at 15 000 X magnification showing more apparent different particle size.

The scanning electron microscopy analysis for the surface of a Vitremer™ sample disc at 5000 X magnification (Figure 5.38a)) showed that despite polishing, cracks were present on the surface of the sample. At 40 000 X magnification (Figure 5.38 (b)), the cracks appear to be quite deep.

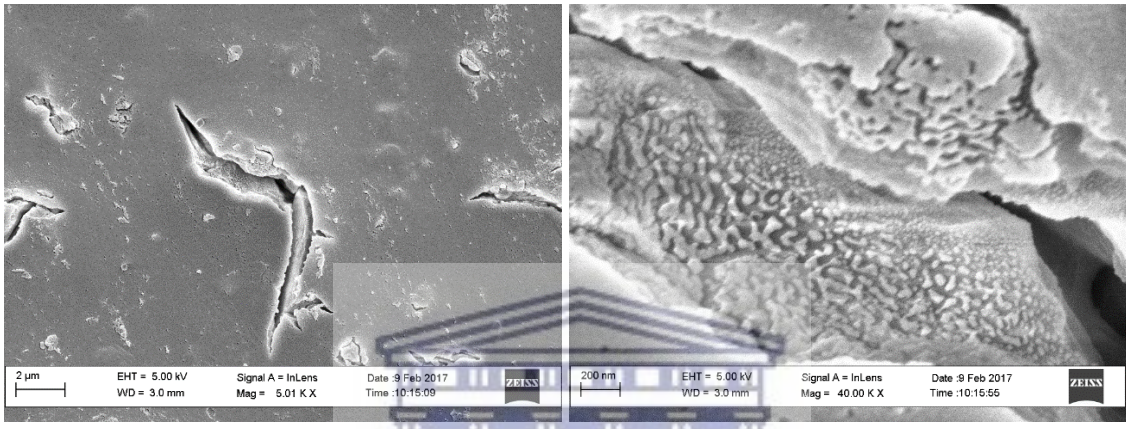

(a) (b)

Figure 5.38: Vitremer™ sample disc viewed at (a) 5000 X magnification showing minor cracks on the surface of the sample disc, (b) 40 000 X magnification showing deep cracks.

5.3.5. ChemFil™ Rock

The scanning electron microscope analysis of the prepared powder of ChemFil™ Rock at 1000 X magnification (Figure 5.39 (a)) showed many large filler particles. At a 15 000 X magnification (Figure 5.39 (b)) smaller filler particles can be seen.

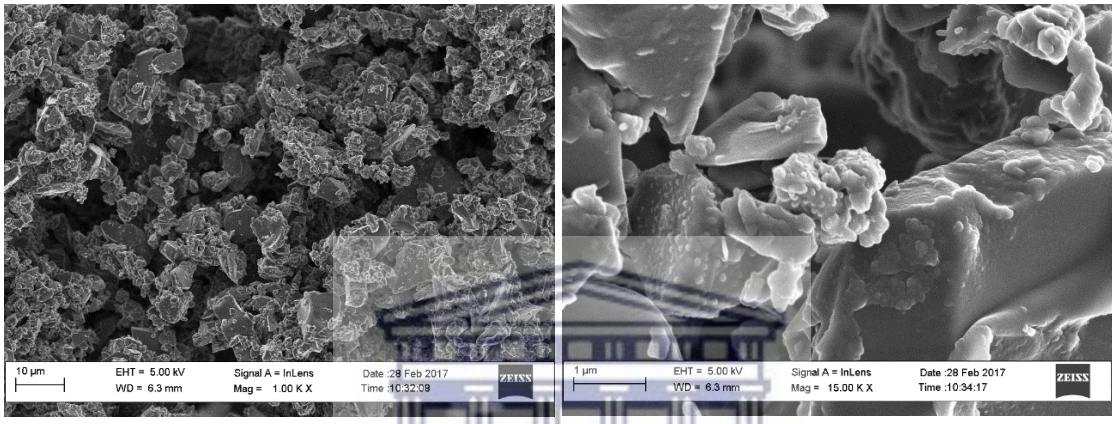

(a) (b)

Figure 5.39: ChemFil™ Rock powder viewed at (a) 1000 X magnification showing large filler particles, (b) 15 000 X magnification showing aggregates of smaller filler particles.

The scanning electron microscopy analysis for the surface of a ChemFil™ Rock sample disc at 5000 X magnification (Figure 5.40a)) showed that despite polishing, cracks were present on the surface of the sample. At 100 000 X magnification (Figure 5.40 (b)), of the crack, smaller clusters of other filler particles can be seen together with zinc filler particles.

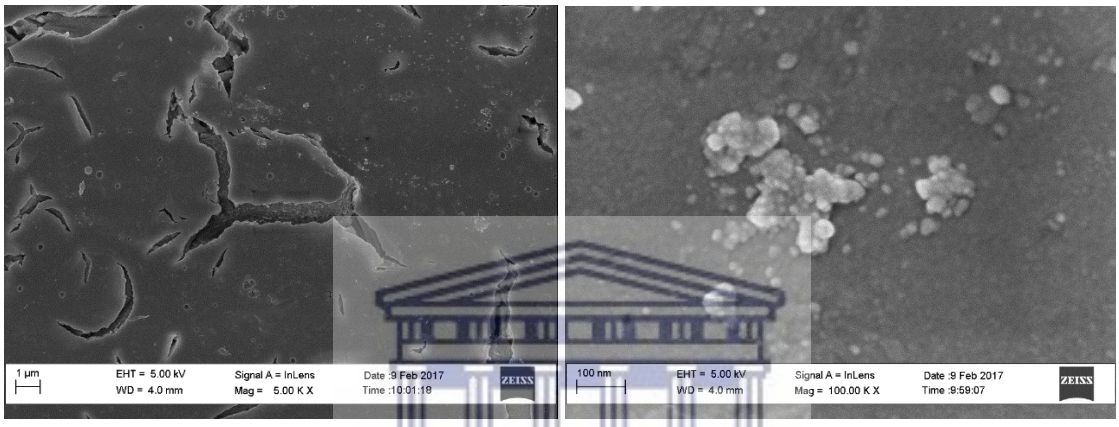

(a) (b)

Figure 5.40: ChemFil™ Rock sample disc viewed at (a) 5000 X magnification showing cracks on the surface of the sample, (b) 100 000 X magnification showing clusters of filler particles.

Chapter 6

Discussion

Conventional and resin-modified glass ionomers have been used for many years. Colour stability of restorative materials can be the difference between success and failure with regards to aesthetics (Postiglione *et al*., 2008). Therefore, it was decided to determine the stainability of the 4 resin-modified and one conventional glass ionomers selected for this study. In the past, conventional glass ionomers were criticised for their lack of colour stability (*Bern et al* in Ahmed and Sajjan, 2005). It was found in the literature that many limitations of conventional glass ionomers were reported which eventually led to the introduction of hybrid materials and compomers which have both the components of glass ionomers and resins, in various percentages (Prabhakar *et al*., 2009). Under oral conditions the aesthetic restorations could be exposed to the combined effects of light, moisture, mechanical wear and staining foods and drinks, which can often result in visibly detectable and aesthetically undesirable colour changes (Ahmed and Sajjan, 2005). Colour changes in aesthetic restorative materials have been attributed to various possible causes, only some of which were included for this study.

Wear or chemical degradation can increase the susceptibility of these materials to extrinsic staining (Villalta *et al*., 2006) as was observed with the ChemFil™ Rock sample discs. Other factors which lead to the susceptibility of extrinsic staining include stain accumulation, dehydration, water sorption, leakage, poor bonding and surface roughness

(Prabhakar *et al*., 2009), of which stainability (stain accumulation) was looked at in this study.

Extrinsic staining of restorations can be a major problem for many individuals especially those who smoke tobacco products or consume large quantities of tea, coffee, cola or red wine (Villalta *et al*., 2006). This is why the standard staining broth recommended by the American Dental Association was used for this study (Table 3.3). This broth is comprised of a combination of ingredients which simulates the ability that foods or beverages which are consumed daily have to stain a restorative material.

It is for this reason it could be expected that this staining could be a more accurate representation of a staining broth as it simulates the *in-vivo* situation more closely (Maart *et al*., 2016). Therefore, the present study was conducted to evaluate the degree of colour stability of resin-modified glass ionomer cements and a conventional glass ionomer cement.

Staining and Spectrophotometry

In this study, samples of various glass ionomer restorative materials were stained in a broth over a period of 7 days. Following this the stainability of materials was determined using different tests. The rationale being that some of the relatively newer materials which were chosen were compared for their stainability, giving an indication of their long lasting aesthetic ability.

Discolouration can be evaluated using various instruments. Spectrophotometers and colorimeters have been used to measure colour changes in dental materials (Ishikawa-Nagai *et al*., 2010) as the use of instrument measurements eliminates the subjective

interpretation of visual colour comparison and photograph comparison. Therefore, the Konica Minolta CM-2600d Spectrophotometer was used in this study. But, in contradiction to what the literature highlights as a more reliable instrument for determining colour change, it was still decided to include visual colour comparison in this study. The reason for this is based on what initiated this study, that is, anecdotal evidence indicating the replacement of restorations due to a visually perceptible change in colour over time. It was anticipated that a correlation between the stainability observed subjectively (visually) and the objective measurement (using a spectrophotometer) would therefore be found for the materials tested in this study. According to the literature, colour differences of composites can be visually perceived by the human eye once the overall mean colour change value equals 3.3 (Ruyter *et al*., 1987). After immersion in the broth for 7 days, all colour differences caused by staining solutions were visually perceptible in this study. Furthermore, the literature states that hydrophilic materials stain more than hydrophobic materials and glass ionomer cements exhibit more colour change than composites because of its hydrophilicity (Prabhakar *et al*., 2009). This is important as often the reason for replacement of an aesthetic restoration would be that the patient notices a visually perceptible change in the colour of the restoration.

Colour stability, in this study was assessed by determining the colour differences between the baseline colour and after 7 days following staining in the said broth. Mean colour differences were calculated for each specimen group as stated in the methods. For all materials there was an increase in staining when the colour difference between the baseline and the 7 day readings was assessed. Ketac™ N100 showed the highest total colour change for the unpolished surface whilst ChemFil™ Rock showed the least. The

colour change readings for Vitremer™, Riva™ Light Cure and Fuji II LC® were between these two extremes. Even though the least change was noted in ChemFil™ Rock, it does not have as great an impact on aesthetics as it is indicated for posterior use only. For the polished surfaces, the highest colour change was seen with Fuji II LC®, followed by Vitremer™, Ketac™ N100 and Riva™ Light Cure. Similar to the unpolished staining of the ChemFil™ Rock samples, the polished surfaces showed the least colour change. As stated above, this does not have a great impact on aesthetics of the restoration when using this material as it is indicated for posterior use only.

To determine the direction of the colour change, the spectrum was divided into lightness/brightness, red/green chroma and yellow/blue chroma scales to determine the exact nature of the colour change *i.e.* to determine whether the total colour change was influenced by any of these components.. In the lightness/brightness direction, the unpolished surfaces of all the sample discs for the materials used decreased, with Ketac™ N100 showing the biggest drop in lightness following the exposure to the broth for the full testing period. In the lightness/brightness direction for the polished surfaces, all the sample discs of the materials used in this study showed a decrease in this direction. Ketac™ N100 recorded the least lightness with the smallest change after immersion in the staining broth for the 7 day period.

In the red/green direction for the unpolished surfaces of the sample discs for Fuji II LC®, ChemFil™ Rock and Vitremer™, there was a decrease on this scale. Whereas with Riva™ Light Cure and Ketac™ N100 there was an increase, indicating that these materials absorbed more colour (making it darker) from this part of the spectrum during the staining process. In the red/green direction for the polished surfaces of the samples in the study

all the samples showed a decrease on the red/green scale, except for ChemFil™ Rock, which showed an increase. This is an indication that it absorbed more colour from this range after being in the broth, resulting in the samples becoming darker.

In the yellow/blue direction for the unpolished surfaces of the samples used in this study, all the samples showed an increase on this scale, with Ketac™ N100 showing the highest increase and ChemFil™ Rock the lowest, indicating absorption of less pigment from the broth. For the polished surfaces of all the samples used in this study, Fuji II LC® showed the biggest increase in colour change compared to ChemFil™ Rock. This would mean that Fuji II LC® absorbed more yellow/blue pigment and thus results in restorations appearing yellower to the naked eye.

Light Microscopy

When all the samples discs from the five selected materials were assessed visually and under the light microscope for surface changes, stain deposits were visible to varying degrees on both the polished and unpolished surfaces. This is in line with the literature which indicates that the roughness of materials might affect plaque formation or inhibit its removal (Prabhakar *et al*., 2009). The rate at which deposits accumulate on materials varies between individuals and can be affected by factors such as dietary intake, saliva composition, surface texture and porosity of the material (Xie *et al*., 2000).

Currently, the vast majority of the literature on glass ionomer cements deals with properties such as polishability, lustre and ease of handling without specifying composition or microstructure (Iqbal, 2012). This study is therefore an attempt to

correlate staining of glass ionomer cements with surface structure for both polished and unpolished surfaces. Therefore, it was decided to compare unpolished glass ionomer surfaces to polished surfaces as anecdotal evidence suggests that clinicians neglect to polish glass ionomer restorations. The researcher wanted to observe the effect of polishing on the surface and whether this would influence staining which was then tested. In this study, unpolished surfaces represent a matrix finish which is a smooth finish as seen without any magnification when the samples were prepared. These surfaces were compared to the polished surfaces (also viewed without any magnification at preparation) which had a disrupted surface morphology as a result of polishing. This study wanted to highlight the importance of the finished restoration and the effect of polishing the surface of glass ionomer cements and indirectly, its clinical implications. No varnish or gloss was considered in this study as according to the respective manufacturers' instructions, only Vitremer™ and Fuji II LC® Capsule have recommendations for the use of a gloss/varnish. The instructions for the handling of Ketac™ N100, ChemFil™ Rock and Riva™ Light Cure make no mention of the use of a finishing gloss/varnish. Abdel Hamid *et al*. (2018) showed no statistically significant difference between the overall values of gloss coated and uncoated glass ionomer surfaces at various aging periods with tea and distilled water. This ties in with the results of the staining of the various sample discs which all stained significantly on both the polished and unpolished surfaces.

Visual Assessment of Depth Penetration

For the depth of staining of the samples, all the materials showed only surface staining and mild penetrative staining, except for Ketac™ N100 where stains were observed

penetrating deeper. This was seen mainly in the areas of voids or crevices on the surface which may have been created as a result of the sample preparation. Ketac™ N100, being a two-paste system where, while mixing, voids could have been incorporated. Overall, Ketac™ N100 showed the highest staining in the mean overall colour difference. Both Vitremer™ and ChemFil™ Rock reacted similarly and seemed most stable with regards to colour change. These results are similar to that found by other researchers (Vance *et al.*, 2015). Vance *et al*. (2015) found the nano-ionomer Ketac™ N100 showing the worst colour stability in a staining solution as compared with traditional resin-modified glass ionomers and attributes this increase in colour change for nano-ionomers to their chemical composition. Vance *et al*. (2015) concludes that clinicians should be aware that nano resin-modified glass ionomers are more susceptible to colour change which will likely occur, particularly if the patient consumes a diet rich in substances which stain (Vance *et al.*, 2015).

A clinical trial by Perdigao (2012) showed that colour mismatching was more prevalent for Ketac™ Nano which is also a nano-filled ionomer compared to Fuji II LC® (Perdigão *et al*., 2012). Again, these results are similar to the ones obtained in this study. A possible explanation for the increase in stain uptake for Ketac™ Nano is the introduction of porosities which occur as a result of the mixing procedure prior to placement, leaving a behind rough surface that may enhance plaque accumulation and staining (Priyadarshini *et al*., 2017). When exposed to dark beverages, nano-filled glass ionomer (Ketac™ Nano) was more susceptible to staining and translucency changes than composites and this increased staining was correlated with a decrease in translucency, compromising clinical aesthetics (Tan *et al*., 2015). The results obtained in this study are similar to the Tan *et*

al. study where Ketac™ N100 showed the highest stain uptake corresponding to a decrease in the translucency/lightness.

SEM

Surface structure of glass ionomer cements plays an important role in the stainability of the material (Bagheri *et al*., 2005). Again, this was evident with Ketac™ N100 where there were several voids and porosities on the surface as observed in the SEM images. Intrinsic factors as a result of changes in the filler, matrix or silane coating or extrinsic factors such as adsorption or absorption of stains, may cause discolouration of aesthetic materials (Prabhakar *et al*., 2009). The intrinsic colour of aesthetic materials may change when the materials aged by exposure to various physical-chemical conditions, such as ultraviolet exposure, thermal changes and humidity (Sarkis, 2012; Iazzetti *et al*., 2000). This study therefore also attempted to establish the relationship between surface structure and stainability of the glass ionomer materials.

Prabhakar *et al.* (2009) compared surface roughness and found that glass ionomer cements demonstrated a more significant increase in surface roughness than composites. This group of researchers also observed that the roughness was due to the inclusion of voids which might be incorporated during the mixing or insertion of the material. Prabhakar *et al.* (2009) showed that colour stability and ability to resist stain may be potentiated by the surface conditions of the restorative material. A rougher surface affects colour by increasing the scattering of the light incidence (Prabhakar *et al*., 2009). This may explain the reason for Ketac™ N100 taking on the most stains in this study. This may

also be a result of the light scattering off the increased number of smaller filler particles as seen in Ketac™ N100.

Scanning electron microscopic (SEM) analysis is an efficient and acceptable method of studying surface morphology, filler size and distribution, interface adhesion and porosity (Xie *et al*., 2000).

Figures 5.26 to 5.30 and figures 5.32, 5.34, 5.36, 5.38 and 5.40 illustrate representative regions of the unstained surfaces for the 4 resin-modified glass ionomers and 1 conventional glass ionomer tested in this study at various magnifications.

SEM analysis was also done for the powder only (and one paste) for the respective materials tested. Many of the cracks observed in the microstructures may be caused by dehydration during preparation for SEM analysis, and the paths of crack propagation typically may be linked to microstructural porosities or voids. For Ketac™ N100, the void size and depth were generally greater than for the other materials especially on the polished surface. This may explain the higher colour change observed in Ketac™ N100 compared to the other materials. ChemFil™ Rock showed large particles appearing in clusters with open matrix spaces in between for both polished and unpolished surfaces. These particles may be tightly bound to the matrix which may explain the fewer number of voids on this surface resulting in least amount of stain uptake. Comparing the five materials, Vitremer™ showed a more integrated and highly fused smooth surface texture. This may explain the small amount of stain uptake on the surface of Vitremer™. Riva™ Light Cure exhibited different sizes of glass particles and more cracks were observed after

polishing. Fuji II LC® exhibited a smooth surface and a more tightly integrated glass particle–polymer matrix surface and less exposed glass particles.

Chapter 7
Conclusion

ChemFil™ Rock was found to be the most colour stable, that is, it absorbed the least colour, on both the polished and unpolished surfaces of all 5 materials tested for this study using 3 different types of tests (CIELAB colour evaluation; light microscope views and SEM images). The conclusion for this study does however refute the null hypothesis but the use of ChemFil™ Rock does not impact on aesthetics because it is indicated for posterior use only.

When considering the overall results for the remaining four resin-modified glass ionomer cements, the best results were obtained from Riva™ Light Cure, followed closely by Ketac™ N100 and then Vitremer™. Fuji II LC® absorbed the most colour on the polished surfaces, while Ketac™ N100 absorbed the most colour on the unpolished surfaces. If one were therefore to consider only the polished surfaces (since manufacturers all recommend polishing), then Riva™ Light Cure would be the most colour stable resin-modified glass ionomer to use for an aesthetic result, followed by Ketac™ N100 and both these materials can be used anteriorly and posteriorly.

Ketac™ N100 showed the highest overall colour change for the CIELAB colour evaluation; had the least amount of lightness at baseline and took on the most stains in the yellow/blue scale. Ketac™ N100 also showed the most voids when examined under SEM which may explain its high tendency for staining.

Both Vitremer™ and ChemFil™ Rock showed similar patterns of staining as Ketac™ N100. Vitremer™ having the highest lightness value. In the red/green colour scale, Vitremer™ and ChemFil™ Rock for both polished and unpolished surfaces were the least affected by this colour direction. At baseline Fuji II LC®, however, had the highest red/green component in its colour range. Both Vitremer™ and ChemFil™ Rock behaved similarly and seemed most stable with regards to colour change when viewed under SEM. Both these materials appeared fairly smooth on the SEM images explaining its lower rate of staining.

In this study, it was demonstrated by using the CIELAB colour evaluation, that all glass ionomer cements stained when exposed to the staining broth. Ketac™ N100 showed the highest overall colour change compared to the other materials tested. Both Vitremer™ and ChemFil™ Rock showed similar patterns of staining.

In the lightness/brightness scale, Ketac™ N100 had the least amount of lightness at baseline compared to the other materials with Vitremer™ having the highest lightness value.

In the red/green colour scale, Vitremer™ and ChemFil™ Rock for both polished and unpolished surfaces were the least affected by red/green colour direction. At baseline Fuji II LC® has the highest red/green component in its colour range.

On the yellow/blue scale Ketac™ N100 took on the most stains in this direction. At baseline ChemFil™ Rock had the least amount of yellow/blue in its baseline colour with Riva™ Light Cure having the highest amount of yellow/blue at baseline.

On the SEM images Ketac™ N100 showed the most voids which may explain its high tendency for staining, possibly as a result of void incorporation during mixing. Both

Vitremer™ and ChemFil™ Rock behaved similarly and seemed most stable with regards to colour change. Both these materials appeared fairly smooth on the SEM images, explaining its lower rate of staining.

The smaller the particles, the less the likelihood for absorption of colour as space in the material is filled by the smaller particles. However, the literature has shown that a nano-filled resin-modified glass ionomer absorbed more colour than the traditional resin-modified glass ionomers it was compared to (Vance *et al*., 2015). This correlates strongly to the findings in this study where it was found that Ketac™ N100 sample discs absorbed more colour, especially on the unpolished surfaces.

From this finding and other findings in this study, it can be concluded that polishing of conventional and resin-modified glass ionomer cements is essential in attempting to minimise the colour uptake by these restorations.

Chapter 8
Limitations and Recommendations

- This is an *in vitro* study and performed under ideal laboratory conditions where variables like conditions for microbiological inclusion in the broth are under controlled, ideal conditions. In the clinical situation, these conditions may vary. A variety of bacteria are present in the mouth which may influence the colour change. Also, the number of staining components added to the broth are limited to the recommendations of the American Dental Association and this may vary from individual to individual.

- Another limitation of this study is that it did not consider the effect of the mechanical modification of these materials that occurs during tooth brushing or occlusal wear. Perhaps surface modifications may influence staining.

- This study did not consider the effect of finishing gloss or varnish and did not measure surface roughness. Perhaps measuring surface roughness could have allowed for a better correlation between the polished and unpolished surfaces with regards to stainability, and especially when these are used clinically.

- This study was performed on one conventional and 4 resin-modified glass ionomer cements. Further studies should be done where more cements are tested. This may then give a broader indication on how glass ionomer cements react when exposed to a staining broth.

- This study should be followed up with a randomised clinical trial. A long term clinical study would give a better indication of the performance of these materials *in vivo*.

Chapter 9

References

3M ESPE (2007a) *3M ESPE Ketac™ N100 Light-Curing Nano-Ionomer Restorative and Nano-Ionomer Primer Instructions for use*.

3M ESPE (2007b) *An exclusive preview of a new resin modified glass ionomer from 3M™ ESPE™*. Available at: http://multimedia.3m.com/mws/media/439989O/ketac-n100-technical-data-sheet.pdf (Accessed: 20 June 2017).

3M ESPE (2007c) *Ketac™ N100 Light-Curing Nano-Ionomer Restorative*. Available at: http://mws9.3m.com/mws/media/443480O/ketac-n100-brochure-ebu.pdf (Accessed: 20 June 2017).

3M ESPE (2012a) *3M ESPE Vitremer Instructions For Use*.

3M ESPE (2012b) *Vitremer Technical Product Profile*. Available at: http://multimedia.3m.com/mws/media/44495O/vitremertm-core-buildup-restorative.pdf.

Abdel Hamid, D. M. *et al*. (2018) 'Effect of surface protection, staining beverages and aging on the color stability and hardness of recently introduced uncoated glass ionomer restorative material', *Future Dental Journal*. Elsevier.

Abu-bakr, N. *et al.* (2000) 'Color Stability of Compomer after Immersion in Various Media', *Journal of Esthetic Dentistry*, 12(5), pp. 258–263.

Ahmed, K. I. and Sajjan, G. (2005) 'Color stability of ionomer and resin composite restoratives in various environmental solutions: An invitro reflection spectrophotometric study', *Journal of Conservative Dentistry*, 8(1), pp. 45–51.

American Dental Association (2008) *In-office whitening agents: laboratory testing methods*. Available at: http://www.ada.org/sections/scienceAndResearch/pdfs/0804_whitening_testmethods.pdf.

Ayad, N. M. (2007) ‘Susceptibility of restorative materials to staining by common beverages: an in vitro study.’, *The European journal of esthetic dentistry : official journal of the European Academy of Esthetic Dentistry*, 2(2), pp. 236–247.

Bagheri, R., Burrow, M. F. and Tyas, M. (2005) ‘Influence of food-simulating solutions and surface finish on susceptibility to staining of aesthetic restorative materials’, *Journal of Dentistry*, 33(5), pp. 389–398.

Barry, T., Clinton, D. and Wilson, A. (1979) ‘The structure of a glass ionomer cement and its relationship to setting’, *Journal of Dental Research*, 58, pp. 1072–1079.

Berger, S. B. *et al.* (2011) ‘Surface Roughness and Staining Susceptibility of Composite Resins after Finishing and Polishing’, *Journal of Esthetic Restorative Dentistry*, 23(1), pp. 34–44.

Bhardwaj, Archana *et al.* (2014) ‘Nanotechnology in dentistry: Present and future.’, *Jioh*, 6(1), pp. 121–126.

Brune, D. and Smith, D. (1982) ‘Microstructure and strength properties of silicate and glass ionomer cements.’, *Acta odontologica Scandinavica*, 40(6), pp. 389–96. Available at: http://www.ncbi.nlm.nih.gov/pubmed/6962661.

Burkinshaw, S. M. (2004) ‘Colour in relation to dentistry. Fundamentals of colour science’, *British Dental Journal*, 196(1), pp. 33–41.

Cardoso, M. V. *et al.* (2010) ‘Towards a better understanding of the adhesion mechanism of resin-modified glass-ionomers by bonding to differently prepared dentin’, *Journal of Dentistry*, 38(11), pp. 921–929.

Chinelatti, M. A. *et al.* (2004) ‘Clinical performance of a resin-modified glass-ionomer and two polyacid-modified resin composites in cervical lesions restorations: 1-Year follow-up’, *Journal of Oral Rehabilitation*, 31(3), pp. 251–257.

Chu, S., Devigus, A. and Mielesszko, A. (2004) *Fundamentals of color, shade matching and communication in esthetic dentistry*. 3rd edn. Chicago: Quintessence Publications.

Commission Internationale de l'Eclairage (CIE) (1978) 'Recommendations on uniform color spaces, color-difference equations, psychometric color terms', *Paris: Bureau Central de la CIE*, Supplement(15), p. E-1.3.1.

Coutinho, E. *et al.* (2009) 'Bonding effectiveness and interfacial characterization of a nano-filled resin-modified glass-ionomer', *Dental Materials*, 25(11), pp. 1347–1357.

Crisp, S. *et al.* (1974) 'Reactions in Glass Ionomer Cements: II. An Infrared Spectroscopic Study', *Journal of Dental Research*, 53(6), pp. 1414–1420.

Crisp, S., Lewis, B. G. and Wilson, A. D. (1979) 'Characterization of glass-ionomer cements 5. The effect of the tartaric acid concentration in the liquid component', *Journal of Dentistry*, 7(4), pp. 304–312.

Crisp, S. and Wilson, A. D. (1974) 'Reactions in Glass Ionomer Cements: III. The Precipitation Reaction', *Journal of Dental Research*, 53(6), pp. 1420–1424.

Crisp, S. and Wilson, A. D. (1976) 'Reactions in glass ionomer cements: V. effect of incorporating tartaric acid in the cement liquid', *Journal of Dental Research*, 55(6), pp. 1023–1031.

Culbertson, B. M. (2001) 'Glass-ionomer dental restoratives', *Progress in Polymer Science (Oxford)*, 26(4), pp. 577–604.

Dentsply (2011) *Dentsply Chemfil Rock Sccientific Compedium*. Available at: https://www.dentsply.com/content/dam/dentsply/pim/manufacturer/Restorative/Direct_Restoration/Glass_Ionomers/Classic_Glass_Ionomers/ChemFil_Rock/ChemFil-Rock-nhg3c1d-scientific-en-1402 (Accessed: 6 June 2017).

Endo, T. *et al.* (2010) 'Surface texture and roughness of polished nanofill and nanohybrid resin composites', *Dental Materials Journal*, 29(2), pp. 213–223. Available at: http://joi.jlc.jst.go.jp/JST.JSTAGE/dmj/2009-019?from=CrossRef.

Francisconi, L. F. *et al.* (2009) 'Glass Ionomer Cements And Their Role In The Restoration Of Non-Carious Cervical Lesions', *Journal of Applied Oral Science*, 17(5), pp. 364–369.

GC (2008) *Fuji II LC A Perfect Choice*. Available at: http://sea.gcasiadental.com/Upload/product/pdf/13/Brochure-GC-Fuji-II-LC-CAPSULE.pdf (Accessed: 6 June 2017).

GC (2013) *GC Fuji II LC CAPSULE Instructions for Use*. Available at: http://www.gcamerica.com/products/operatory/GC_Fuji_II_LC/Fuji_II_LC_Caps_IFU.pdf (Accessed: 6 June 2017).

Ghinea, R. *et al.* (2011) 'Influence of surface roughness on the color of dental-resin composites', *Journal of Zhejiang University - Science B (Biomedicine & Biotechnology)*, 12(7), pp. 552–562.

Horn, D. J., Bulan-Brady, J. and Hicks, M. L. (1998) 'Sphere spectrophotometer versus human evaluation of tooth shade.', *Journal of endodontics*, 24(12), pp. 786–790.

https://pocketdentistry.com/2-3-glass-ionomer-cements-and-resin-modified-glass-ionomer-cements/ (no date). Available at: https://pocketdentistry.com/2-3-glass-ionomer-cements-and-resin-modified-glass-ionomer-cements/.

HunterLab (1996) *CIE L * a * b * Color Scale, Applications Note: Insight on Color*. Available at: http://cobra.rdsor.ro/cursuri/cielab.pdf.

Iazzetti, G. *et al.* (2000) 'Color Stability of Fluoride-Containing Restorative Materials', *Operative Dentistry*, 25(6), pp. 520–525.

Iqbal, K. (2012) 'Particle Size Variations In The Glass Component of Glass-Ionomer Dental Cements', *Journal of Ayub Medical College Abbottabad*, 24(2), pp. 41–43.

Ishikawa-Nagai, S. *et al.* (2005) 'Reproducibility of tooth color gradation using a computer color-matching technique applied to ceramic restorations', *Journal of Prosthetic Dentistry*, 93(2), pp. 129–137.

Ishikawa-Nagai, S. *et al.* (2010) 'Spectrophotometric Analysis of Tooth Color Reproduction on Anterior All-Ceramic Crowns: Part 1: Analysis and Interpretation of Tooth Color', *Journal of Esthetic and Restorative Dentistry*, 22(1), pp. 42–52.

Jarad, F. D., Russell, M. D. and Moss, B. W. (2005) 'The use of digital imaging for colour matching and communication in restorative dentistry', *British Dental Journal*, 199(1), pp. 43–49.

Jhaveri, H. M. and Balaji, P. R. (2005) 'Nanotechnology : The future of dentistry', *Nanotechnology*, 5(1), pp. 15–17.

Johnston, W. M. (2009) 'Color measurement in dentistry', *Journal of Dentistry*, 37(SUPPL. 1), pp. 2–6.

Joiner, A. (2004) 'Tooth colour: A review of the literature', *Journal of Dentistry*, 32(SUPPL.), pp. 3–12.

Judd, D. B. (1968) 'Ideal Color Space', *Palette*, 30, pp. 21–28.

Kanchanavasita, W., Anstice, H. M. and Pearson, G. J. (1998) 'Long-term surface micro-hardness of resin-modified glass ionomers', *Journal of Dentistry*, 26, pp. 707–712.

Khashayar, G. (2013) *Color Science in Dentistry*.

Khoroushi, M. and Keshani, F. (2013) 'A review of glass-ionomers: From conventional glass-ionomer to bioactive glass-ionomer', *Dental Research Journal (Isfahan)*, 10(4), pp. 411–420.

Khurshid, Z. *et al.* (2015) 'Advances in nanotechnology for restorative dentistry', *Materials*, 8(2), pp. 717–731.

Kielbassa, A. M. *et al.* (2009) 'In vitro comparison of visual and computer-aided pre- and post-tooth shade determination using various home bleaching procedures', *Journal of Prosthetic Dentistry*. The Editorial Council of the Journal of Prosthetic Dentistry, 101(2), pp. 92–100. Available at: http://dx.doi.org/10.1016/S0022-3913(09)60001-9.

Kleverlaan, C. J., Van Duinen, R. N. B. and Feilzer, A. J. (2004) 'Mechanical properties of glass ionomer cements affected by curing methods', *Dental Materials*, 20(1), pp. 45–50.

Landa, E. R. and Fairchild, M. D. (2005) ‘Charting Color from the Eye of the Beholder’, *American Scientist*, pp. 436–443.

Lang, B. R., Jaarda, M. and Wang, R.-F. (1992) ‘Filler particle size and composite resin classification systems’, *Journal of Oral Rehabilitation*, 19, pp. 569–584.

Lohbauer, U. (2010) ‘Dental glass ionomer cements as permanent filling materials? - Properties, limitations and future trends’, *Materials*, 3(1), pp. 76–96.

Maart, R. *et al.* (2016) ‘The whitening effect of four different commercial denture cleansers on stained acrylic resin’, *South African Dental Journal*, 71(3), pp. 106–111.

Malhotra, N. *et al.* (2011) ‘Effect of three indigenous food stains on resin-based, microhybrid-, and nanocomposites’, *Journal of Esthetic and Restorative Dentistry*, 23(4), pp. 250–257.

McCabe, J. F. (1998) ‘Resin-modified glass-ionomers’, *Biomaterials*, 19, pp. 521–527.

Minolta Co. Ltd. (1994) *Radiometric Instruments Operations*. 2-Chome, Azuchi-Machi, Chuo-Ku. Osaka 564-8556, Japan.

Moshaverinia, A. *et al.* (2011) ‘A review of powder modifications in conventional glass-ionomer dental cements’, *Journal of Materials Chemistry*, 21, pp. 1319–1328.

Mount, G. J. and Mackinson, O. F. (1978) ‘Clinical characteristics of a glass ionomer cement’, *British Dental Journal*, 145(3), pp. 67–71.

Nicholson, J. W. (1998) ‘Chemistry of glass-ionomer cements: A review’, *Biomaterials*, 19(6), pp. 485–494.

Park, J. K. *et al.* (2010) ‘Effect of staining solutions on discoloration of resin nanocomposites’, *American Journal of Dentistry*, 23(1), pp. 39–42.

Perdigão, J., Dutra-Corrêa, M. and Saraceni, S. (2012) ‘Randomized clinical trial of two resin-modified glass ionomer materials: 1-year results’, *Journal of Operative Dentistry*, 37(6), pp. 591–601.

Phillips, S. and Bishop, B. M. (1985) ‘An in vitro study of the effect of moisture on glass-ionomer cement’, *Quintessence International*, 2, pp. 175–177.

Postiglione, B. *et al.* (2008) ‘Color stability evaluation of aesthetic restorative materials’, *Brazilian Oral Research*, 2222(33), pp. 205–10205.

Prabhakar, A. *et al.* (2009) ‘Effect of Surface Treatment With Remineralizing on the Color Stability and Roughness of Esthetic Restorative Materials’, *Rev Clin Pesq Odontol*, 5(1), pp. 19–27.

Priyadarshini, B. I. *et al.* (2017) ‘One-year comparative evaluation of Ketac Nano with resin-modified glass ionomer cement and Giomer in noncarious cervical lesions: A randomized clinical trial.’, *Journal of conservative dentistry : JCD*. Wolters Kluwer -- Medknow Publications, 20(3), pp. 204–209.

Prosser, H. J., Richards, C. P. and Wilson, A. D. (1982) ‘NMR spectroscopy of dental materials. II. The role of tartaric acid in glass-ionomer cements’, *J Biomed Mater Res.*, 16, pp. 431–445.

Purdue University Radiological & Environmental Management Division Of Environmental Health And Public Safety (no date). Available at: https://www.purdue.edu/ehps/rem/laboratory/equipment safety/Research Equipment/sem.html (Accessed: 4 October 2017).

Ruyter, I. E., Nilne, K. and Möller, B. (1987) ‘Color stability of dental composite resin materials for crown and bridge veneers’, *Journal of Dental Materials*, 3(5), pp. 246–251.

Saito, S. (1978) ‘Characteristics of glass ionomer and its clinical application. 1. Relations between hardening reactions and water.’, *International Journal of Dental Materials*, 8, pp. 1–16.

Sarkis, E. (2012) ‘Color change of some aesthetic dental materials : Effect of immersion solutions and finishing of their surfaces’, *The Saudi Dental Journal*. King Saud University, 24(2), pp. 85–89. doi: 10.1016/j.sdentj.2012.01.004.

Saunders, S. A. (2009) ‘Current practicality of nanotechnology in dentistry. Part 1: Focus on nanocomposite restoratives and biomimetics’, *Clinical, Cosmetic and Investigational Dentistry*, 1, pp. 47–61.

SDI (2016) *SDI Riva Bond LC Light Cured Adhesive For Direct Restorations Instructions For Use*. Available at: https://www.sdi.com.au/downloads/instructions/INST_SHEET_RIVA_BOND_LC.pdf (Accessed: 6 June 2017).

SDI (no date) *No Title*. Available at: https://www.sdi.com.au/en-eu/product/riva-light-cure/ (Accessed: 6 June 2017).

Sidhu, S. K. and Nicholson, J. W. (2016) ‘A Review of Glass-Ionomer Cements for Clinical Dentistry’, *Journal of Functional Biomaterials*, 7(3), p. 16. Available at: http://www.mdpi.com/2079-4983/7/3/16.

Smith, D. C. (1998) ‘Development of glass-ionomer cement systems.’, *Biomaterials*, 19(6), pp. 467–78.

Soares, L. E. S. *et al.* (2012) ‘Scanning electron microscopy and roughness study of dental composite degradation’, *Microscopy and Microanalysis*, 18(2), pp. 289–294.

Swapp, S. (2017) *Scanning Electron Microscopy (SEM)*. Available at: https://serc.carleton.edu/research_education/geochemsheets/techniques/SEM.html (Accessed: 4 October 2017).

Tan, B. *et al.* (2015) ‘Effect of Beverages on Color and Translucency of New Tooth-Colored Restoratives’, *Operative Dentistry*, 40(2), pp. E56–E65.

Topcu, F. T. *et al.* (2009) ‘Influence of different drinks on the colour stability of dental resin composites.’, *European Journal of Dentistry*, 3(1), pp. 50–6. Available at: http://www.pubmedcentral.nih.gov/articlerender.fcgi?artid=2647959&tool=pmcentrez&rendertype=abstract.

Upadhya, N. P. and Kishore, G. (2005) ‘Glass Ionomer Cement-The Different Generations’, *Trends Biomater. Artif. Organs*, 18(2). Available at: http://www.sbaoi.org (Accessed: 2 October 2018).

Vance, M. *et al.* (2015) ‘Color and gloss of nano-filled resin-modified glass ionomers and resin composites’, *Journal of Esthetic and Restorative Dentistry*, 27(5), pp. 293–299.

Villalta, P. *et al.* (2006) ‘Effects of staining and bleaching on color change of dental composite resins’, *Journal of Prosthetic Dentistry*, 95(2), pp. 137–142.

Walls, A. (1986) ‘Glass polyalkenoate (glass-ionomer) cements: a review’, *Journal of Dentistry*, 14(6), pp. 231–246.

Wilson, A. D. (1968) ‘Dental silicate cements: VII. Alternative liquid cement formers.’, *Journal of Dental Research*, 47(6), pp. 1113–1136.

Wilson, A. D., Crisp, S. and Ferner, A. J. (1976) ‘Reactions in glass ionomer cemennts, IV Effect of chelating comonomers on setting behaviour.’, *Journal of Dental Research*, 55(3), pp. 489-495.

Xie, D. *et al.* (2000) ‘Mechanical properties and microstructures of glass-ionomer cements.’, *Dental materials : official publication of the Academy of Dental Materials*, 16(2), pp. 129–138.